GFZ
Helmholtz Centre
POTSDAM

GeoMod2014

Modelling in Geosciences

Programme & Extended Abstracts

31 August - 5 September 2014

Editors:
Kirsten Elger
Øystein Thordén Haug
Malte Ritter

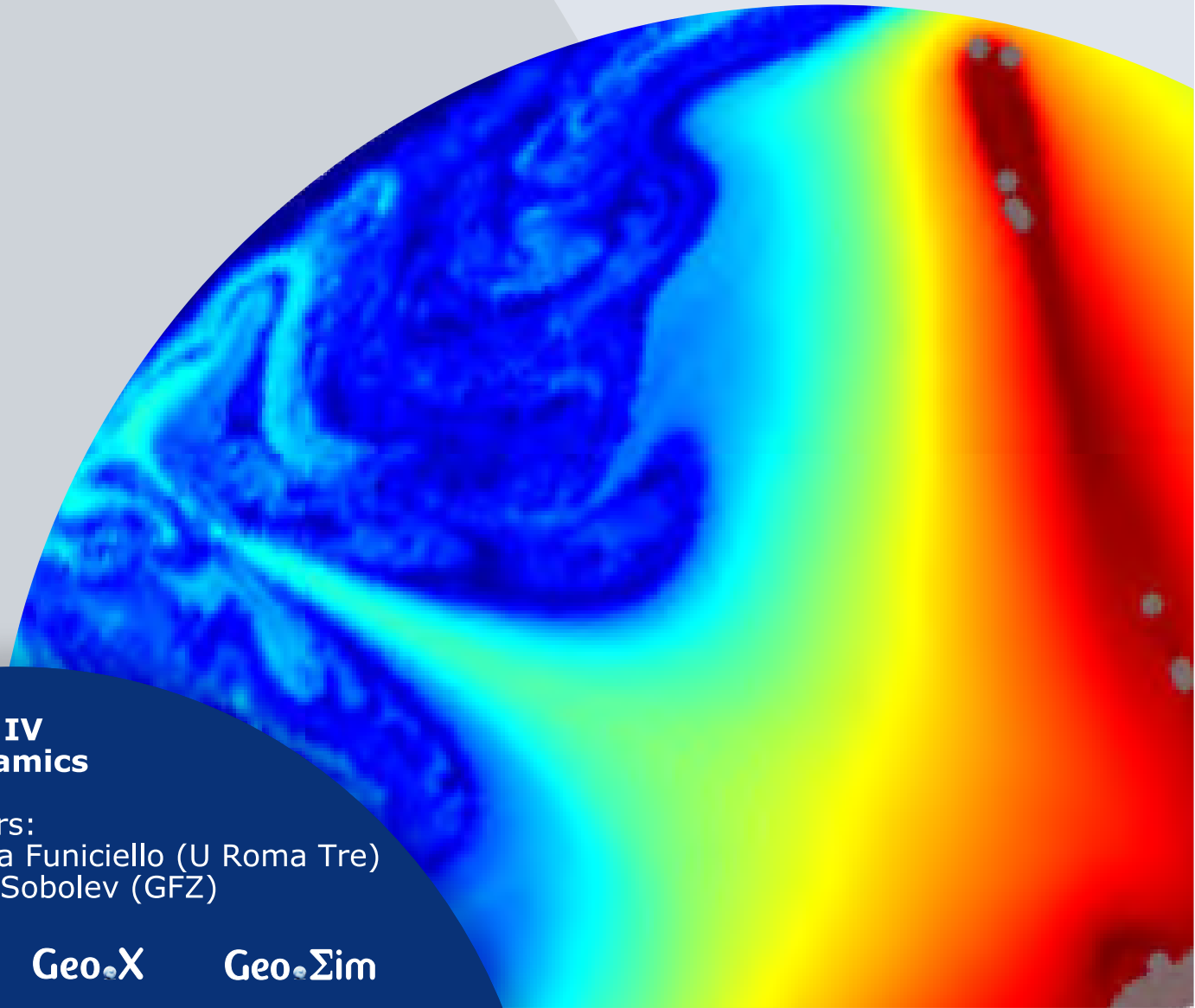

Session IV
Geodynamics

Conveners:
Francesca Funiciello (U Roma Tre)
Stephan Sobolev (GFZ)

DFG GeoX GeoSim

Recommended Citation

Elger, K; Haug, Ø. T.; Ritter, M. C. (Eds), (2014): Proceedings of GeoMod2014 – Modelling in Geosciences: Programme and Extended Abstracts 31 August–5 September 2014, GeoMod2014 – Modelling in Geosciences (Potsdam 2014), Potsdam: GFZ German Research Centre for Geosciences. DOI: http://doi.org/10.2312/GFZ.geomod.2014.001.

Disclaimer and Copyright

Imprint

Publisher
Helmholtz Centre Potsdam
GFZ German Research Centre for Geosciences
Telegrafenberg
14473 Potsdam
Published in Potsdam, Germany

Editors
Kirsten Elger
Øystein T. Haug
Malte C. Ritter

doi: 10.2312/GFZ.geomod.2014.001

About this book

This volume contains the extended abstracts of contributions presented during GeoMod 2014 at the Helmholtz Centre Potsdam GFZ German Research Centre for Geosciences (GFZ Potsdam), showing the state of the art of the tectonic modeling community.

GeoMod is a biennial conference dedicated to latest results of analogue and numerical modelling of lithospheric and mantle deformation. It started in 2002 in Milan as RealMod2002, then moved to Lucerne (GeoMod2004), Florence (2008), Lisbon (2010), and Lausanne (2012).

GeoMod2014 took place from 31 August to 3 September 2014 with 138 participants from 25 countries on all continents. The scientific programme of GeoMod2014 was organized in seven topical sessions listed below. The conference was followed by a 2-day short course on "Constitutive Laws: from Observation to Implementation in Models" (including lectures, lab visits, and practical exercises), as well as a 1-day hands-on tutorial on the ASPECT numerical modelling software.

GeoMod2014 focused on rheology and deformation at a wide range of temporal and spatial scales: from earthquakes to long-term deformation, from microstructures to orogens and subduction systems. For the first time, the discipline of volcanotectonics was included, while the (mantle) geodynamics community was more strongly represented than in previous editions. The bridge to field geology has traditionally been strong. At GeoMod 2014, fitting to the focus on rheology, the rock mechanics community was also represented. We thank our sponsors DFG, GFZ Potsdam and Geo.X, the conveners and all participants for contributing to a successful conference.

The GeoMod2014 Committee

The Scientific Committee
Onno Oncken
Georg Dresen
Stephan Sobolev
Matthias Rosenau
Karen Leever

The Organising Committee
Kirsten Elger
Franziska Alberg
Students support: Zahra Amirzada, Felix Eckelmann, Øystein Thordén Haug, Shaoyang Li, Malte Ritter, Tasca Santimano, Sarah Schröder, Johannes Wagner

Sessions, Conveners, and keynote speakers

(Seismo-)tectonics
Conveners: Boris Kaus (U Mainz), Onno Oncken (GFZ/FU Berlin),
Keynotes: Kelin Wang (Geological Survey Canada, Alberta), Bertrand Maillot (U Cergy-Pontoise)

Tectonics & Surface Processes
Conveners: Fabien Graveleau (U Lille), Niels Hovius (GFZ/U Potsdam),
Keynotes: Ritske Huismans (U Bergen), Stéphane Dominguez (U Montpellier II)

Volcanism and Volcanotectonics
Conveners: Olivier Galland (U Oslo), Eoghan Holohan (GFZ)
Keynotes: Rikke Pedersen (U Iceland), Olivier Roche (U BP Clermont-Ferrand)

Geodynamics
Conveners: Francesca Funiciello (U Roma Tre), Stephan Sobolev (GFZ),
Keynotes: Anne Davaille (U Paris-Sud), Bernhard Steinberger (GFZ)

Rheology
Conveners: Georg Dresen (GFZ/U Potsdam), Hiroki Sone (GFZ),
Keynotes: Yuri Fialko (U California), Laurent Montési (U Maryland)

Fluids and Deformation
Conveners: Stephen Miller (U Bonn), Marcos Moreno Switt (GFZ),
Keynotes: Boris Galvan (U Bonn), Takeshi Tsuji (U Kyushu)

Methods and Materials (poster-only session)
Conveners: Matthias Rosenau (GFZ), Marcel Frehner (ETH Zürich)

Short course on "Constitutive Laws: from Observation to Implementation in Models"
Lecturers: Onno Oncken (GFZ Potsdam), Matthias Rosenau (GFZ Potsdam), Fabio Corbi (GFZ Potsdam), Georg Dresen (GFZ Potsdam), Stephan Sobolev (GFZ Potsdam), Sascha Brune (U Sydney)

Hands-on tutorial on "ASPECT: a next-generation geodynamic modelling software"
(Advanced Solver for Problems in Earth's ConvecTion)
Lecturers: Anne Glerum (Utrecht University), Juliane Dannberg (GFZ Potsdam). Supervised by Wolfgang Bangerth (Texas A&M University, ASPECT main developer), Stephan Sobolev (GFZ Potsdam), Bernhard Steinberger (GFZ Potsdam).

Contents

Session IV.

Geodynamics

Session Description: Geodynamics

Conveners: Francesca Funiciello (U Roma Tre), Stephan Sobolev (GFZ)

We are living in the time when initially observational-qualitative geology is rapidly turning into the quantitative-predictive science where numerical and analogue modelling are essential. Both these modelling techniques have their strong and weak sides and their combination is potentially very desirable, but is not often practiced. In this session we would like to focus at geodynamic problems where both modelling techniques could best cooperate. Those include, but are not limited to deformation of lithosphere, subduction, mantle convection and plumes. We invite contributions of numerical and analogue modellers in all these fields and particularly welcome joint numerical-analogue modelling approaches and ideas on efficient cross-technique collaboration.

Anomalous structure of the oceanic lithosphere in the North Atlantic and Arctic oceans: preliminary analysis based on bathymetry, gravity and crustal structure

O. Barantseva, I. M. Artemieva, H. Thybo, M. Herceg

IGN, University of Copenhagen, Denmark
e-mail: *olba@ign.ku.dk*
session: *Geodynamics*

We present preliminary analysis of the crustal and upper mantle structure of the oceanic lithosphere in the North Atlantic and Arctic oceans with the specific goals of establishing factors that control variations in crustal thickness, and recognizing upper mantle structure which, together with the crustal structure, controls the bathymetry.

In comparison to continents, oceanic crust and upper mantle is commonly believed to have a simple structure, and in young oceans (< 80 Ma) bathymetry usually follows the square-root-of-age law. However, this is not true for the Northern Atlantic, northwards from the Charlie Gibbs transform zone. Although the Northern Atlantic ocean started opening ca. 65 Ma, it has anomalously thick crust and anomalously shallow bathymetry that does not follow theoretical predictions. These anomalies may, in part, be controlled by mantle processes at around Iceland. Further north and into the Arctic ocean, spreading rate decreases rapidly, having effect on the structure of the oceanic lithosphere. In the Arctic Ocean the main geodynamic factor that controls the crustal and lithospheric development, is the presence of a unique system of ultraslow mid-ocean ridges.

Our analysis is based on modeling of gravity anomalies caused by subcrustal anomalous masses. The calculations are based on removing the gravitational effect of water, crust and the deep mantle from the observed gravity field. The bathymetry is based on the global NOAA database ETOPO1. For crustal correction we use a part of the global model CRUST1.0, and for comparison, a regional seismic model EUNAseis. Gravity data is derived from GOCE satellite data. As a result we aim at understanding the links between the deep lithosphere dynamics, ocean spreading, ocean floor bathymetry, heat flow and structure of the oceanic lithosphere in the region where classical models of evolution of the oceanic lithosphere appear to be unreasonable.

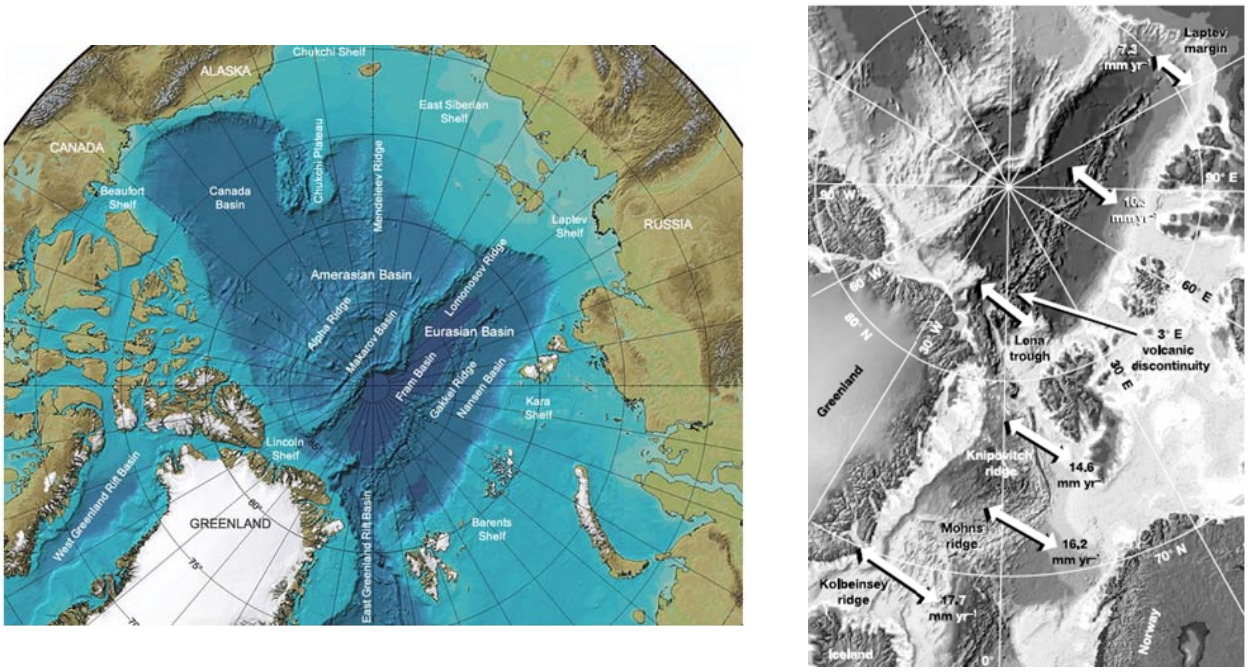

Fig. 1.: Simplified map of the area of study. North-Atlantic and Arctic transitional ridge system.

Constraining the rheology of the lithosphere through geodynamic inverse modelling

Tobias Baumann, Boris Kaus* Anton Popov

Institute of Geosciences, Center for Computational Sciences & VAMOS research center, Johannes-Gutenberg University, Mainz, Germany
**presenting author*
e-mail: *kaus@uni-mainz.de*
session: *Geodynamics*

Abstract

Understanding the physics of lithospheric deformation requires good constraints on lithospheric rheology and in particular on the effective viscosity. Typically, rheology is determined from laboratory experiments on small rock samples, which are extrapolated to geological conditions - an extrapolation over 10 orders of magnitude in deformation rates. Ideally, we thus need a new independent method that allows constraining the effective rheology of the lithosphere directly from geophysical data, which is the aim of this work.

Our method uses the fact that the geodynamically controlling parameters of lithospheric deformation are its effective viscosity and density structure. By appropriately parametrising the rheological structure of the lithosphere we perform instantaneous forward simulations of present-day lithospheric deformation scenarios with a finite element method to compute the gravity field as well as surface velocities. The forward modelling results can be compared with observations such as Bouguer anomalies and GPS-derived surface velocities. More precisely, we automatise the forward modelling procedure with a Markov-Chain Monte Carlo method, and in fact solve a joint geodynamic and gravity inverse problem. The resulting misfit can be illustrated as a function of rheological model parameters and a more detailed analysis allows constraining probabilistic parameter ranges.

Yet, the lithosphere has non-linear rheologies that can be plastic or temperature-dependent powerlaw creep depending on stresses. As the thermal structure of the lithosphere is in general poorly constrained, and only affects the dynamics of the lithosphere in an indirect manner, we developed a parameterised rheology that excludes a direct temperature dependency. To test the accuracy of this approximation we perform lithospheric-scale collision forward models that incorporate a temperature-dependent visco-plastic rheology to create synthetic surface observations. In a second step, we deploy these synthetic data sets to perform a joint inversion, using our simplified parameterized rheology. Results show that we can recover the rheology of the lithosphere reasonably well, provided that lithospheric layers contribute to the large-scale dynamics. In addition, we have applied the models to the India-Asia collision zone, and first results are consistent with the Tibetan plateau having a weak lower crust, but the Indian mantle lithosphere having large viscosities.

Acknowledgements

Funding was provided by the European Research Council under the European Community's Seventh Framework Program (FP7/2007-2013) / ERC Grant agreement #258830. Numerical computations have been performed on MOGON (ZDV Mainz computing center) and JUQUEEN (Jülich high-performance computing center).

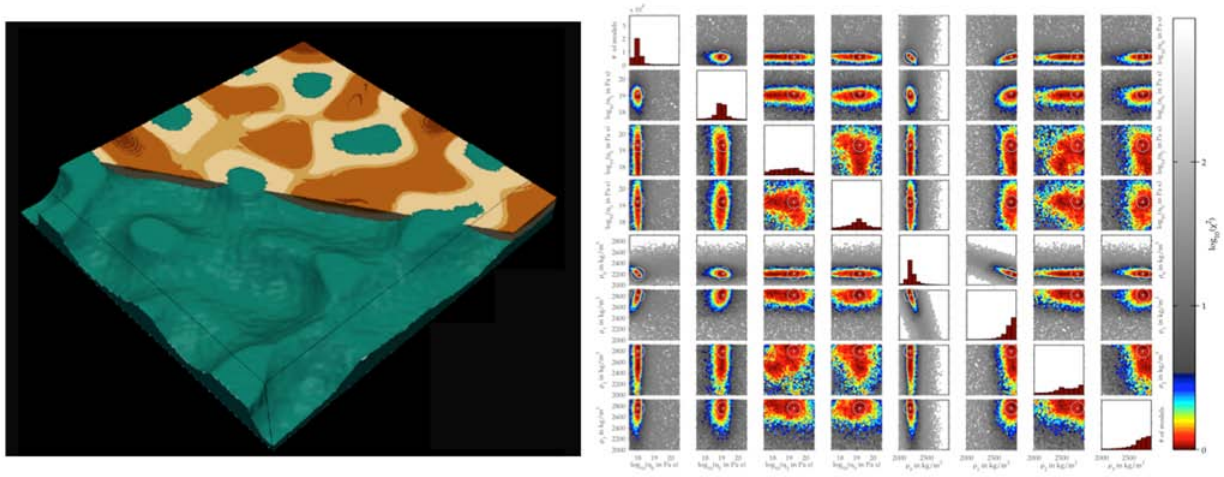

Fig. 1.: Left: 3D model of salt tectonics in the presence of sedimentation and erosion ("downbuilding"), of which we use one snapshot to define the geometry of our model. From this snapshot, we compute the gravity anomalies and the surface velocities, which forms our synthetic dataset. Right: In a next step, out inversion method runs many forward models in which density and viscosity of each of the layers is varied in an automatic fashion and the resulting model output is compared with the data which gives one misfit value per simulation (dots on these plots). Models that fit the data well have red colors. Results show that we can retrieve the true data (larger circles) very well, provided that the layers are not too thin (pictures taken from Baumann et al. 2014).

References

Baumann T., Kaus B., Popov A. (2014). Constraining effective rheology through parallel joint geodynamic inversion. Tectonophysics. DOI:10.1016/j.tecto.2014.04.037

A new model for the architecture of magma-poor rifted margins

Sascha Brune[1,2], Christian Heine[1], Marta Pérez-Gussinyé[3], Stephan V. Sobolev[2]

[1] *EarthByte Group, School of Geosciences, The University of Sydney, Australia*
[2] *Geodynamic Modelling Section, GFZ German Research Centre for Geosciences, Potsdam, Germany*
[3] *Royal Holloway College, University of London, UK*
e-mail: *sascha.brune@sydney.edu.au*
session: *Geodynamics*

Magma-poor rifted margins often exhibit highly extended continental crust with a thickness of less than 10 km. The width of these thin crustal regions varies from 70 km off Iberia (Whitmarsh et al., 2001) to 200 km in the Central South Atlantic segment (Contrucci et al., 2004). The respective conjugate margin, however, is often restricted to few tens of kilometres resulting in large scale crustal asymmetry (Hopper et al., 2004; Unternehr et al., 2010). Seismic observations as well as kinematic reconstruction of the Iberia/Newfoundland conjugates suggest that an array of ocean-ward younging sequential faults is responsible for the typical asymmetric architecture (Ranero and Perez-Gussinye, 2010). Up to now, no thermo-mechanically verified model exists that explains the existence of highly thinned crust, margin asymmetry, and sequential fault activity simultaneously.

Here, we use thermo-mechanical modelling (SLIM3D, Popov and Sobolev, 2008) to understand the spatio-temporal evolution of the Iberia/Newfoundland and the Brazil/Angola passive margins. Our finite element model involves an elasto-visco-plastic rheology formulation that allows for the self-consistent generation of faults and ductile shear zones as well as stress- and temperature-dependent viscosity. We constrain our experiments with detailed plate kinematic history of the pre-break up and early seafloor spreading phase, laboratory-based rheology, and melt fraction evaluation of mantle upwelling. Our results are consistent with observed fault patterns, crustal thickness, and basin stratigraphy.

We propose rift migration as a key process during magma-poor margin formation (for more detail, see Brune et al., 2014). Our numerical models show that steady-state rift migration is maintained by sequential faulting in the brittle crust and balanced by lower crustal flow (Fig. 1). Hence, the degree of rift migration is controlled by the lower crustal viscosity adjacent to the moving rift, whereas the viscosity of the lower crust is a function of lower crustal composition, initial thermal structure, intensity of strain softening and most importantly extension velocity. By demonstrating how rift velocity affects the final margin width, we explain the formation of highly thinned crust and the along-strike asymmetry variation of the Central South Atlantic segment (Fig. 2). The effect of initial lower crustal viscosity was most important to shape the Iberia-Newfoundland margins. Their structure is best described with an initially decoupled, moderately asymmetric fault phase that is followed by crust-mantle coupling, sequential faulting, and low degree rift migration. Rift migration may be also relevant for other highly thinned and asymmetric margin pairs such as Antarctica–India, the North-East Atlantic, the Southern South Atlantic segment and the East Australia/Lord Howe Rise conjugate.

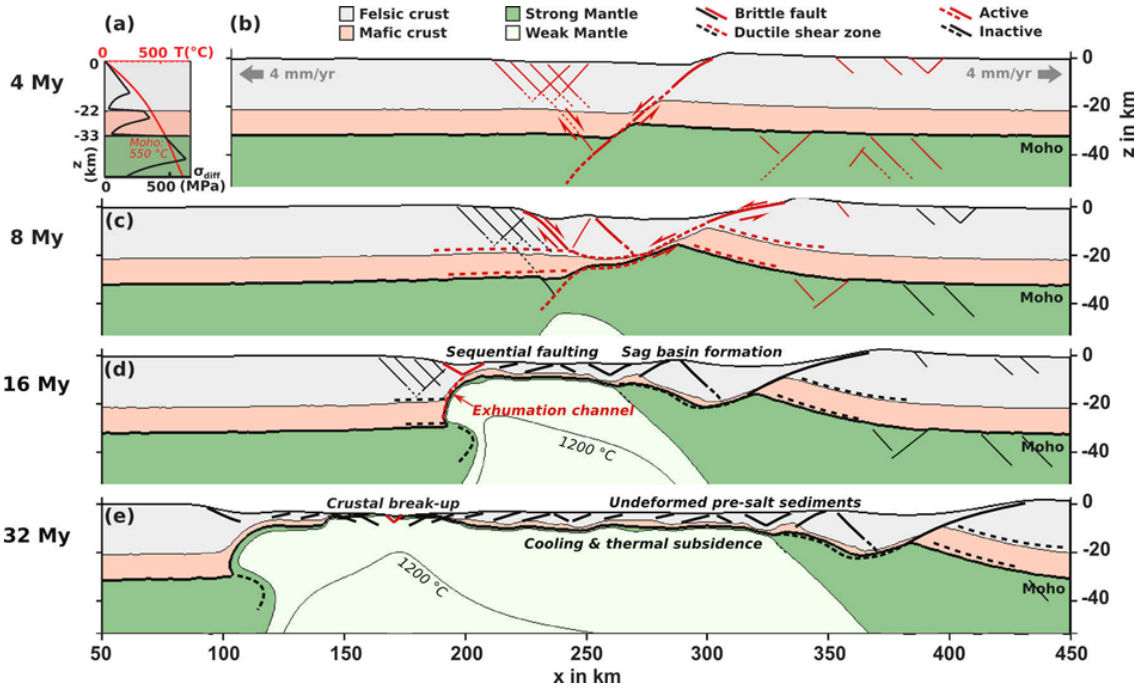

Fig. 1.: Active faults are shown in red, inactive faults in black. Brittle faults are indicated with solid lines, ductile shear zones with dashed lines. The wide margin is formed through rift migration and sequentially active faulting towards the future ocean. Hence, undisturbed pre-salt sediments pre-dating breakup are predicted by our model to be deposited in the landward part of the margin.

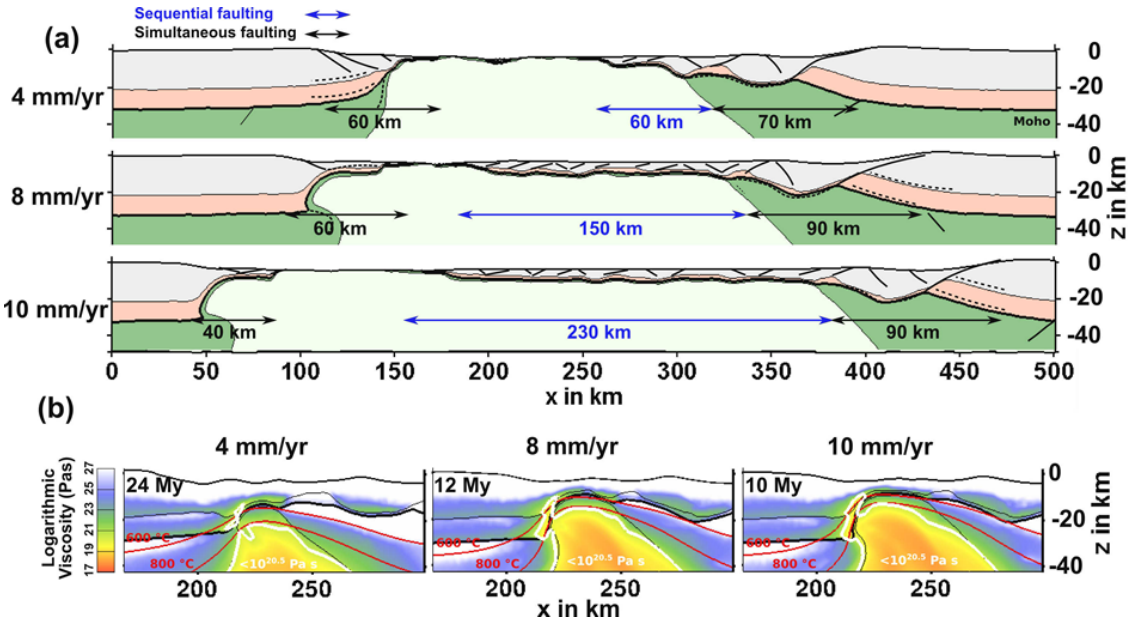

Fig. 2.: **(a)** Conjugate margin structure for 4, 8, and $10\,\mathrm{mm/a}$ full rift velocities. The width of simultaneously faulted areas is indicated by black arrows, while sequentially faulted domains are depicted by blue arrows. The width of the wide margin increases with rift velocity. The reason for this behaviour is shown in **(b)**: Higher velocities lead to advection of the isotherms to shallower depths. This heats the lower crust more efficiently forming a weaker and larger exhumation channel (see white iso-viscosity line that cuts into the lower crust).

References

Brune, S., Heine, C., Perez-Gussinye, M., Sobolev, S.V., 2014. Rift migration explains continental margin asymmetry and crustal hyperextension. Nature Communications (in press.) doi:10.1038/ncomms5014

Contrucci, I., Matias, L., Moulin, M., Geli, L., Klingelhofer, F., Nouze, H., Aslanian, D., Olivet, J.L., Rehault, J.P., Sibuet, J.C., 2004. Deep structure of the West African continental margin (Congo, Zaire, Angola), between 5 degrees S and 8 degrees S, from reflection/refraction seismics and gravity data. Geophys. J. Int. 158, 529–553.

Hopper, J.R., Funck, T., Tucholke, B.E., Larsen, H.C., Holbrook, W.S., Louden, K.E., Shillington, D., Lau, H., 2004. Continental breakup and the onset of ultraslow seafloor spreading off Flemish Cap on the Newfoundland rifted margin. Geology 32, 93–96. doi:10.1130/G19694.1

Popov, A.A., Sobolev, S.V., 2008. SLIM3D: A tool for three-dimensional thermo mechanical modeling of lithospheric deformation with elasto-visco-plastic rheology. Phys. Earth Planet. Inter. 171, 55–75. doi:10.1016/j.pepi.2008.03.007

Ranero, C.R., Perez-Gussinye, M., 2010. Sequential faulting explains the asymmetry and extension discrepancy of conjugate margins. Nature 468, 294–299. doi:10.1038/nature09520

Unternehr, P., Peron-Pinvidic, G., Manatschal, G., Sutra, E., 2010. Hyper-extended crust in the South Atlantic: in search of a model. Pet. Geosci. 16, 207–215. doi:10.1144/1354-079309-904

Whitmarsh, R.B., Manatschal, G., Minshull, T.A., 2001. Evolution of magma-poor continental margins from rifting to seafloor spreading. Nature 413, 150–154. doi:10.1038/35093085

Oblique extensional structures from initial deformation to breakup: Insights from numerical 3D lithospheric-scale experiments

Sascha Brune

EarthByte Group, School of Geosciences, The University of Sydney, Australia
Geodynamic Modelling Section, GFZ German Research Centre for Geosciences, Potsdam, Germany
e-mail: *sascha.brune@sydney.edu.au*
session: *Geodynamics*

Oblique extension takes place when the relative velocity of two diverging plates is at an angle to the zone of deformation. Brittle deformation is accommodated by complex normal fault systems that are controlled by reactivation of pre-rift structures, extension direction, erosion, sedimentation, melting and dyke dynamics. The relative impact of these processes on the observed fault pattern, however, is difficult to deduce from field-based studies alone. This study provides insight in crustal stress patterns and fault orientations by employing a laterally homogeneous, 3D rift setup with constant extension velocity and direction (Fig. 1). While previous analogue models elucidated the fault patterns of initial rift phases, the entire rift evolution from the beginning of extension to breakup has not be addressed so far. In order to validate the model, I explicitly compare its results to a set of analogue experiments that have been conducted on crustal scale (Clifton et al., 2000) and lithospheric scale (Agostini et al., 2009). Despite the simplicity of the setup, the presented rift models feature a large variety of fault orientations that are solely due to the three-dimensionality of oblique rift systems.

The presented numerical models cover all possible rift obliquities (i. e. rift-orthogonal extension, low obliquity, high obliquity, strike-slip deformation) by extending a previous study that focused on the moderately oblique Gulf of Aden Rift (Brune and Autin, 2013). Hence, model results are applicable to diverse oblique rifts that existed in the past or are active at present day, such as the presently active Main Ethiopian Rift (Corti, 2008), the Gulf of California Rift (Bennett and Oskin, 2014) the Equatorial Atlantic Rift (Heine and Brune, 2014), and the Antarctica/Australia Rift (Whittaker et al., 2007). Moreover, the model yields insight in oblique mid ocean ridges like the Reykjanes and Mohns Ridge (Dauteuil and Brun, 1993) and the South West Indian Ridge (Montési et al., 2011).

Rift evolution is computed using the finite element model SLIM3D that features realistic, elasto-visco-plastic rheology and a free surface. The modelled lithospheric segment involves crustal and mantle layers accounting for self-consistent necking of the lithosphere. Along-strike model sides use a periodic boundary condition that mimics an infinitely long rift zone. Despite recent advances, 3D numerical experiments still require relatively coarse resolution so that individual faults are poorly resolved. This issue is addressed by employing a simple post-processing method that uses the surface stress-tensor to evaluate stress regime (extensional, strike-slip, compressional) and preferred fault azimuth (Brune and Autin, 2013). The described method is applicable to any geodynamic model and easy to introduce.

The evolution of a moderately oblique rift system is illustrated in Fig. 2. Initial small-scale faults strike with an azimuth that exactly in the middle between the rift-parallel and the extension

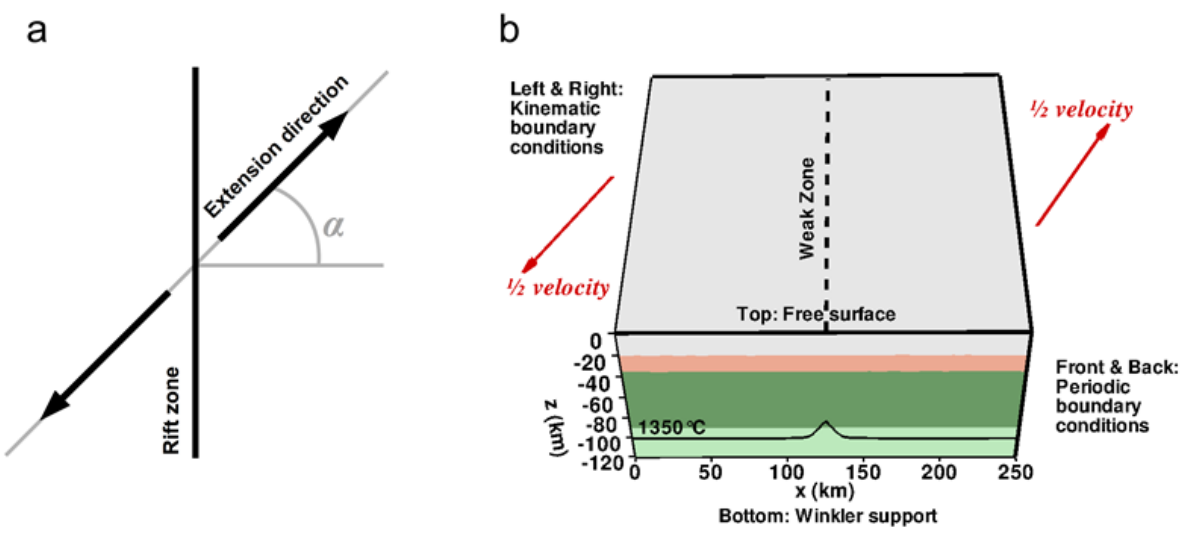

Fig. 1.: (a) Fundamental geometry of oblique extension. The angle of obliquity α is defined as the angular difference between extension velocity and rift normal. **(b)** The numerical model setup involves four layers: felsic crust (grey), mafic crust (red), strong mantle (olive), and weak mantle (light green). Extensional velocities are prescribed at the boundaries in x-direction.

orthogonal direction. This agrees with previous analogue experiments and theoretical considerations (Withjack and Jamison, 1986). The small-scale faults coalesce into an en-échelon system at 6 My. The phase of en-échelon deformation is accompanied with smoothly varying fault orientations that exceed the rift-parallel azimuth of 0° (Fig. 2c). At 11 My, pronounced rift-parallel faults emerge adjacent to the rift centre. This takes place at the end of the en-échelon deformation when strong lithospheric necking occurs below the central part of the rift. Simultaneously, a thin, strike-slip dominated area emerges in the rift centre indicating strain-partitioning. The latest stages of rifting show intermediate fault orientations while additional extension-orthogonal fault azimuths emerge during breakup.

While fault directions are often used to infer palaeo plate movements, this study shows that local changes in crustal stress field and fault orientation may arise intrinsically during rift maturation and may not require plate motion changes. These changes follow a characteristic temporal pattern that is linked to the maturity of the rift system. In natural rift systems this pattern might be modified by additional heterogeneities, erosion, sedimentation, melting and dyke dynamics.

References

Agostini, A., Corti, G., Zeoli, A., Mulugeta, G., 2009. Evolution, pattern, and partitioning of deformation during oblique continental rifting: Inferences from lithospheric-scale centrifuge models. Geochem. Geophys. Geosystems 10, Q11015. doi:10.1029/2009GC002676

Bennett, S.E.K., Oskin, M.E., 2014. Oblique rifting ruptures continents: Example from the Gulf of California shear zone. Geology G34904.1. doi:10.1130/G34904.1

Brune, S., Autin, J., 2013. The rift to break-up evolution of the Gulf of Aden: Insights from 3D numerical lithospheric-scale modelling. Tectonophysics 607, 65–79. doi:10.1016/j.tecto.2013.06.029

Clifton, A.E., Schlische, R.W., Withjack, M.O., Ackermann, R.V., 2000. Influence of rift obliquity on fault-population systematics: results of experimental clay models. J. Struct.

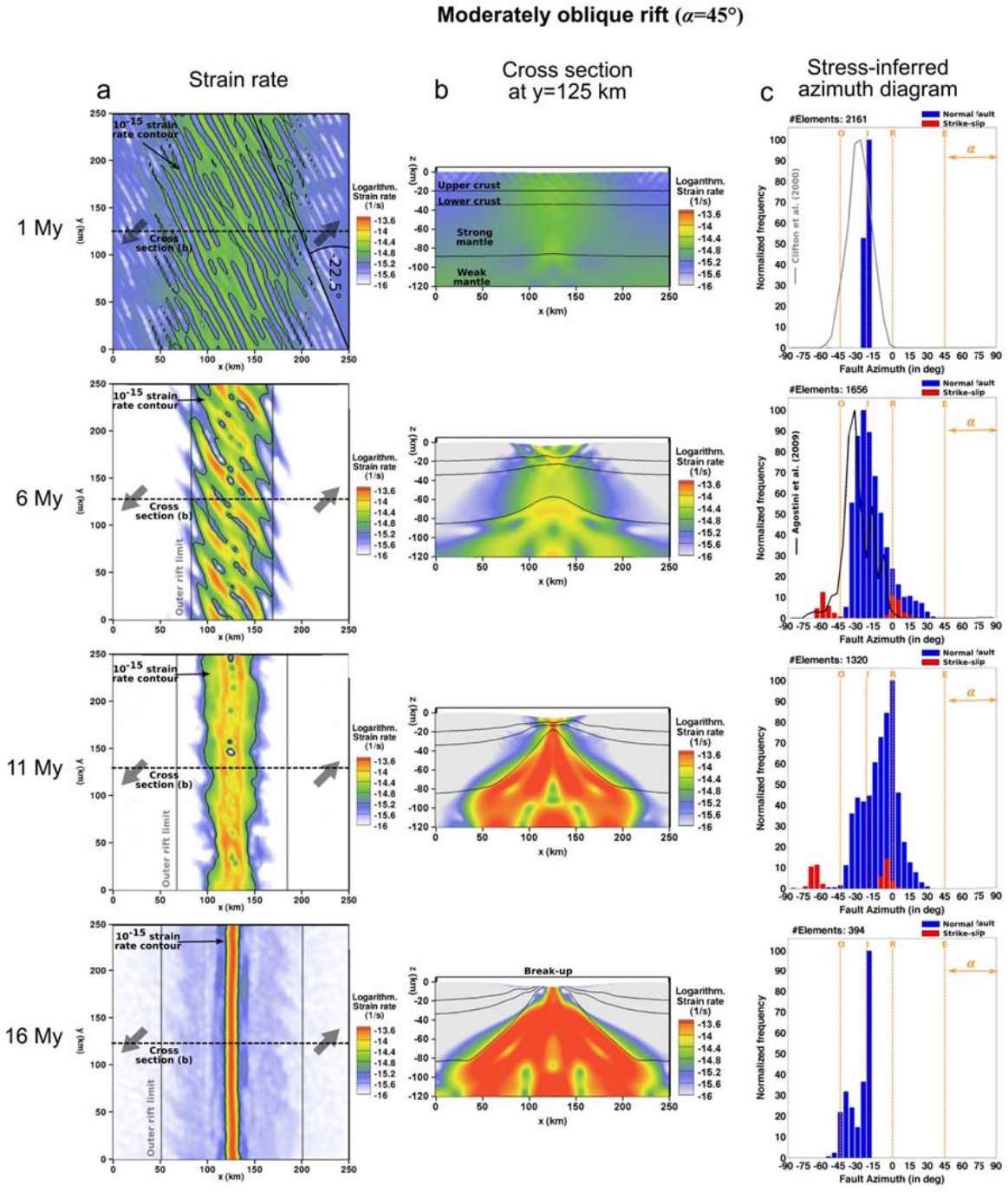

Fig. 2.: (a) The surface strain rate at 1 My shows small-scale shear zones that correspond excellent to the theoretically derived value ($-22.5°$, Withjack and Jamison, 1986). Further evolution involves rotating sigmoidal shear zones and basin-ward localization until crustal break-up is achieved. **(b)** Cross sections show the degree of lithospheric necking. **(c)** Azimuth diagram depicting the characteristic evolution of stress-inferred fault directions at the model surface. Abbreviated directions indicate the rift-parallel azimuth (R), intermediate fault orientation (I), extension-orthogonal direction (O), and the direction of extension (E). For comparison, fault distributions of analogue experiments by Clifton et al. (2000) and Agostini et al. (2009) are plotted at 1 My, and 6 My, respectively.

Geol. 22, 1491–1509. doi:10.1016/S0191-8141(00)00043-2

Corti, G., 2008. Control of rift obliquity on the evolution and segmentation of the main Ethiopian rift. Nat. Geosci. 1, 258–262. doi:10.1038/ngeo160

Dauteuil, O., Brun, J.P., 1993. Oblique Rifting in a Slow-Spreading Ridge. Nature 361, 145–148. doi:doi:10.1038/361145a0

Heine, C., Brune, S., 2014. Oblique rifting of the Equatorial Atlantic: Why there is no Saharan Atlantic Ocean. Geology 42(3), 211–214. doi:10.1130/G35082.1

Montési, L.G.J., Behn, M.D., Hebert, L.B., Lin, J., Barry, J.L., 2011. Controls on melt migration and extraction at the ultraslow Southwest Indian Ridge 10°–16°E. J. Geophys. Res. Solid Earth 116, B10102. doi:10.1029/2011JB008259

Whittaker, J.M., Müller, R.D., Leitchenkov, G., Stagg, H., Sdrolias, M., Gaina, C., Goncharov, A., 2007. Major Australian-Antarctic Plate Reorganization at Hawaiian-Emperor Bend Time. Science 318, 83 –86. doi:10.1126/science.1143769

Withjack, M.O., Jamison, W.R., 1986. Deformation produced by oblique rifting. Tectonophysics 126, 99–124. doi:10.1016/0040-1951(86)90222-2

Initial models of the influence of collision-phase inheritance on continental rifting

Susanne Buiter[1,2], Joya Tetreault[1], Reza Khabbaz Ghazian[3,1]

[1] *Geological Survey of Norway, Trondheim, Norway*
[2] *The Centre for Earth Evolution and Dynamics, University of Oslo, Norway*
[3] *Statoil ASA, Oslo, Norway*
e-mail: *susanne.buiter@ngu.no*
session: *Geodynamics*

Numerical experiments of continental rifting often start from laterally homogeneous crustal layers with an inserted prescribed inhomogeneity to trigger deformation. Some examples of the prescribed inhomogeneity are a thermal anomaly, a variation in Moho geometry, or an inherited weak region. This approach has the advantage of controlling the location of rifting and keeping the rift buffered from boundary effects of the model domain. Yet a review of present-day passive margins quickly reveals that most passive margins are built on former collision zones. This is perhaps not surprising as continents are long-lived and therefore have undergone several deformation phases, increasing the likelihood of a rift forming at or near a suture. But collision zones can also act as intrinsic rift-localizers for several reasons: rifting at a suture may be initiated by extensional collapse of the mountain chain, the thicker crustal root of orogens and their associated increase in heat producing elements makes orogens thermally weak, and inherited thrust faults form large-scale heterogeneities.

Here we use 2-D numerical experiments to explore the role of inherited crustal structures on continental rifting and passive margin formation by actually making inherited collision zones. We first examine a series of experiments in which we explicitly prescribe collisional structures, such as increased Moho depth and inherited thrust zones. Differences in extension duration (the time from rift initiation to break-up) and crustal shear zone patterns result from varying the prescribed collisional structures. Overall the experiments have relatively fast break-up and develop short crustal tapers. Our second series of experiments builds a Wilson Cycle of subduction, collision, and extension. Closure of a 60 Ma ocean leads to continental collision and slab break-off, followed by some tens of kilometres of slab eduction. We use this set-up to investigate how extension localizes on a former continental collision zone. We will present first results of the roles of post-collision thermal equilibration time, lower crustal rheology, and shear zone healing on the evolution of passive margins that develop on continental collision zones.

Modelling subsidence history of rift-type basins

Mauro Cacace[1], Magdalena Scheck-Wenderoth[1,2]

[1]*Helmholtz Centre Potsdam GFZ – German Research Centre for Geosciences, Potsdam, Germany*
[2]*RWTH Aachen University, Department of Geology, Geochemistry of Petroleum and Coal, Aachen, Germany*
e-mail: *cacace@gfz-potsdam.de*
session: *Geodynamics*

This contribution aims to revaluate the character and evolution of large-scale crustal post-rift subsidence of basins that formed and evolved within extensional tectonic settings. Continental margins and intra-continental basins have been conventionally explained in terms of time-dependent thermal contraction of a thermal anomaly formed at the time of basin initiation. A common feature of models based on generic principles is to predict a post-rift subsidence component decaying exponentially in time with a rate controlled by the thermal diffusivity of the mantle lithosphere only. It has being now recognized that additional thermal and mechanical processes may modify (retarding, reducing or enhancing) the overall thermal subsidence pattern. However, their impact on the resulting 3D basin evolution is still to be quantified yet. Such processes comprise regional compensation to time varying sediment loading and internal thermal stresses, non–linear lithosphere thickening due to coupling between 3D conductive mantle cooling and thermal blanketing by low conductive sediments, and accelerated subsidence in response to vertical advection of the mantle lithosphere in response of mechanical loading by sediments and eustatic sea level changes. Conventional models which are based on first-order principles and which do not consider these "low-order" thermo-mechanical interactions are likely to result inadequate to explain the subsidence history as observed in many of the world's continental margin and intra-continental sedimentary basins.

The aim of this contribution is to analyze quantitatively the post-rift evolution of basins formed under extensional tectonics by means of 3D numerical modelling taking into account the dynamic coupling between sedimentation, lithospheric flexure and thermal contraction on the distribution, both in time and space, of the basin subsidence. We present and describe a quantitative tool to assist studies on the evolution of rift-type basins by means of a 3D thermo-mechanical program to model sedimentary basins evolution comprising: (1) uniform or non-uniform lithospheric stretching and related initial subsidence; (2) time-varying thermal evolution and associated subsidence/uplift component; (3) time-dependent loading distributions (sedimentation and sea level changes) and resulting vertical deformation; and (4) thermal effects on the mechanical structure of the lithosphere in terms of EET variations both in time and space by means of different rheologies. Versatility of the program stems from its modular structure that enables to address a variety of lithospheric processes and to account for the coupling among those, see Figure 1.

Efforts have been made to integrate into a unified modelling platform up-to-date concepts of the thermo-mechanical behaviour of the lithosphere in response to internal and external forcing. Active sediment deposition is considered to occur in time in the overlying basin domain. The thermal state and evolution of the forming basin is fully coupled with the evolving thermal configuration of the deeper crustal and mantle lithosphere. The thermal evolution of the system is governed by 3D conduction considering the effects of thermal

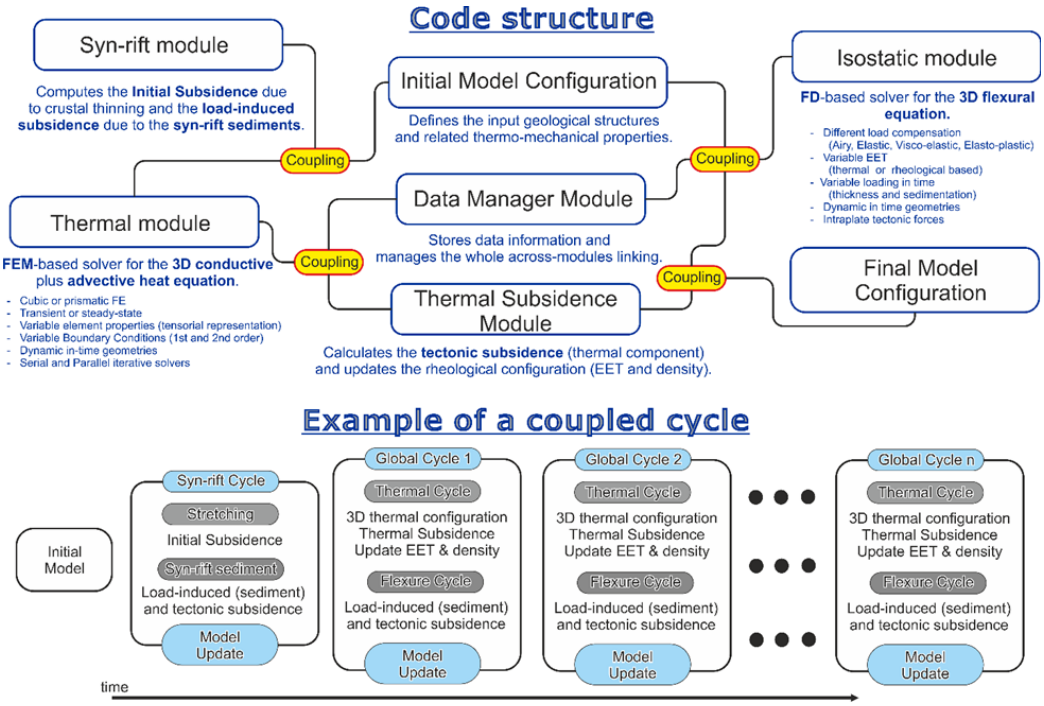

Fig. 1.: (Upper Figure) Schematic representation of the code structure illustrating the different modular components and combinations of across-modules coupling available. (Lower Figure) Example of a coupled cycle to model the subsidence evolution of a rift-type basin.

cooling as well as sediment loading and/or sea level changes. The lithosphere-asthenosphere boundary (LAB) is modelled as a thermal boundary whose location and geometry change in time in response to the computed thermal evolution. Lithospheric deformation occurs due to mechanical loading (sedimentation and sea-level changes) as well as time-dependent thermal stresses (bending moment and intraplate forces) due to a varying thermal configuration.

Applicability of the program to complex geological systems is ensured by accounting for variations through time and space of all rock properties, whether thermal or mechanical, as well as loading functions, sedimentation, thermal and intraplate stresses. Functional dependency of rock thermal properties on computed state variables (pressure and temperature) are considered. In this regard, the program enables not only to model the temporal evolution of a basin in a self-consistent way based and depending on the physics implemented, but it also offers enough flexibility to incorporate detailed information of the sedimentary succession and of the deeper crustal and mantle configuration as preserved at present. Therefore, data-based 3D lithosphere-scale geological model can be used to derive input parameters (lithosphere geometry and sediments thickness), while backward in time backstripping of these models can assist the forward modelling efforts by providing constraints on the configuration of the basin at the time of its initiation. The main advantages are (1) to determine how the rifting processes producing a 3D spatially variable stretching of the lithosphere, including syn-rift sediment deposition, might impact the post-rift evolution of the basin and the associated accumulation space for the sedimentary systems; and (2) to quantify the impact of the flexural behaviour of the lithosphere in response to both the post-rift thermal evolution (i. e. lithosphere cooling) and sedimentation history (i. e. gradual loading) on the post-break up vertical movement.

Strain localization during compression of a laterally heterogeneous lithosphere

Elisa Calignano[1], Dimitrios Sokoutis[1,2], Ernst Willingshofer[1]

[1]*Faculty of Geosciences, Department of Earth Sciences, Utrecht University, Budapestlaan 4, PO Box 80021, 3508 TA Utrecht, The Netherlands*
[2]*Department of Geosciences, University of Oslo, PO Box 1047 Blindern, N-0316 Oslo, Norway*
e-mail: *E.Calignano@uu.nl*
session: *Geodynamics*

Introduction

First order large scale stress fields, associated with active plate tectonic processes, interact with lateral heterogeneities in the lithosphere and generate strain redistribution [Zoback, 1992].

Continental lithosphere exhibits lateral variation in its mechanical properties, as evidenced from observations and supported by mechanical models [Audet and Bürgmann, 2011; Burov, 2011; Ranalli, 1997; Tesauro et al., 2012]. Lateral variation of strength in the lithosphere has been proven to be an important factor controlling the localization of deformation and far-field strain transmission [Sokoutis et al., 2005; Tommasi and Vauchez, 1997; Willingshofer et al., 2005; Ziegler et al., 1998]. Numerous modelling studies investigated the localization of deformation in compressional settings in case of lithospheric weak zones flanked by stronger domains. Such models have been successfully applied to examples of rift inversion [Brun and Nalpas, 1996; Cerca et al., 2004] or compression of weak orogenic wedges at plate boundaries [Willingshofer et al., 2005].

In this contribution, we focus on the strain redistribution resulting from the presence of a stronger rheological heterogeneity embedded in a weak lithosphere. To this purpose we use lithospheric scale analogue models. The experiments have been grouped in two sub-series characterized by different investigated parameters. First we investigated the role of varying convergence velocity and thickness of the upper brittle mantle when a strong lithospheric domain strikes perpendicular to the convergence direction. Both these parameters play an important role in the crust-mantle coupling. Subsequently we kept these two parameters constant and we varied the orientation of the rheological boundaries with respect to the convergence direction. In fact, reactivated lithosphere heterogeneities are often observed to strike oblique with respect to the main horizontal stress field.

Experimental set-up and modelling procedure

Figure 1 illustrates the set-up and different geometrical configurations for the presented experiments. Strength envelopes are representative for the very initial stage of deformation. All experiments consisted of three domains with different mechanical properties: two external blocks shared the same lithospheric stratification (reference lithosphere) and one central block where the increase in strength with respect to the reference lithosphere was achieved by increasing the brittle/ductile ratio in the crust.

The reference model lithosphere was defined by a four layers rheological stratification (brittle upper crust/ductile lower crust/brittle upper mantle/ductile upper mantle) representative for a stabilized lithosphere, characteristic for regions with low geothermal gradient [Afonso and Ranalli,

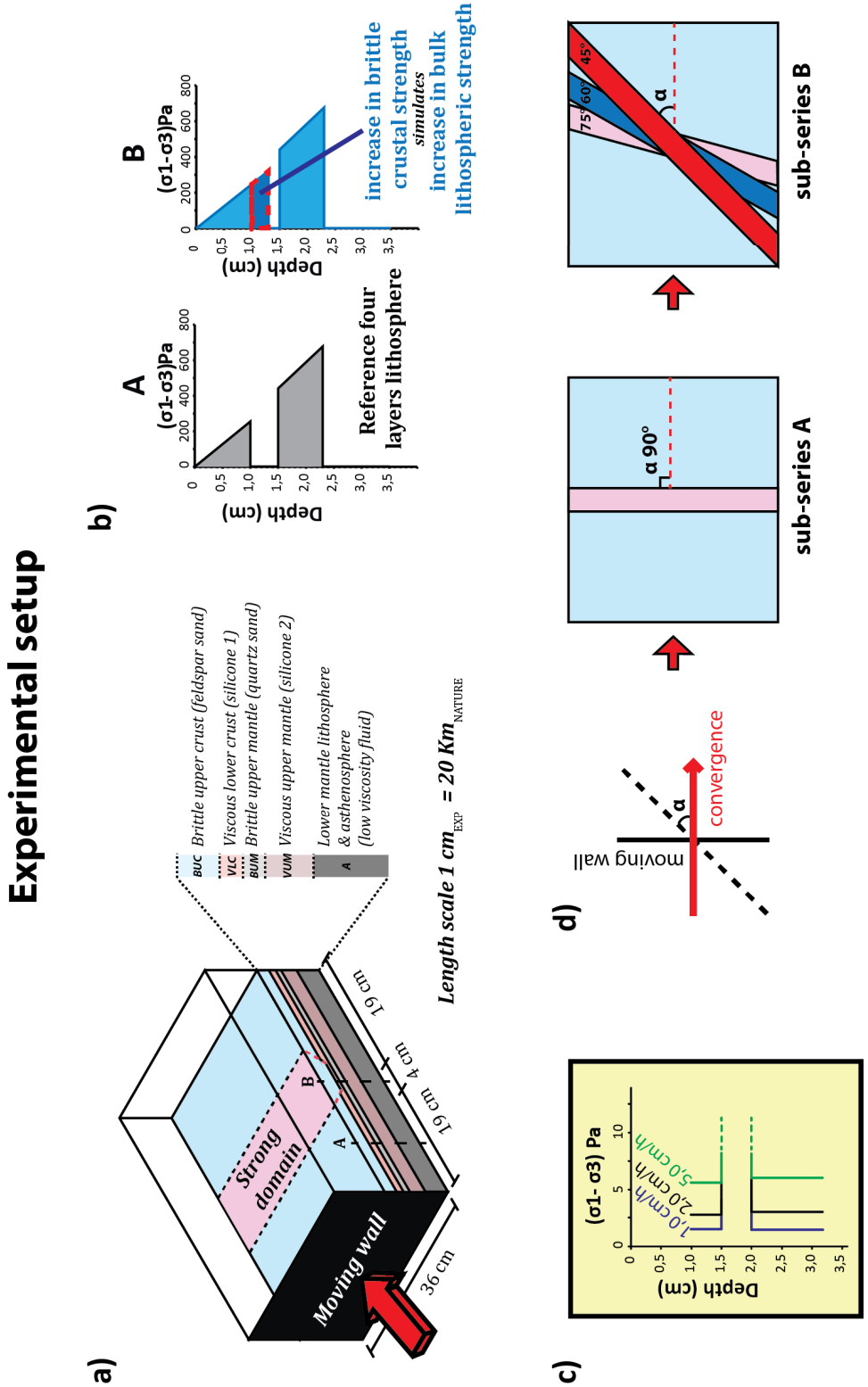

Fig. 1.: a) Sketch of the experimental set-up; **b)** representative strength profiles calculated for a convergence velocity of 1 cm/h; **c)** effect of different convergence velocities on the strength on the ductile layers and crust-mantle coupling; **d)** top view of the experiments: in sub-series A the strong domain has been kept parallel to the moving wall, while in sub-series B different obliquity angle have been tested.

2004] (Figure 1a).

The brittle crust and brittle upper mantle were simulated with dry feldspar and quartz sand respectively, while the lower crust and ductile lithospheric mantle were represented with silicone mixtures characterized by viscous non-Newtonian behaviour. The model lithosphere was resting on a high density and low viscosity fluid mixture representing the lower lithospheric mantle and asthenosphere. This facilitated the isostatic compensation. The density of the lithospheric mantle was lower than the asthenospheric fluid in all experiments, so that subduction was impeded.

The models were built inside a transparent Plexiglas box with dimensions 36 cm x 42 cm x 15 cm equipped with an internal moving wall. Experiments have been performed in normal gravity field. Deformation was monitored during the experiments with top view pictures and laser scanning at regular time intervals. At the end of each experiment the model was cut in cross sections parallel to the convergence direction in order to visualize the internal deformation at the latest experimental stage.

Preliminary Results

Experimental outcomes confirmed the role of lateral strength contrast in the lithosphere as an important factor controlling strain redistribution in compressional settings (Figure 2, 3).

In presence of a strong domain oriented perpendicular to the convergence direction deformation always localized along the rheological boundaries (Figure 2). Strain rate governed the geometry of the deep lithospheric structure. High convergence velocity resulted in asymmetry of the lithospheric root and main transport direction towards the moving wall (Experiment 1). A more symmetric deep lithospheric root characterized experiments with low convergence velocity (Experiment 2).

Brittle/ductile ratio in the lithospheric mantle determined the absence (low B/D) or presence (high B/D) of faults in the upper brittle mantle and the width of the area affected by upper crustal faults. Distributed deformation in the upper brittle crust characterized Experiment 3 where the increased brittle mantle thickness enhanced the decoupling along the ductile lower crust (Figure 2).

When the strong domain was oblique to the convergence direction, deformation resulted only partially localized along the rheological boundaries, due to the along-strike increase in distance from the moving wall (Figure 3 b). Two main thrust systems with different transport direction developed, connected by a complex transition zone (Figure 3 b).

The presented modelling results provide valuable insight for the strain localization in intraplate settings under various rheological and geometrical configurations and are applicable to natural areas.

References

Afonso, J. C., and G. Ranalli (2004), Crustal and mantle strengths in continental lithosphere: is the jelly sandwich model obsolete?, Tectonophysics, 394, 221–232, doi:10.1016/j.tecto.2004.08.006.

Audet, P., and R. Bürgmann (2011), Dominant role of tectonic inheritance in supercontinent cycles, Nat. Geosci., 4, 184–187, doi:10.1038/ngeo1080.

Brun, J.-P., and T. Nalpas (1996), Graben inversion in nature and experiments, Tectonics, 15, 677–687, doi:10.1029/95TC03853.

Burov, E. B. (2011), Rheology and strength of the lithosphere, Mar. Pet. Geol., 28, 1402–1443, doi:10.1016/j.marpetgeo.2011.05.008.

Cerca, M., L. Ferrari, M. Bonini, G. Corti, and P. Manetti (2004), The role of crustal heterogeneity in controlling vertical coupling during Laramide shortening and the development of the Caribbean-North America transform boundary in southern Mexico: insights from analogue models, Geol. Soc. Lond. Spec. Publ., 227, 117–139, doi:10.1144/GSL.SP.2004.227.01.07.

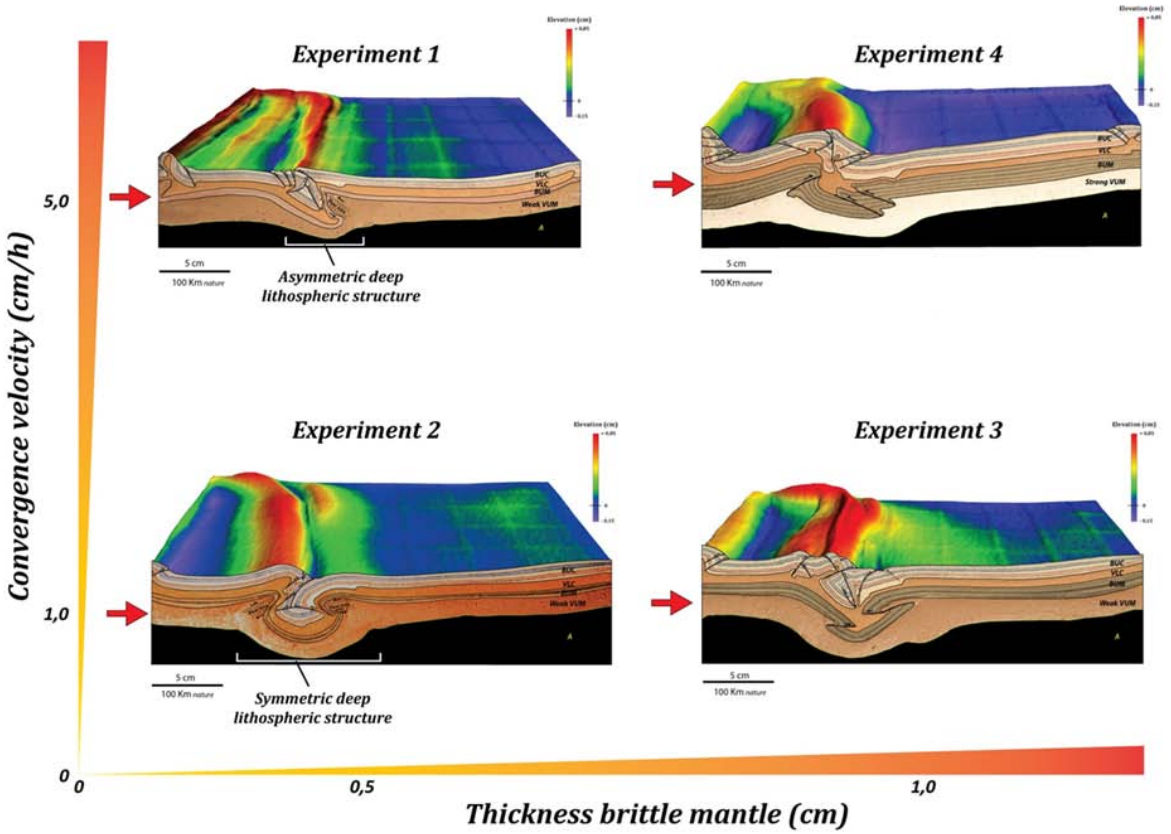

Fig. 2.: Experimental results for sub-series A. Representative cross sections and DEM (Digital Elevation Models) of the experiments' surface at 20 % bulk shortening for different convergence velocities and thickness of the brittle upper mantle.

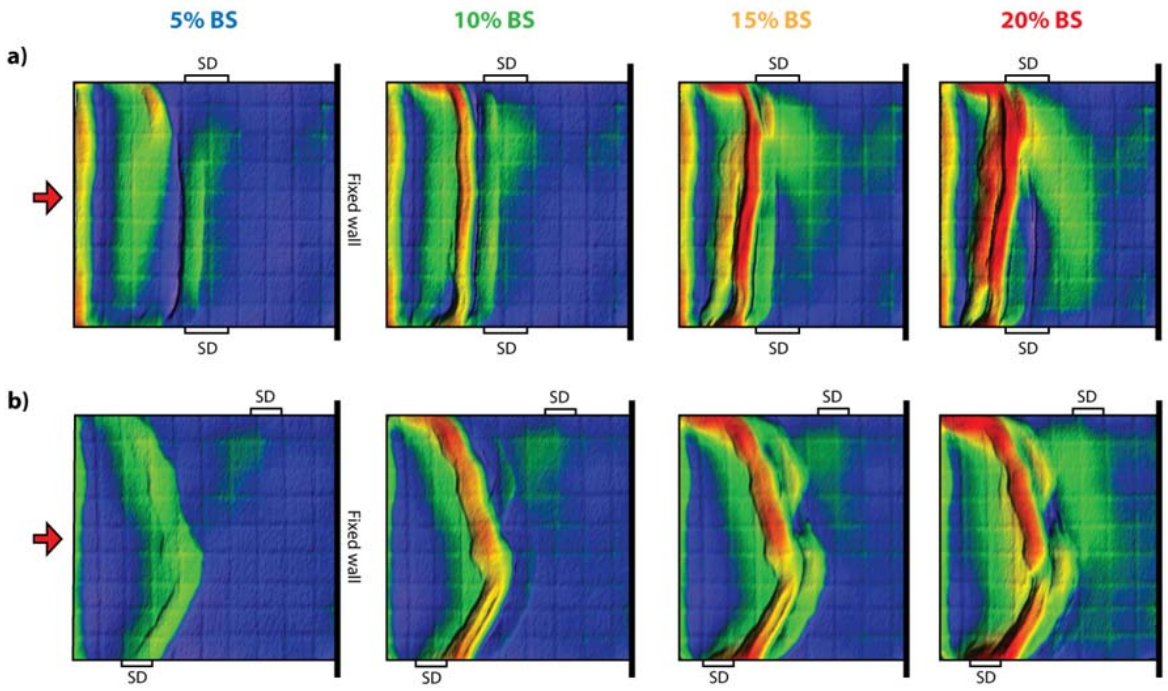

Fig. 3.: Comparison of experiments with different orientation of the strong domain. The evolution at subsequent bulk shortening (% BS) steps is shown with the help of DEMs. **a)** Experiment 3 (sub-series A): the strong domain (SD) strikes perpendicular to the convergence direction; **b)** Experiment 5 (sub-series B): the strong domain (SD) strikes at 60° to the convergence direction. Convergence velocity is $1\,\mathrm{cm\,h^{-1}}$ for both experiments.

Ranalli, G. (1997), Rheology of the lithosphere in space and time, Geol. Soc. Lond. Spec. Publ., 121, 19–37, doi:10.1144/GSL.SP.1997.121.01.02.

Sokoutis, D., J.-P. Burg, M. Bonini, G. Corti, and S. Cloetingh (2005), Lithospheric-scale structures from the perspective of analogue continental collision, Tectonophysics, 406, 1–15, doi:10.1016/j.tecto.2005.05.025.

Tesauro, M., M. K. Kaban, and S. A. P. L. Cloetingh (2012), Global strength and elastic thickness of the lithosphere, Glob. Planet. Change, 90–91, 51–57, doi:10.1016/j.gloplacha.2011.12.003.

Tommasi, A., and A. Vauchez (1997), Continental-scale rheological heterogeneities and complex intraplate tectono-metamorphic patterns: insights from a case-study and numerical models, Tectonophysics, 279, 327–350, doi:10.1016/S0040-1951(97)00117-0.

Willingshofer, E., D. Sokoutis, and J.-P. Burg (2005), Lithospheric-scale analogue modelling of collision zones with a pre-existing weak zone, Geol. Soc. Lond. Spec. Publ., 243, 277–294, doi:10.1144/GSL.SP.2005.243.01.18.

Ziegler, P. A., J.-D. van Wees, and S. Cloetingh (1998), Mechanical controls on collision-related compressional intraplate deformation, Tectonophysics, 300, 103–129, doi:10.1016/S0040-1951(98)00236-4.

Zoback, M. L. (1992), First- and second-order patterns of stress in the lithosphere: The World Stress Map Project, J. Geophys. Res. Solid Earth, 97, 11703–11728, doi:10.1029/92JB00132.

3-D numerical modeling of subduction evolution of the western Mediterranean region

M. V. Chertova[1], W. Spakman[1,2], A.P. van den Berg[1], T. Geenen[3], D.J.J. van Hinsbergen[1]

[1] *University of Utrecht, Utrecht, the Netherlands*
[2] *Centre of Earth Evolution and Dynamics (CEED), University of Oslo, 0316 Oslo, Norway*
[3] *SURFsara, Amsterdam, the Netherlands*
e-mail: *M.V.Chertova@uu.nl*
session: *Geodynamics*

This research is focused on various aspects of the evolution of the western Mediterranean region. This region underwent a long and complicated history of slab rollback and lithosphere tearing, for which the only direct observations come from its geological history and present day mantle structure inferred by tomographic data. Different tectonic reconstructions were proposed for this region based on these observations. Despite the general agreement on the initiation of subduction rollback around 35Ma and slab buoyancy being a major driving force leading to the present day slab under the Rif-Gibraltar-Betic (RGB) these reconstructions propose distinctly different initial configuration of the subduction zone, as well as temporal evolution of the region during 35 Ma to 0 Ma. We categorize all tectonic reconstructions into three different evolution scenarios and based on this in the first part of the research we investigated the evolution of the region employing 3D thermo-mechanical numerical modeling. The criteria to discriminate between these reconstructions are fits between observed and predicted slab and major subduction evolution temporal constraints, which are Mid-Miocene (16 Ma) thrusting of the Kabylides onto the African margin and a stalled subduction under the RGB arc since the Tortonian (~8 Ma).

The first scenario (S 1) proposes that subduction rollback started from a 300 km long trench to the southeast from Baleares. Initially rollback occurred southward with a rotation to westward, but changed its direction to westward after reaching the African margin (e. g. Rosenbaum et al. 2002; Spakman and Wortel 2004; van Hinsbergen et al. 2014). In the second scenario (S 2) a long trench from Gibraltar to Baleares is assumed with predominantly southward rollback (e. g. Gueguen et al. 1998; Faccenna et al. 2004). In the last, third scenario (S 3), it is proposed that subduction has started at the African margin with predominantly northwestward rollback (Verges and Fernandez 2012).

From these scenarios we configured three different initial buoyancy conditions in terms of initial geometry of subduction zone at 35Ma and optimize developed models by fitting the major morphological and temporal constraints varying the parameters for non-linear rheology implemented in our models and the geometrical settings within a range appropriate for each reconstruction scenario.

We obtained a good match between present-day mantle structure tomography (Spakman and Wortel 2004, Bezada et al. 2013) and predicted slab morphology for subduction models based on S 1 (Fig. 2). For S 3 we could simulate the curved slab structure under Betics in top 200 km, however, the deep part of the slab extends far to the south under the Africa, which is inconsistent with tomographic constraints. For the scenario S 2 we could not find a subduction model that reasonably fits the observed mantle structure under Gibraltar (Fig. 2).

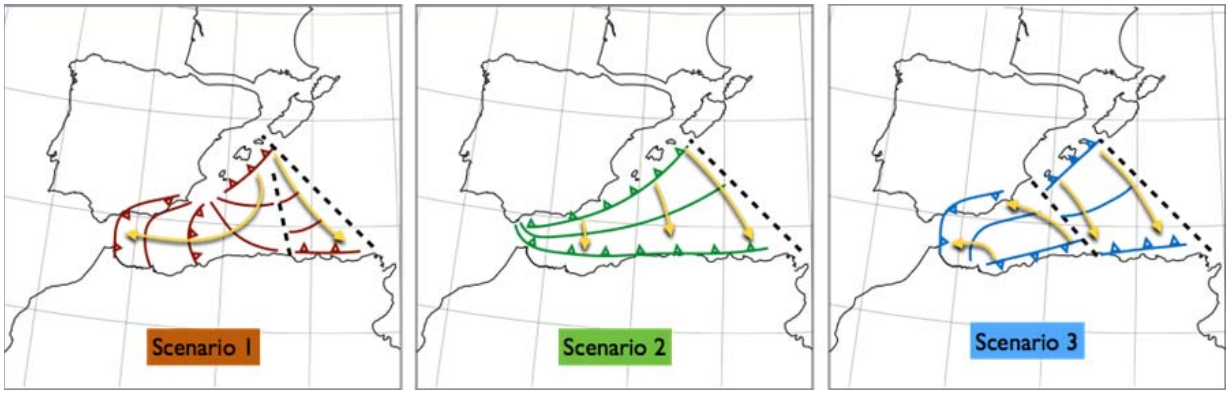

Fig. 1.: An illustration of rollback as portrayed in the three different reconstruction scenarios: scenario 1 (S 1), scenario 2 (S 2) and scenario 3 (S 3). Dashed lines represent proposed transform faults regions.

We concluded from our experiments that only models with the subduction evolution starting from a short NW-dipping subduction zone under Baleares at 35 Ma defining scenario S 1 can successfully predict trench rollback to the African margin of the RGB- and Kabylides slabs, westward tearing of the African margin and slab rotation by more than 180°, a dominant westward opening of the Algerian basin, and, finally a resulting slab under Gibraltar around 8 Ma.

This part of the research provides us with the favorable subduction framework for future investigations of the geological/tectonic evolution of the western Mediterranean region. Based on this we continued our research with investigation on the influence of absolute plate motions on the subduction evolution of this region. For a regional Earth subduction zone absolute plate motions might be an important factor controlling the subduction evolution and present-day stress field.

So far, instantaneous models of the western Mediterranean region as well as tectonic reconstructions only utilize relative plate motion reference frames with fixed Europe or Africa. However, only when considering the evolution of this region in an absolute plate motion frames for Africa and Iberia one can investigate the coupling between plate motion, mantle, and subduction. By using 3D thermo-mechanical modeling, we evaluate the impact of adopting four different absolute plate motion frames on subduction evolution of the western Mediterranean region during the last 35 Ma. The first one is determined from the global moving hotspot reference frame (GMHRF) of Doubrovine et al. (2012) and three are invented frames: a motion model with an African plate fixed to the mantle, a model with a fixed Iberian plate and a model in which Africa motion is twice that of GMHRF. We kept the same relative Africa-Iberia convergent motion in all motion frames.

The numerical experiments started from the same paleogeography, rheology and subduction settings conforming to subduction scenario S 1. The models demonstrated distinctly different 3-D subduction evolution showing a critical sensitivity of slab morphology evolution on absolute plate motions adopted. We achieved the best results in terms of fitting present day mantle structure and major temporal constraints with the model based on GMHRF (Fig. 3). The model with faster Africa demonstrated significant decrease in lithosphere tearing and associated rollback and resulted in slab stalling at the longitude of the eastern Betics. The African-fixed or Iberia-fixed reference frames led to a too early slab arrival at Gibraltar (Fig. 3). The model with Iberia fixed also resulted in a slab located to the north of the tomographically observed slab with continental lithosphere involved into subduction process during the final phase of the rollback (Fig. 3).

Our models demonstrated a strong correlation between the increase in northward Africa mo-

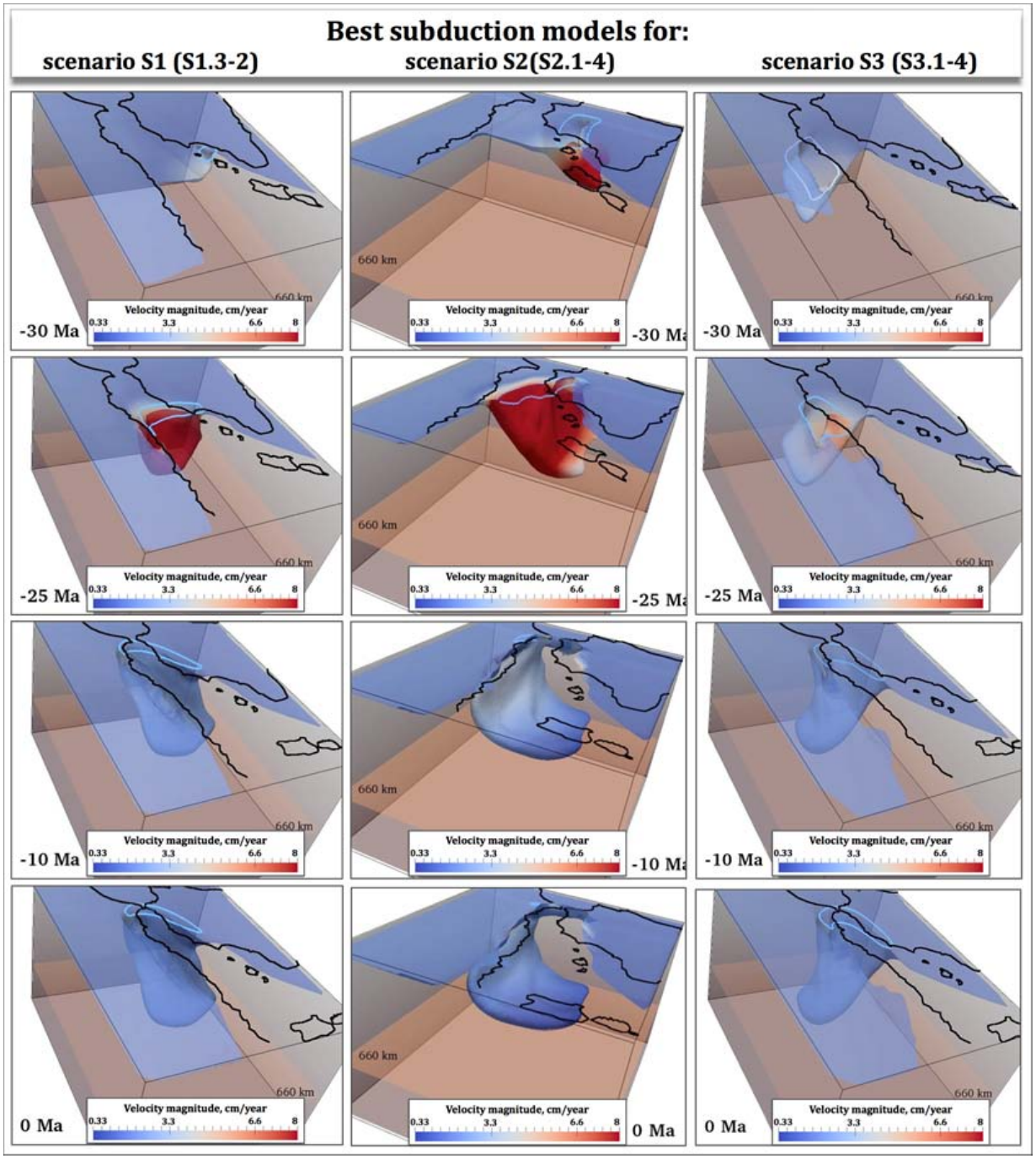

Fig. 2.: 3-D view on the evolution of the best model obtained for each reconstruction scenario. Left: model based on S 1, starting from a short trench at the Baleares margin, view from SE. Middle: model based on scenario S 2, starting from a long initial subduction zone and long slab, view from NE. Right: model based on scenario S 3, starting from a trench at the African margin, view from SE. Blue contours at the surface show the shape of the slab at depth of $200\,\mathrm{km}$.

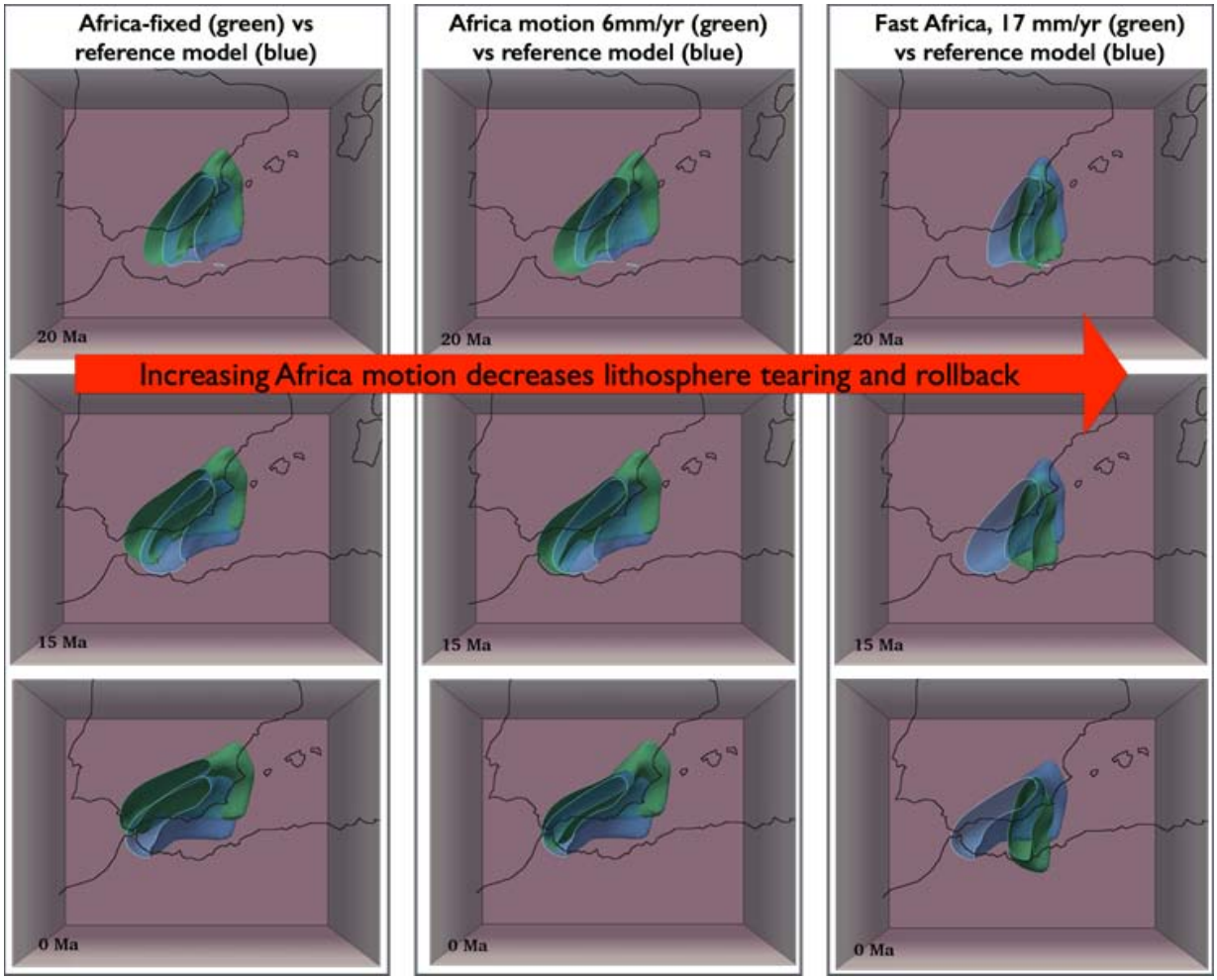

Fig. 3.: Slab morphology in the four subduction models at 20 Ma and 15 Ma. The reference model is shown in blue in all panels and belongs to a northward Africa motion of 8 mm/a. The first column shows the Africa-fixed model; the second column the Iberia-fixed model; the third column shows the model with two-times faster Africa. The 1400 K isotherm is shown from 200 km downward. The coastlines are shown in absolute plate motion frame of the reference model, i. e. GMHRF.

tion and a decrease in the speed of westward slab rollback along the African margin (Fig. 3). We relate this to an increased slab-mantle coupling and this provided new insight into propagation and dynamics of subduction transform edge propagator (STEP) faults as proposed by Govers and Wortel (2005). We conclude that absolute plate motions of the subducting and overriding plates can induce important dynamic slab-mantle couplings that may strongly affect subduction evolution. Furthermore, accurate absolute plate motion constraints are crucial for modeling subduction evolution and dynamics in natural settings and visa versa, modeling of natural subduction may provide novel constraints on absolute plate motions.

References

Bezada M.J., and E.D. Humphreys (2012), Contrasting rupture processes during the April 11, 2010 deep-focus earthquake beneath Granada, Spain, Earth and Planetary Science Letters, 353–354, 38-46, doi: 10.1016/j.epsl.2012.08.001.

Doubrovine, P. V., B. Steinberger, and T.H. Torsvik (2012), Absolute plate motions in a reference frame defined by moving hotspots in the Pacific, Atlantic and Indian oceans. Journal of Geophysical Research, 117, B09101, doi: 10.1029/2011JB009072.

Govers, R. and M.J.R. Wortel (2005), Lithosphere tearing at STEP faults: Response to edges of subduction zones, Earth and Planetary Science Letters, 236 (1-2), pp. 505-523.

Gueguen, E., C. Doglioni, and M. Fernandez (1998), On the post-25 Ma geodynamic evolution of the western Mediterranean, Tectonophysics, 298, 1–3, 259-269, doi: 10.1016/S0040-1951(98)00189-9.

Faccenna C., C. Piromallo, A. Crespo-Blanc, L. Jolivet, and F. Rossetti (2004), Lateral slab deformation and the origin of the western Mediterranean arcs. Tectonics;23:TC1012. doi:10.1029/2002TC001488.

Rosenbaum, G., G.S. Lister, and C. Duboz (2002), Reconstruction of the tectonic evolution of the western Mediterranean since the Oligocene. Journal of the Virtual Explorer, 8, 107–130.

van Hinsbergen, D.J.J., R.L.M. Vissers, and W. Spakman (2014), Origin and consequences of western Mediterranean subduction, rollback, and slab segmentation, Tectonics

Vergés, J., and M. Fernàndez (2012), Tethys–Atlantic interaction along the Iberia–Africa plate boundary: The Betic–Rif orogenic system, Tectonophysics, 579, 144-172, doi:10.1016/j.tecto.2012.08.032.

Spakman W., and M.J.R. Wortel (2004), A tomographic view on western Mediterranean geodynamics. In: Ziegler P., editor. The TRANSMED Atlas-The Mediterranean Region From Crust to Mantle. Berlin: Springer, pp. 31-52.

Surface manifestations of low-buoyancy mantle plumes: Insights from geodynamic modeling

Juliane Dannberg, Stephan V. Sobolev

German Research Centre for Geosciences Potsdam GFZ, Germany
e-mail: *dannberg@gfz-potsdam.de*
session: *Geodynamics*

According to widely accepted models, mantle plumes ascend from the lower mantle and cause massive melting when their heads reach the base of the lithosphere. Classical geodynamic models consider plumes as purely thermal and thus predict a flattening of the plume head to a disk-like structure and thin plume tails. However, there are seismic observations and paleo-topography data that are difficult to explain with this classical approach. In addition, geochemical data indicate that plumes have a different composition than the average mantle material and it has been suggested a long time ago that subducted oceanic crust could be recycled by mantle plumes (Hofmann & White, 1981).

While recent numerical models have considered a different chemistry (Sobolev et al., 2011, Ballmer et al., 2013) to explain complex plume shapes or zoning within plumes, they are either restricted to only a part of the plume evolution or use simplified material models. However, due to the high density of recycled oceanic crust, thermo-chemical plumes are expected to have much smaller buoyancy than thermal plumes. Therefore it is especially important to incorporate realistic material properties as they can influence the plume dynamics crucially, and determine if a plume reaches the lithosphere or remains in deeper parts of the mantle.

We perform numerical experiments in 3D spherical shell geometry to investigate the dynamics of the plume ascent, the interaction between plume- and plate-driven flow and the dynamics of melting in a plume head. For that purpose, we use the finite-element code ASPECT (Kronbichler et al., 2012), which allows for complex temperature-, pressure- and composition-dependent material properties. Moreover, our models incorporate phase transitions (including melting) with the accompanying rheological and density changes, Clapeyron slopes and latent heat effects for the peridotite and eclogite phase, mantle compressibility and a highly temperature- and depth-dependent viscosity.

We study under which conditions low-buoyancy plumes ascend through the whole mantle, their internal chemical zoning and the structures they form in the upper mantle. We then compare these results to observations of dynamic topography, geochemical trends and melting degrees of ocean island basalts, buoyancy fluxes and seismic tomography.

Modeling shows that high plume buoyancy results in plumes directly advancing to the base of the lithosphere, while plumes with slightly lower buoyancy pond in a depth of 300 km to 400 km and form pools or a second layer of hot material (Figure 1). These structures become asymmetric and finger-like channels begin to form when the plume gets entrained by a quickly moving overlying plate (Figure 2). Our models also suggest that thermo-chemical plumes ascend in the mantle much slower compared to thermal plumes and have thicker plume tails. The conversion of plume excess temperatures to anomalies in seismic velocity shows that thermo-chemical low-buoyancy plumes can explain a variety of features observed by seismic tomography much better than purely thermal plumes.

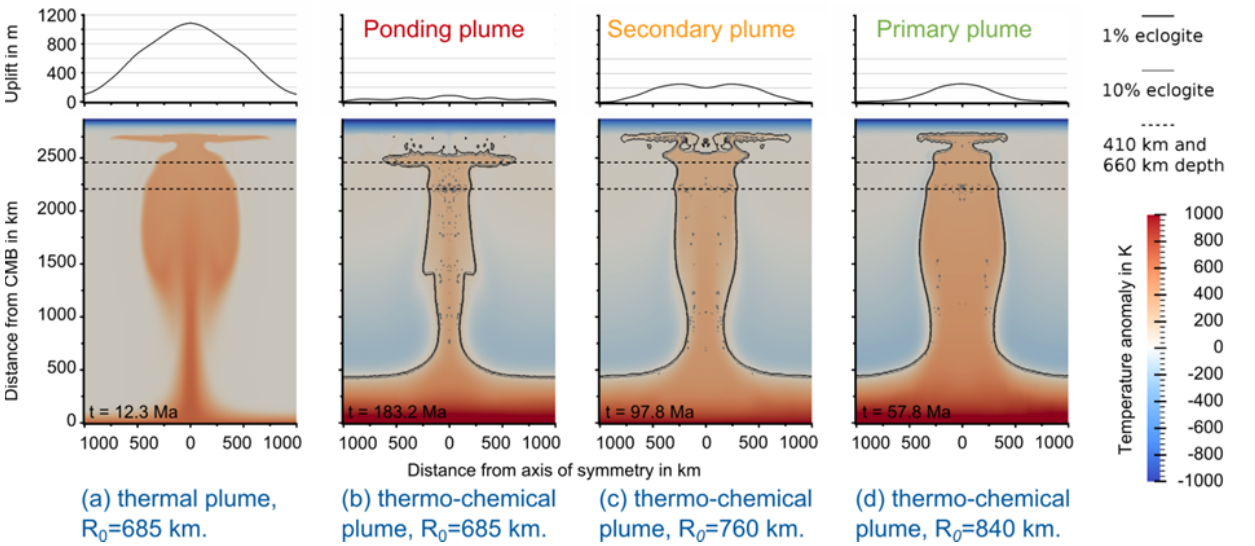

Fig. 1.: Snapshots of a thermal (a) and three thermo-chemical (b, c, d) plumes with different volumes, and the generated surface uplift. Colors represent excess temperature, the solid lines are isolines of chemical composition and dashed lines mark $410\,\mathrm{km}$ and $660\,\mathrm{km}$ depth. In dependence of their initial temperature and buoyancy flux thermo-chemical plumes show three different regimes: Primary plumes (d) ascend directly to the lithosphere, plumes with slightly lower buoyancy pond in $300\,\mathrm{km}$ to $400\,\mathrm{km}$ depth and generate smaller secondary plumes (c), and even lower buoyancy leads to plumes not reaching the lithosphere, but staying below $300\,\mathrm{km}$ depth. The surface uplift caused by a thermo-chemical plume is about an order of magnitude smaller than that of a purely thermal plume.

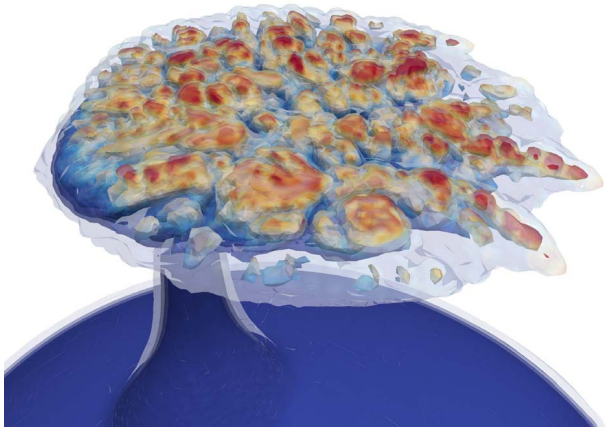

Fig. 2.: A thermo-chemical plume rising from the core-mantle boundary and getting entrained by an overlying, moving plate. The figure shows the isosurface of the chemical composition (fraction of recycled oceanic crust) and colors give an estimate of the melt fraction.

References

Hofmann, A.W, & White, W.M. (1981): Mantle plumes from ancient oceanic crust – Earth and Plaentary Science Letters, 57, 421-436.

Sobolev, S.V. et al. (2011): Linking mantle plumes, large igneous provinces and environmental catastrophes – Nature, 477, 312-316.

Kronbichler, M., Heister, T. & Bangerth, W. (2012): High accuracy mantle convection simulation through modern numerical methods – Geophysical Journal International, 191, 12–29.

Ballmer, M. D., G. Ito, Wolfe, C. J., and Solomon, S. C. (2013): Double layering of a thermochemichal plume in the upper mantle beneath Hawaii – Earth Planet. Science Lett., 376, 155-164.

Plumes to plate tectonics: insights from laboratory experiments

A. Davaille

Laboratoire FAST, CNRS/Université Paris-Sud, Bat. 502, Rue du Belvédère, 91405 Orsay, France
e-mail: *cdavaille@fast.u-psud.fr*
session: *Geodynamics*

Summary

Because laboratory experiments are crucial for exploring new physics and testing theories, they have long played a central role for understanding the physics that governs thermal convection and mantle dynamics. Mantle dynamics on geological time scales is dominated by "fluid" behavior, so that liquids around room temperature, and fluid mechanics techniques, can generally be used. With the development of computer power and lasers, it has become possible in the last years to measure the temperature, velocity, concentration and deformation fields in experimental tanks. Laboratory experiments can therefore also constitute important tools for benchmarking complex numerical codes. Moreover, the rheological characterization of complex fluids has made important progress. I shall review recent results on the dynamics and diversity of mantle plumes and lithospheric intrusions, and on the generation of asymmetric subduction and plate tectonics in the laboratory.

Plume signatures in a complex fluid: velocity, temperature, compositional fields

It is now possible to follow the ascent and growth of a starting plume through both its velocity and temperature fields (fig. 1). Key measurements are then the velocity of the stagnation point located on the top of the plume head V_A, and the velocity of the particles at this point $V_z(A)$. The former will give the same information as following dye (which underlines the maximum deformation) or following shadowgraph (which underlines the maximum temperature gradient), while $V_z(A)$ gives the same value as the uplift of the maximum vorticity centers. The latter constitutes the "true" plume head velocity. The difference $V_A - V_z(A)$ represents plume head growth by thermal diffusion, which remains quite small. We observe that the plume samples mostly the material coming from the thermal boundary layer above the heat source (fig. 1), in agreement with early numerical simulations (Farnetani and Richards, 1995).

When the bottom of the tank contains denser fluid (fig. 2 – left), the interplay of the compositional and thermal buoyancies produces complicated plume morphologies and histories which depend strongly on the buoyancy ratio B (Kumagai et al, 2008).

On the other hand, in a visco-elasto-plastic fluid (e. g. Carbopol), the morphology of plumes is very different from the mushroom-shape observed in newtonian fluids: a plug flow develops inside the plume thermal anomaly, producing a rising finger-shape with strong shear zones confined along its edges (fig. 2 – right)). And two conditions must now be fulfilled for an instability to develop and rise: 1) the Yield number Ψ_0 comparing the buoyancy-induced stress to the yield stress, should be greater than a critical value $\Psi_0 \approx 6$ (Davaille et al, 2013); and 2) the Bingham number B_i, comparing the yield stress to the viscous stresses, needs to be locally smaller

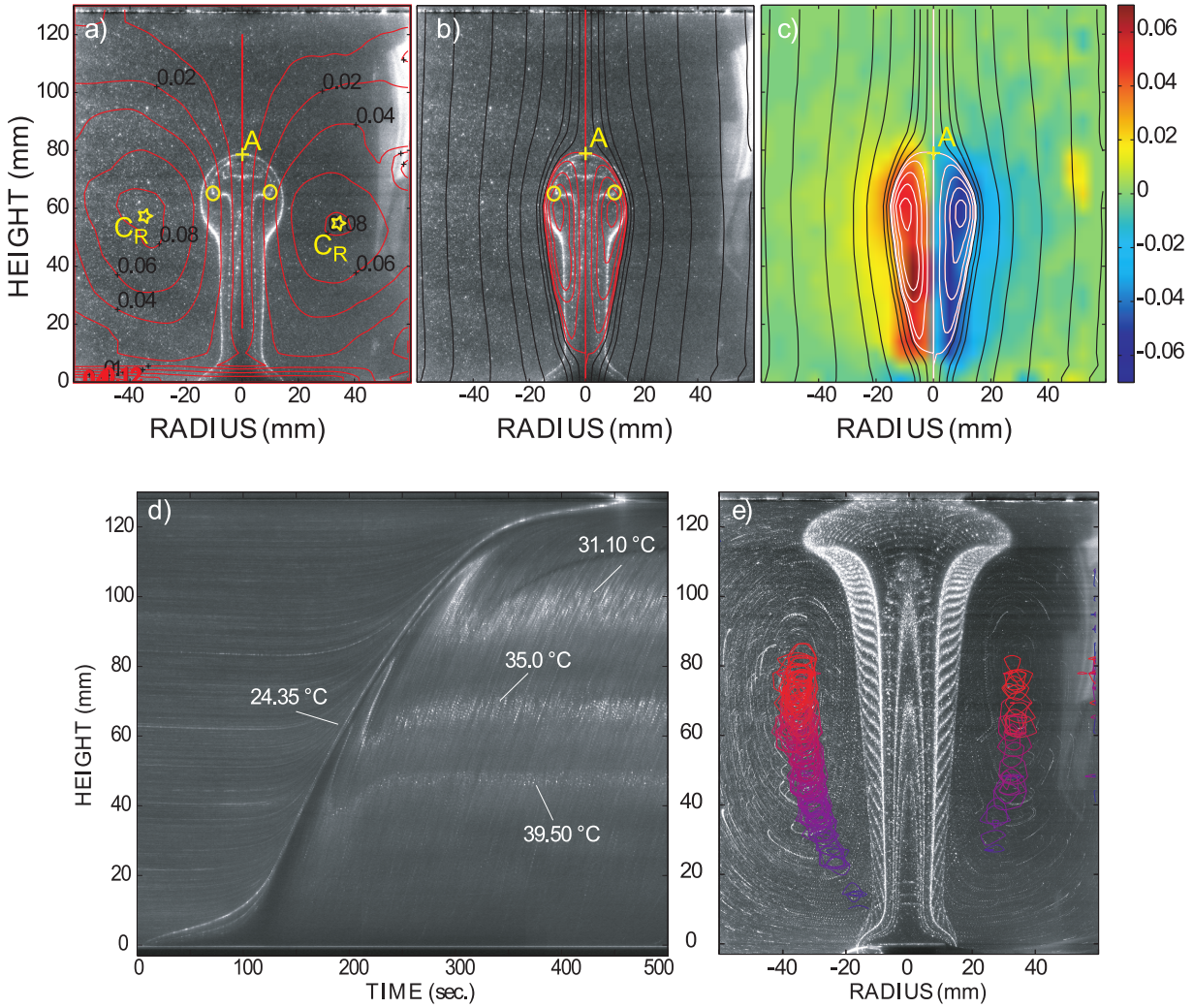

Fig. 1.: Thermal starting plume in sugar syrup ($\gamma = 47$). a) Streamlines in the laboratory reference frame on top of the plume image. The yellow cross represents the stagnation point A at the head top, the stars the rotation centers CR in the laboratory reference frame, and the yellow open circles point to the vorticity extrema. b) Streamlines in the "plume head" reference frame on top of the plume image, and c) on top of the vorticity field. d) Plume uplift through time followed through the image intensity along the plume vertical axis; the bright lines are the isotherms (labelled in white). e) Superposition of the plume images taken every 5 s between t = 100 and t = 500 s. The internal structure of the plume conduit, with its 5 isotherms, appears to be steady. The outer bright line underlines the steady growth of the plume head. The positions of the centers of rotation (corresponding to the position of the maximum values of the stream function) are represented in blue (early times) to red (late times) (adapted from Davaille et al., 2011a).

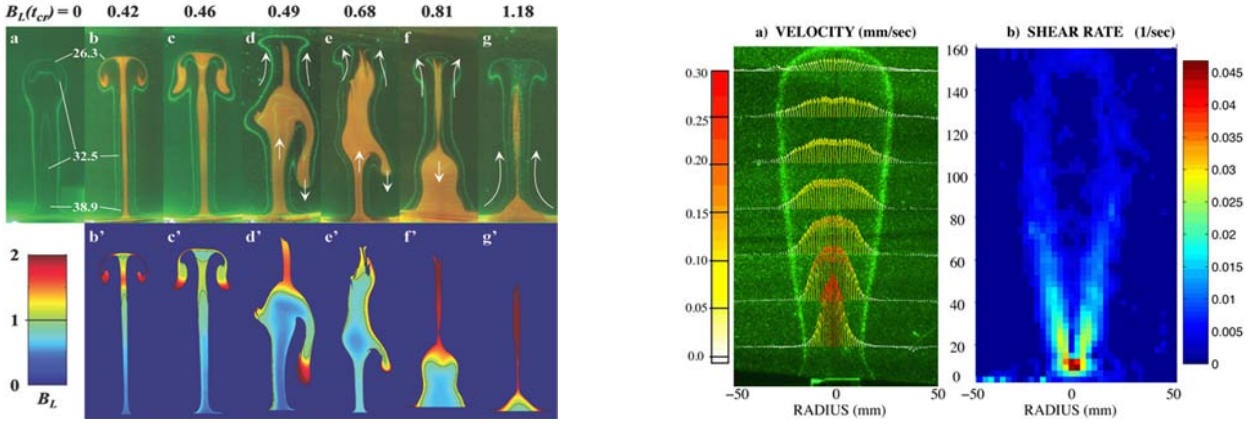

Fig. 2.: Left: Different morphologies as B increases. A thermochemical plume was generated on a flat heater with a constant power. Initially the orange denser material was in a thin layer at the bottom of the tank. The green lines are the isotherms. top) thermal and compositional fields. The white arrows indicate the fluid motions. bottom) local buoyancy ratio.(from Kumagai et al, 2008). Right : Thermal plume in a yield-stress and shear-thinning carbopol gel. a) Temper- ature (visualized by isotherms) and velocity structure. b) shear rate calculated from the velocity fields. Note how deformation is confined on the edges of the thermal finger. (from Davaille et al, 2013).

than 1. Moreover, the instability halts its ascent as soon as $\Psi_0 < \Psi_c$ or $Bi > 1$ (Massmeyer et al, 2013). The experimental finger-shaped plumes show strong similarities with diapiric intrusions in the Earth's lithosphere. A 10 km-diameter purely thermal anomaly could only be emplaced in a partially molten lithosphere (with $\sigma_0 \approx 100$ kPa), but the yield stress of the surrounding matrix could reach up to ~ 50 MPa if the instability also exhibits a chemical density anomaly.

Planetary dynamics: lessons from soft matter

On Earth, seismic tomography studies show that the subduction zones – and therefore the cold plates – distribution delimits two large cells in the mantle (the Pacific and the Indo-Atlantic "boxes"), each cell containing several hot instabilities (plumes). The existence of several scales of convection suggests that the Earth's mantle is in the "mobile lid" regime of convection in a strongly temperature-dependent viscosity (e. g. Solomatov, 1995; Androvandi et al, 2011). Given the mantle physical characteristics, this would imply that the effective viscosity of the lithosphere is not more than ~ 30 to 3000 times more viscous than the bulk mantle, in agreement with estimates using bathymetry and geoid constraints), regional models of subduction, or slab bending (Androvandi et al, 2011).

However, with an actual viscosity contrast across the lithosphere $\geq 10^7$, the Earth should be in the stagnant lid regime, i. e. a one-plate planet like for example Mars. So, if temperature-dependent viscosity is clearly a key ingredient for plate formation, this ingredient alone is not sufficient to generate Plate Tectonics convection. To make plate tectonics work, weakening and shear localization are also required. Moreover, the lithosphere can support over long time periods dormant weak zones (faults or rifts), which can be preferentially reactivated to become new plate boundaries. For years, experimentalists have been looking for an analogue fluid presenting the "right" kind of rheology to allow self-consistent, true plate tectonics. We are now using aqueous colloidal dispersions of nanoparticles, whose rheology depends strongly on the solid particle fraction ϕ_p and on the chemical activity a_χ, being Newtonian at low ϕ_p and low a_χ, and presenting yield stress, elasticity, and brittle

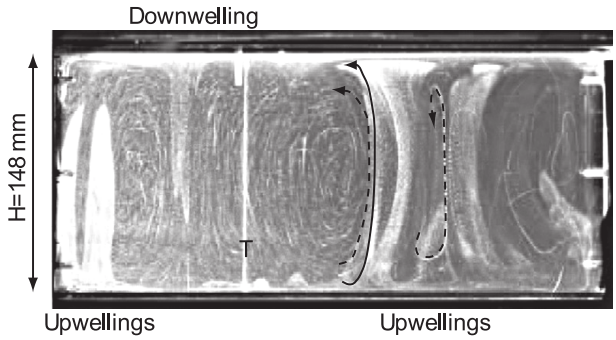

Fig. 3.: Experiment at high Rayleigh number and intermediate viscosity ratio (Rahot = 5.3x107; $\gamma = 142$). Snapshot of a vertical cross-section taken 8 cm from the front lateral wall. The bright lines are isotherms, except the clear straight line labelled 'T' at position x = 110 mm which is the thermocouple probe. Several hot plumes are seen while only one cold downwelling is observed. This situation resembles what is observed on Earth for example in the Pacific "box". (from Androvandi et al, 2011).

properties as ϕ_p or a_χ increase (Di Giuseppe et al, 2012). So by heating these fluids from below, as well as drying them (as an analogue to cooling) from above, several regimes can be observed whereas a visco-elasto-plastic skin forms at the surface and either stays there (convection under a stagnant lid), or breaks and sinks episodically in the fluid (episodic subduction, fig. 4 – left, Di Giuseppe and Davaille, 2010), or presents the continuous motion and renewal of surface plates (fig. 4 – right, Davaille et al, 2011b). The latter regime is close to the continuous plate tectonics observed on Earth, and subduction is always asymmetric.

References

Androvandi S., Davaille A., Limare A., Fouquier A. and Marais C. 2011. At least three scales of convection in a mantle with strongly temperature- dependent viscosity, Phys. Earth Planet. Int. 188, 132-141.

Davaille A., A. Limare, F. Touitou, I. Kumagai, J. Vatteville. 2011a. Anatomy of a laminar starting plume at high Prandtl number, Exp. Fluids, 50, 285-300.

A. Davaille, E. Di Giuseppe, S. Androvandi, M.-C. Renoult and F. Doumenc. 2011b. Convective regimes in "soft matter": implications for the dynamics of planetary interiors, EPSC-DPS 2011 Planetary Sciences, Nantes.

Davaille A., Gueslin B., Massmeyer A., Di Giuseppe E. 2013. Thermal in- stabilities in yield stress fluids: existence and morphology. J. Non-Newtonian Fluid Mech. 193, 144-153.

Di Giuseppe E., A. Davaille . 2010. Episodic Subduction arising from con- vection in a complex-rheology fluid: Insights from laboratory experiments, Geophysical Research Abstract 12, 07954.

Di Giuseppe, E., A. Davaille, E. Mittelstaedt, M. Franois. 2012. Rheo- logical and mechanical properties of silica colloids: from liquid Newtonian to brittle behavior, Rheologica Acta 51, 451-465.

Farnetani C.G., Richards M. A., 1995. Thermal entrainment and melting in mantle plumes, Earth Planet. Sci. Lett., 136, 251-267.

Kumagai I, Davaille A, Kurita K, Stutzmann E . 2008. Mantle plumes: Thin, fat, successful, or failing? Constraints to explain hot spot volcanism through time and space, Geophys. Res. Lett., 35, L16301.

Massmeyer A., E. Di Giuseppe, A. Davaille, T. Rolf, P.J. Tackley . 2013. Numerical simulation of thermal plumes in a Herschel-Bulkley fluid, J. Non- Newtonian Fluid Mech. 195, 32-45.

Solomatov S. 1995 Scaling of temperature- and stress-dependent viscosity convection. Phys. Fluids 7, 266-274.

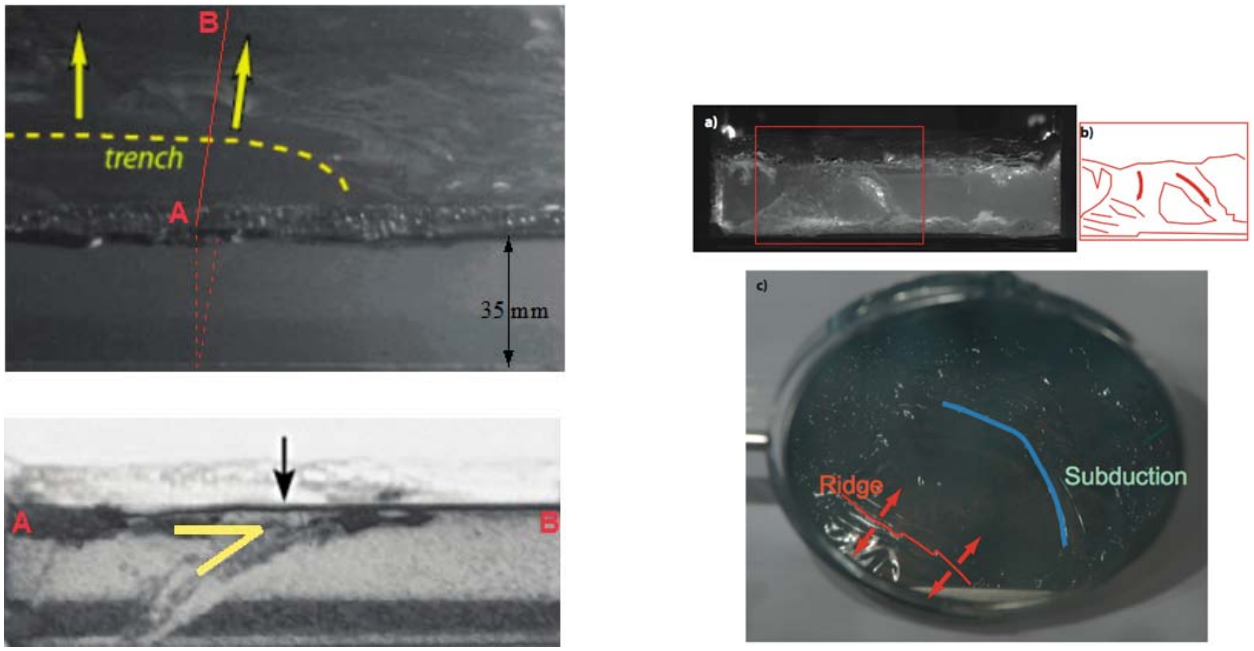

Fig. 4.: Left: Spontaneous asymmetric subduction in a layer of colloids dried from above at constant temperature and humidity. Top) view from above. The "trench" is outlined in yellow and the direction of trench rollback is indicated by the yellow arrows. Bottom) view from the side. The contrast has been enhanced to better see the subducting plate. The trench position is marked with a black arrow. (from Di Giuseppe & Davaille, 2010). Right : Convection in silica colloidal suspension: regime of continuous Plate Tectonics. a-b) View from the side. Two plates coming from the upper skin are subducting towards us. b) is the interpreted cartoon of the inset in a). The left subducting plate is folding and forming a pile on the tank bottom. c) View from the top: a spreading ridge is visible as well as a subduction zone.

Three dimensional laboratory models of subduction: plate interface, overriding plate deformation and energy dissipation

João C. Duarte, Zhihao Chen, Wouter P. Schellart, Alexander R. Cruden

School of Geosciences, Monash University, Melbourne, Australia
e-mail: *joao.duarte@monash.edu*
session: *Geodynamics*

Introduction

Subduction zones are major features on Earth and are believed to be one of the main drivers of plate tectonics and mantle convection. The subducted slabs are negatively buoyant and have the natural tendency to sink into the Earths' mantle, pulling their trailing plates at the surface. Slabs generally have a plane perpendicular component of movement that forces the trench at the surface to migrate (retreat or advance). In such cases, the overriding plate follows the subduction hinge, while remaining in physical contact with the subduction plate and deforming in the meantime.

Several works have used laboratory experiments to investigate a number of natural aspects of subduction (e. g. Kincaid & Olson 1987; Faccenna et al. 1996; Buttles & Olson 1998; Funiciello et al. 2003; Schellart 2004; Boutelier & Cruden 2008). In this work, we present three-dimensional fluid dynamic laboratory experiments of narrow subduction zones with an overriding plate and an interplate rheology. These results are based on and build on recent modelling studies on subduction zones with an overriding plate (Meyer and Schellart, 2013) as well as an interplate rheology (Duarte et al., 2013; Duarte et al., 2014).

Material and methods

In our subduction experiments we use a low viscosity glucose tank (Fig. 1) to simulate an upper mantle reservoir and a mixture of high viscosity silicone and fine iron powder to simulate the subducting plate (negatively buoyant) and overriding plate (neutrally buoyant). Mixtures of petrolatum and paraffin oil with an adjustable rheology are used to lubricate the subduction interface by applying them to the surface of the subducting plate. Our models are scaled using the Reynolds number and the Stokes velocity, insuring that geometry, kinematics, and dynamics (driving and resisting forces) are proportional to the natural example (see Duarte et al., 2013 for a detailed description of the scaling and modelling apparatus). No external velocity or force boundary conditions are applied in our models.

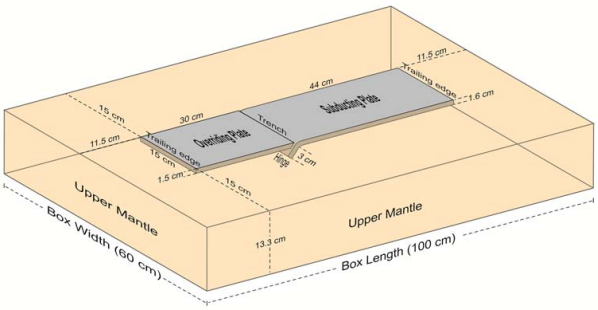

Fig. 1.: Model setup of our reference experiment

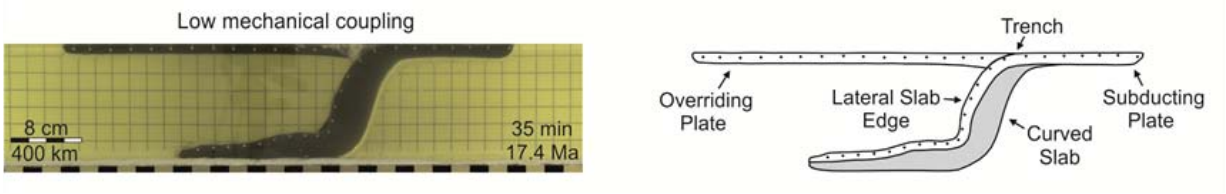

Fig. 2.: Example of a subduction experiment with both a subducting plate and an overriding plate, and an interplate rheology (adapted from Duarte et al., 2013).

Modelling results

The main results are: 1) The shear stresses at the subduction interface have a control on the plate velocity, with high shear stresses correlating with low velocities and vice-versa. Calculations of the interfacial shear force and comparison with natural subduction zones suggest that globally the interfacial shear stresses are low (<33 MPa); 2) In our models of narrow subduction zones the overriding plate always experiences overall extension, with an area of maximum (extensional) deformation localizing at a finite distance from the trench (~ 300 km), and with some shortening often occurring at the forearc. This implies that the extension is mainly driven by the toroidal component of the mantle return flow; 3) Only a small portion of the potential energy of the subducted slab is used to deform the overriding plate (less than 1 %). Considering that the energy dissipated in the slab and in the subduction zone hinge is also minor (less than 30 %), it implies that majority of the energy ($\leq$ 70 %) is dissipated in the ambient sub-lithospheric mantle. Furthermore, our models indicate that overriding plate deformation force is of comparable magnitude as the ridge push force (2×10^{12} N m^{-1} to 3×10^{12} N m^{-1}).

Final remarks

Even though our models of subduction incorporate some simplifications (isoviscous plates and sub-lithospheric mantle, isothermal conditions) the rigorous scaling procedure assures that they are robust at a first order approximation. We thus conclude that in nature the subduction zones interfaces are weak, in narrow subduction systems the overriding plate deformation is mainly controlled by the toroidal component of the mantle return flow and the energy dissipated in the overriding plate during such deformation is relatively low when compared to the potential energy release of the subducted slab.

Acknowledgements

The authors acknowledge financial support from a Discovery Grant DP110103387 from the Australian Research Council. Z.C. was supported by APA and IPRS scholarships.

References

Boutelier, D.A. & Cruden, A.R., 2008. Impact of regional mantle flow onsubducting plate geometry and interplate stress: insights from physical modelling, Geophys. J. Int., 174, 719–732.

Duarte, J.C., Schellart, W.P., Cruden, A.R., 2013. Three-dimensional dynamic laboratory models of subduction with an overriding plate and variable interplate rheology. Geophysical Journal International 195 (1), 47-66.

Duarte, J.C., Schellart, W.P., Cruden, A.R., 2014. Rheology of petrolatum - paraffin oil mixtures: applications to analogue modelling of geological processes. Journal of Structural Geology 63, 1-11.

Faccenna, C., Davy, P., Brun, J.-P., Funiciello, R., Giardini, D., Mattei, M. & Nalpas, T., 1996. The dynamics of back-arc extension: an experimental approach to the opening of

the Tyrrhenian Sea, Geophys. J. Int., 126, 781–795.

Funiciello, F., Faccenna, C., Giardini, D. & Regenauer-Lieb, K., 2003. Dynamics of retreating slabs: 2. Insights from three-dimensional laboratory experiments, J. geophys. Res.-Solid Earth, 108(B4) 2207, doi:10.1029/2001JB000896.

Meyer, C. & Schellart, W.P., 2013. Three-dimensional dynamic models of subducting plate-overriding plate-upper mantle interaction, J. geophys. Res.-Solid Earth, 118, 775–790.

Kincaid, C. & Olson, P., 1987. An experimental study of subduction and slab migration, J. geophys. Res., 92, 13 832–13 840.

Schellart, W.P., 2004. Kinematics of subduction and subduction induced flow in the upper mantle, J. geophys. Res., 109, B07401, doi:10.1029/2004JB002970.

Geometrical transitions of mantle plumes: an insight from numerical simulations

Urmi Dutta, Shamik Sarkar, Nibir Mandal

Department of Geological Sciences, Jadavpur University, Kolkata – 700032, India
e-mail: *urmidutta.geology@gmail.com*
session: *Geodynamics*

Thermo-mechanical instabilities occurs primarily at a seismically distinct zone called D" zone along the core–mantle boundary of the Earth's interior, triggering upwelling of hot and buoyant mantle materials in the form of thermal plumes. Understanding the mechanics of mantle plumes has raised renewed research interest in the last couple of decades, especially in the context of explaining the origin of large igneous provinces, i. e. the Deccan Traps and the Siberian Traps, and hotspots, i. e. the Iceland and Hawaiian Islands. A direction of plume research investigates the upwelling dynamics of plumes and the possible physical factors which may control this process. It has been demonstrated from physical and numerical experiments that the ascent behaviour of mantle plumes can be unsteady, leading to a complex evolutionary path through the mantle. Such an unsteady ascent is largely attributed to the time-dependent variations of plume-head geometry. The present study aims to explore the key physical parameters that may control the plume geometry, a question that still invokes controversies among the researchers.

We ran scaled model experiments by injecting a hot (~60 °C), buoyant viscous fluid (glycerine) into a relatively cold (30 °C) fluid (glycerine) medium. Experiments produced plumes with a bulbous head, which progressively increased in size during their ascent, and subsequently started to curl inwardly at their flanks, giving rise to a mushroom like shape (Figure 1a). On the other hand, the plume head continued to increase in size without any curling when the fluid was injected slowly. The latter condition produced plumes with a bulbous head (Figure 1b), as documented from many seismic tomography.

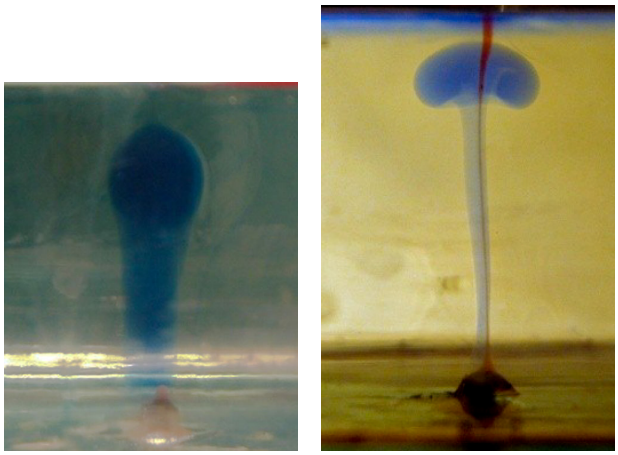

Fig. 1.: Different plume geometry from experiments: (a) Balloon-shaped, (b) Mushroom-shaped plumes.

For a quantitative analysis of these two principal two types: *bulbous-* and *mushroom-shaped* plumes, we performed numerical simulations employing the *Volume of fluid (VOF)* method for multiphase fluid flows. The VOF method applies the flow equations based on volume averaging and tracks the interfaces of two fluid phases using a phase indicator function γ (also denoted as color function or volume fraction). $\gamma = 1$ implies a phase, say Phase 1, whereas $\gamma = 0$ indicates another phase, say Phase 2. The interface between two phases can be tracked with $0 < \gamma < 1$. The VOF formulation assumes that the fluid phases taken for modeling remain in the immiscible state.

Non-dimensionalization of the different parameters in the governing equations is an important step while handling the fluid problems either theoretically or computationally. In our studies we have considered a fluid (*Phase 2*) of lower density (ρ_p), which is injected into a stagnant fluid (*Phase 1*) of higher density (ρ_p), as exercised in the laboratory experiments. Model simulations predict the development of plumes in two principal modes: i) *ballooning mode* and ii) *curling mode*, leading to the bulbous and mushroom-shaped geometry respectively. There can be a transition in the mode of plume ascent as a function of two independent physical variables: density contrast ($\Delta\rho = \frac{\rho_a}{\rho p}$, ρ_a and ρ_p are mantle and plume density respectively) and material influx rate (normalized in terms of Reynolds number $Re = \frac{\rho v d}{\mu}$ where v is the injection velocity and d is length of the cross-sectional area).

The ballooning mode (Figure 2) occurs in a condition of high $\Delta\rho$ ($\sim$1.2) and low Re ($\sim$6), which transforms into the curling mode (Figure 3) as the condition is reversed ($\Delta\rho = 1.1$ and $Re = 18$). We investigated the thermal structures of plumes from temperature profile across the plume head. The ballooning and curling types show contrasting temperature profiles (Figure 4). Ballooning type of plumes are characterized by steeper thermal gradients across their boundaries, as compared to that in the curling type. Secondly, the temperature remains laterally more uniform in case of ballooning. In the advanced stage the profile shows a temperature drop inside the head, which resulted possibly from a secondary convection process operating inside the plume head. The thermal front of a plume migrates laterally with time, and the rate of migration depends on the mode of ascent. The curling mode shows the thermal front migration at much faster rates, about ten times that for the ballooning mode (Figure 4).

Results from this fluid models has been employed to addresses a fundamental question why seismic images rarely detects the curling type of plume geometry, although it is widely reported from various model simulations. The maps of the temperature distribution in close proximity

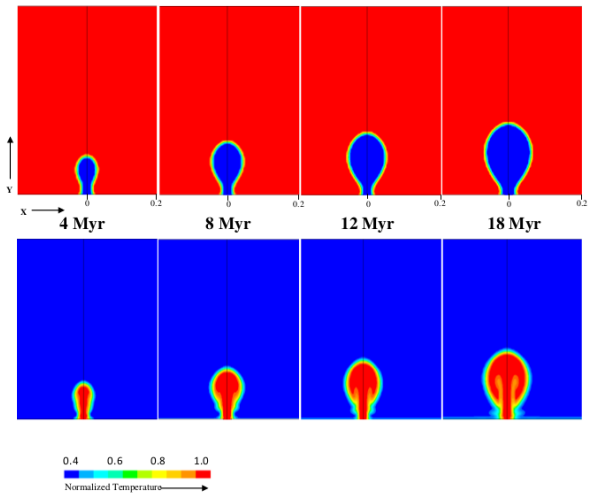

Fig. 2.: Progressive development of a plume in ballooning mode in VOF models. Mapping of the plume shapes by (a) phase and (b) thermal boundary are shown.

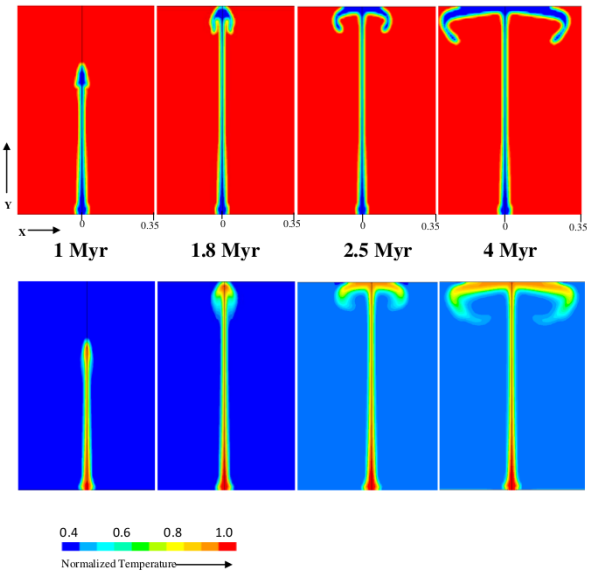

Fig. 3.: Development of plumes by curling mode in models with a low density contrast ($\Delta\rho = 1.1$) and a high influx rate ($Re \approx 20$). (a) Phase and (b) thermal structures.

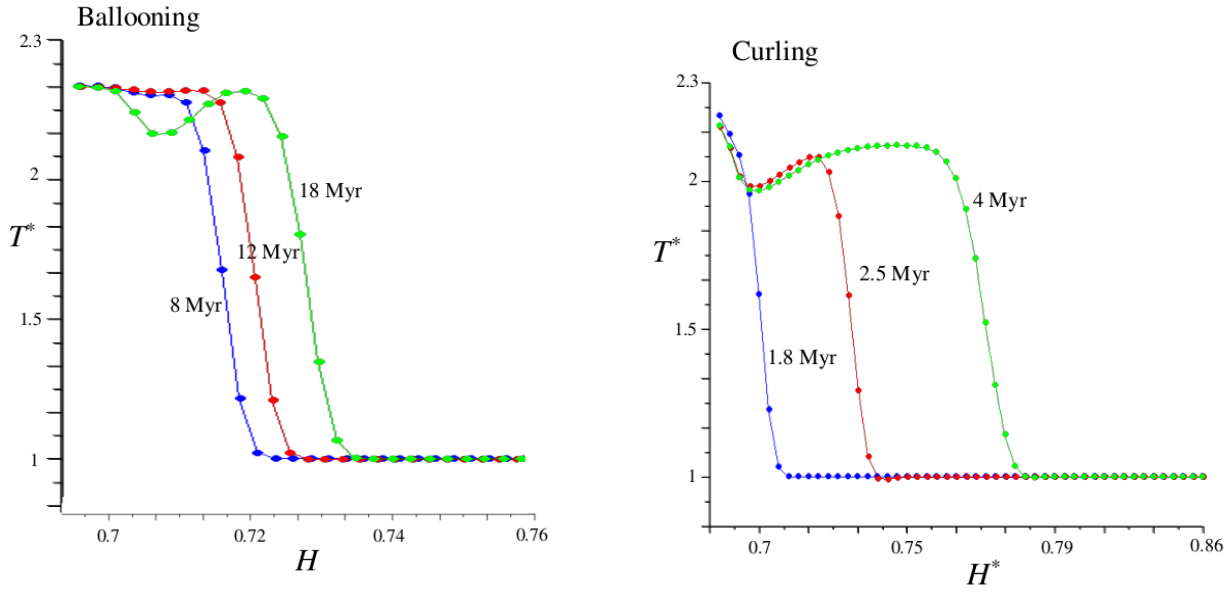

Fig. 4.: Temperature profile of plume head along a horizontal, central line passing through the head. Both temperature and horizontal distance have been shown by their values normalized with respect to the corresponding far-field temperatures and the horizontal model dimension, respectively.

to the plumes suggest that they differ considerably from plume phase boundary in case of the curling mode plume. The thermal structure always reveals a balloon-shaped geometry even if the phase boundary suggests a mushroom-shaped plume head. We infer that seismic tomography perhaps tracks the thermal boundary of plumes, rather than the mantle-plume phase boundary.

References

Dutta, U., Sarkar, S., Baruah, A.,Mandal, N., (2014). "Ascent modes of jets and plumes in a stationary fluid of contrasting viscosity". International Journal of Multiphase Flow, `http://dx.doi.org/10.1016/j.ijmultiphaseflow.2014.02.007`.

Dutta, U., Sarkar, S., Mandal, N., (2013). "Ballooning versus curling of mantle plumes: views from numerical models". Current Science. 104 (7), 893–903.

Thermo-mechanically coupled subduction with a free surface using ASPECT

Menno Fraters[1], Anne Glerum[1], Cedric Thieulot[1,2], Wim Spakman[1,2]

[1] *Utrecht University, Geosciences, Earth Sciences, Utrecht, Netherlands*
[2] *Centre of Earth Evolution and Dynamics, Oslo, Norway*
e-mail: *menno.fraters@outlook.com*
session: *Geodynamics*

ASPECT (Kronbichler et al., 2012), short for Advanced Solver for Problems in Earth's ConvecTion, is a new Finite Element code which was originally designed for thermally driven (mantle) convection. It has, among others, the following advantages and properties:

1. Modern numerial methods: linear and nonlinear solvers, stabilization of transport dominated processes;

2. adaptive mesh refinement;

3. Build from the ground up for parallelism (a high scalability on multiple processors);

4. Trivial to go from 2D to 3D

5. Build upon the well maintained and supported liberies deal.ii, Trilinos and p4est.

Here we present an application of ASPECT to modeling of fully thermo-mechanically coupled subduction. Our subduction model contains three different compositions: a crustal composition on top of both the subducting slab and the overriding plate, a mantle composition and a sticky air composition, which allows for simulating a free surface for modeling topography build-up. We implemented a visco-plastic rheology using frictional plasticity and a composite viscosity defined by diffusion and dislocation creep. The lithospheric mantle has the same composition as the mantle but has a higher viscosity because of a lower

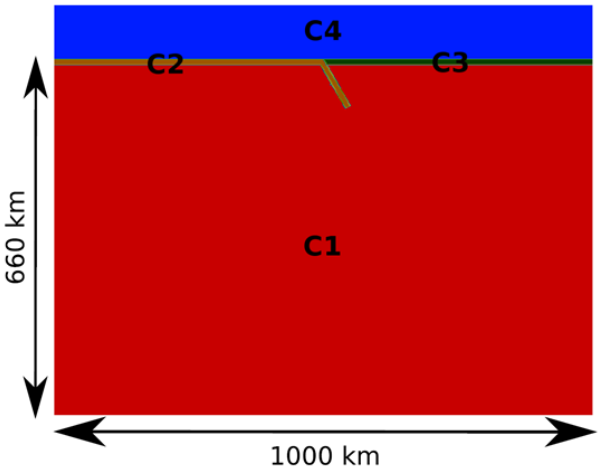

Fig. 1.: Model setup. C1 is mantle material, C2 and C3 are crust materials and C4 is a sticky air material.

temperature. The temperature field is implemented in ASPECT as follows: a linear temperature gradient for the lithosphere and an adiabatic geotherm for the sublithospheric mantle. Initial slab temperature is defined using the analytical solution of McKenzie (1970). The plates can be pushed from the sides of the model, and it is possible to define an additional independent mantle in/out flow through the boundaries.

We show that this model produces good results:

1. the free surface works in building reasonable topography;

2. the deformation is highly localized in the overriding and subducting plate in clear visible shear bands;

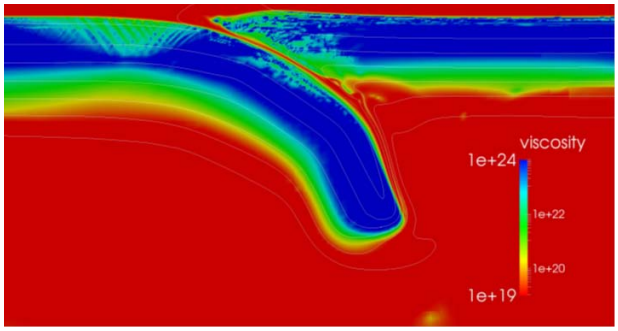

Fig. 2.: The viscosity field of the model described above after 1 myr where the plates are pushed from both sides.

3. a self-consistent evolution of the evolution of the subduction channel through the viscoplastic rheology;

4. transfer of crustal material from the subducting plate to the overriding plate;

5. Slab shape depending on mantle flow.

This setup is then used to investigate the western Mediterranean subduction and subsequent rollback. About 30Ma this rollback was initiated (Van Hindsbergen et al, 2014) and pulled Sardinia and Corsica from Iberia as a big block. We will show a preliminary set of models and results, highlighting the codes capabilities, such as the Adaptive Mesh Refinement, topography development, the influence of mantle flow on the subduction evolution, and the investigation into this blocklike behavior of Sardinia and Corsica.

References

Kronbichler, M., Heister, T., and Bangerth, W. (2012), High accuracy mantle convection simulation throughmodern numerical methods, Geophysical Journal International,191, 12-29, doi:10.1111/j.1365-246X.2012.05609.

McKenzie, D.P. (1970), Temperature and potential temperature beneath island arcs, Teconophysics, 10,357-366, doi:10.1016/0040-1951(70)90115-0.

Van Hinsbergen, D.J.J., Vissers, R.L.M. and Spakman, W. (2014), Origin and consequences of western Mediterranean subduction, rollback, and slab segmentation, Tectonics, doi:10.1002/2013TC003349

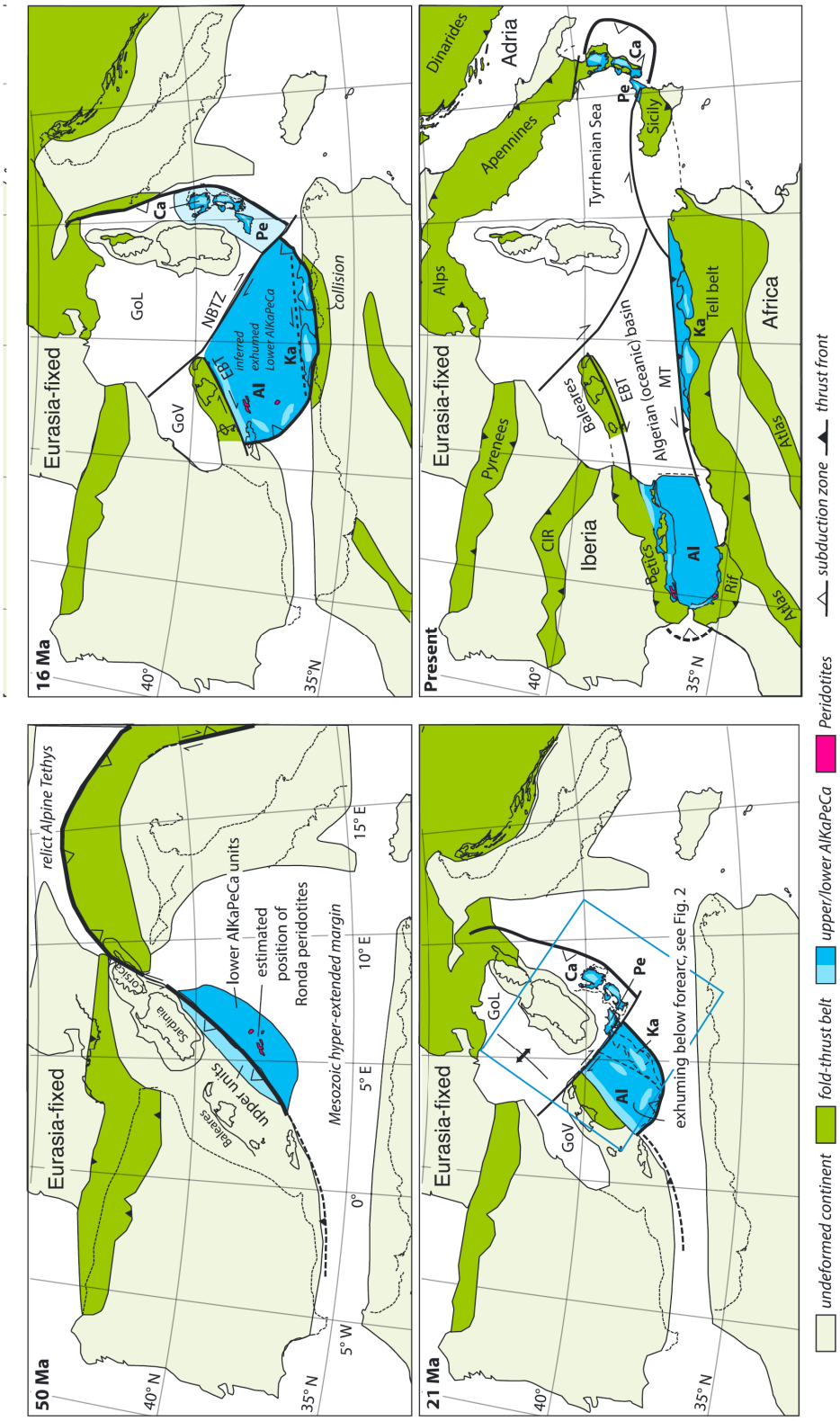

Fig. 3.: Western Mediteranian subduction and rollback history (Van Hindsbergen, 2014)

The Role of the Initial Condition in Numerical Models of the Present-day Mantle Flow Field

E. H. Fritzell, A. L. Aller, G. E. Shephard

CEED, Sem Sælands vei 24, Nedre Blindern, 0371 Oslo
e-mail: *evahfr@student.geo.uio.no*
session: *Geodynamics*

To perform any numerical model of convection in Earth's mantle, initial internal conditions (e. g., temperature and composition), boundary conditions (e. g., the velocity fields at the surface and the core-mantle boundary), and parameters such as the mantle viscosity profile must be imposed. Such conditions and parameters are crucial for simulating mantle convection, however, none are fully constrained, and assumptions on their values must be made. Using palaeomagnetically-derived tectonic plate motion velocities as time-dependent surface boundary conditions in numerical convection models, it is possible to simulate convective flow within Earth's mantle for periods encompassing several hundreds of Ma. Recent work has shown that such models can, to first-order, successfully reproduce the global present-day lower mantle velocity signature inferred from seismic tomography. For such models, assumptions must be made on the initial conditions and surface kinematics, along with a mantle viscosity profile. In this project, we will study the effect of the assumed initial condition on the resulting 3D flow field in simulations of mantle convection. We will investigate whether the assumption of an initial condition affects the present-day mantle dynamical structure on both local and global scales and aim to determine the time-dependence of the effect of initial conditions. We will investigate both isochemical (i. e., purely thermal) and thermochemical (thermal and compositional) modes of convection in Earth's mantle, and simulate convection over time periods of several hundreds of Ma. We will use the finite-element mantle convection code CitcomS in parallel with the interactive plate tectonic reconstruction software, Gplates, to simulate convection in Earth's mantle with palaeomagnetically-derived tectonic plate motion velocities as time-dependent surface boundary conditions. We will quantitatively and qualitatively compare predicted present-day mantle structure to inferences from alternative seismic tomography models and aim to determine the effect of initial conditions on numerical model results.

3-D computational modeling of the continental plate collision near South Island, New Zealand

Lev Karatun[1], Cedric Thieulot[2], Russel Pysklywec[1]

[1] *Department of Earth Sciences, University of Toronto*
[2] *University of Utrecht*
e-mail: *lev.karatun@mail.utoronto.ca*
session: *Geodynamics*

The orogenic zone at the South Island of New Zealand is of particular current interest in geodynamics/tectonics research as an active and young continental collision. These characteristics make the region amenable to studying the (enigmatic) nature of continental plate collisions using present-day geophysical/geological observables.

The fundamental nature of the lithospheric deformation, especially the deformation of the mantle lithosphere (sub-crustal lithosphere), at the South Island is unresolved. Two end-member behaviours have been proposed: mantle lithosphere may be accommodated by subduction-like underthrusting of one plate along a narrow shear zone (Beaumont et al., 1996); or it may be shortened by distributed thickening of a viscous mantle lithosphere root (Molnar et al., 1999; Stern et al., 2000). It may also be that lithosphere is deforming by a combination of these two, with a temporal transition from one to another (Pysklywec et al., 2002). An important feature of the South Island tectonics is the highly oblique nature of the plate collision: strike-slip motion ($\sim 4\,\mathrm{cm/a}$) along the boundary exist at the same time with convergent motion ($\sim 1\,\mathrm{cm/a}$). Moreover, the convergence velocity varies along the boundary owing to the proximity of the Euler pole of rotation. To the north, Hikurangi west-dipping subduction and to the south, Peysegur east-dipping subduction may also be modifying the collision in a type of subduction scissor (Pysklywec et al., 2010). However, previous studies on modelling the dynamics of the South Island collision have not included these important factors in the direction parallel to the plate boundary; instead considering this as a two-dimensional problem.

In the research we are conducting 3D geodynamical modelling to explore these tectonic questions for the collision. We are using a newly-developed code "Elefant" by Cedric Thieulot which has been designed for geodynamical simulations at crustal and lithospheric scales. It solves the Stokes and heat transport equations using finite element methods, relying on open-source solvers – MUMPS and SPLIB.

The code is very versatile and offers such features as:

- The so-called Arbitrary Lagrangian-Eulerian method (Donea et al., 2004) meaning that the grid deforms vertically allowing a free surface, but stays intact along the horizontal axes
- Lagrangian markers used to track the material displacements
- Velocity- and pressure-based boundary conditions allowing more realistic and flexible constraints for the models
- Diverse available rheologies – brittle, viscous and visco-plastic

Elefant has been thoroughly benchmarked and optimised for using on supercomputers; it scales well for 100+ cores. The NZ models are currently

being tested and running on the SciNet cluster – Canadas largest supercomputer.

The input parameters of the model is 4-layered structure with convergence occurring alongside with the strike-slip motions along the weak zone representing the Alpine fault. Here, I will show the first results of the work – general structures formed, material displacements, velocities, strain rate, and character of deformation from the forward computational modelling.

References

Beaumont, C., Kamp, P.J.J., Hamilton, J., and Fullsack, P., 1996, The continental collision zone, South Island, New Zealand: Comparison of geodynamical models and observations, Journal of Geophysical Research, 101, 3333–3359, doi: 10.1029/95JB02401.

Donea, J., Huerta, A., Ponthot, J., and Rodriguez-Ferran, A., 2004, Arbitrary Lagrangian-Eulerian Methods, Encyclopedia of Computational Mechanics, 1.

Molnar, P., et al., 1999, Continuous deformation versus faulting through the continental lithosphere of New Zealand, Science, 286, 516–519.

Pysklywec, R.N., Beaumont, C., and Fullsack, P., 2002, Lithospheric deformation during the early stages of continental collision: Numerical experiments and comparison with South Island, New Zealand, Journal of Geophysical Research, v. 107, p. 1–19, doi: 10.1029/2001JB000252.

Pysklywec, R. N., Ellis, S., Gorman, A. R., 2010, Three-dimensional mantle lithosphere deformation at collisional plate boundaries: A subduction scissor across the South Island of New Zealand, Earth and Planetary Science Letters, 289, 334-346.

Stern, T., Molnar, P., Okaya, D., Eberhart-Philips, D., 2000, Teleseismic p wave delays and modes of shortening the mantle lithosphere beneath South Island, New Zealand, Journal of Geophysical Research, 105 (8), 21615–21631.

Featuring lithosphere rheology in models of glacial isostatic adjustment

Volker Klemann[1], Magdala Tesauro[1], Zdenek Martinec[2,3], Ingo Sasgen[1]

[1] *German Research Centre for Geosciences, Germany*
[2] *Dublin Institute for advanced Studies, Ireland*
[3] *Charles University in Prague Chech Republic*
e-mail: *volkerk@gfz-potsdam.de*
session: *Geodynamics*

It is common to treat the lithosphere as a purely elastic plate parameterized by its flexural rigidity or effective elastic thickness if glacial isostatic adjustment processes are modeled. Furthermore, the viscous or viscoelastic mantle structure underlying the elastic plate is considered in a spherical, i. e. 1D symmetry. These assumptions downgrade the lithosphere to a thin plate where its rheological characteristics and structural features are neglected; but the assumptions are widely accepted as the horizontal extensions of the classical glacial loads in Scandinavia and North America are too large as to be sensitive to small-scale lateral variations of lithospheric strength. Likewise, the presently observed fading adjustment process due to the loading processes dating back several thousands of years is governed by the large-scale flow of mantle material.

To proof the validity of such an assumption, we apply the spectral finite element code VILMA which is based on Martinec (2000) where the field equations of a self-gravitating viscoelastic continuum are solved in the time domain and which allows for lateral variations in viscosity structure (Klemann et al., 2008) but also power-law rheology. On the two latter aspects we focus in this study where we investigate the influence of a rheologically constrained lithosphere with lateral variability in temperature and structure, which is based on Tesauro et al. (2012), on the response to glacial loading processes.

As a case example, we discuss the evolution of viscosity on a cross section that cuts the Laurentide ice sheet from its centre to the periphery and we apply a power-law rheology, where the effective viscosity is determined from the load induced stress field, σ, which is determined from the viscoelastic deformations of the earth:

$$\eta_{\text{eff}} = \frac{1}{A|\sigma|^{n-1}} \exp \frac{E}{RT} \qquad (1)$$

Here, A, E and n are material dependent quantities following from the considered earth structure and the temperature, T , follows from the considered thermal state of the lithosphere.

For reference, Fig. 1 shows the effective viscosity for a homogeneous shear-stress state of 1 MPa and 10 MPa, respectively, on this cross section. The increase of viscosity with radius is mainly due to the temperature decrease. Lateral heterogeneity reflects structural features of the lithosphere. Qualitatively, one can expect that the effective viscosity is lowest during the termination phase when the fast ice retreat induces largest changes in the stress state and, so, enhances the sub-lithospheric material transport.

This is shown in Fig. 2, where the viscosity in the mantle lithosphere drops by more than one magnitude during the termination phase and increases afterwards again.

Furthermore, we extend this study to more recent and smaller scale processes like the Little Ice Age and present time loading processes in tectonically active regions like Southern Patagonia, Antarctic Peninsula or Alaska.

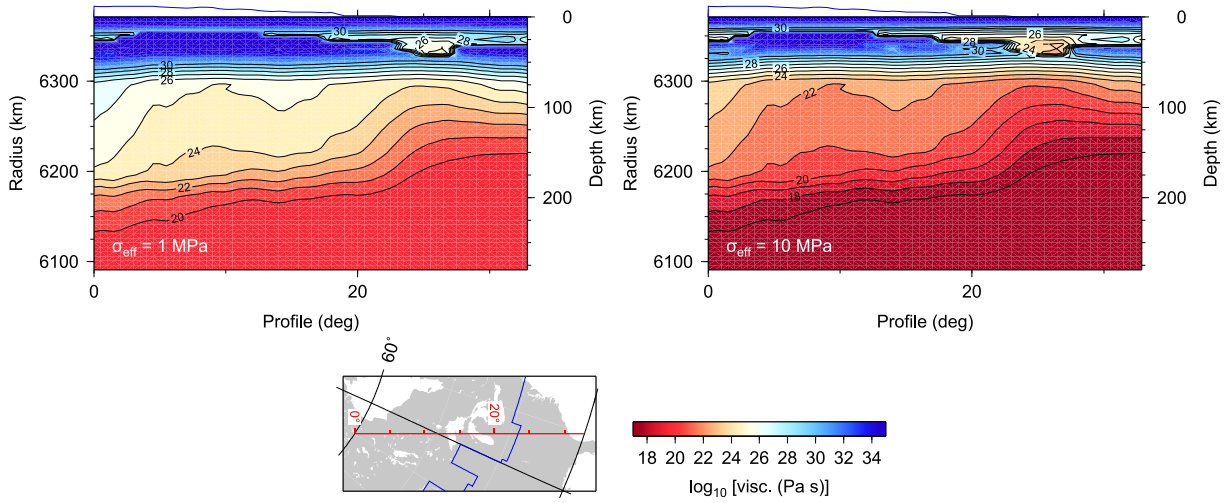

Fig. 1.: Effective viscosity for homogeneous stress state of $1\,\mathrm{MPa}$ and $10\,\mathrm{MPa}$. For orientation, the extension of the Laurentide ice sheet is shown at the top of each plot in blue. The map below shows the chosen profile from west of Hudson Bay towards Florida in red and the maximum extension of the adopted ice-sheet model again in blue.

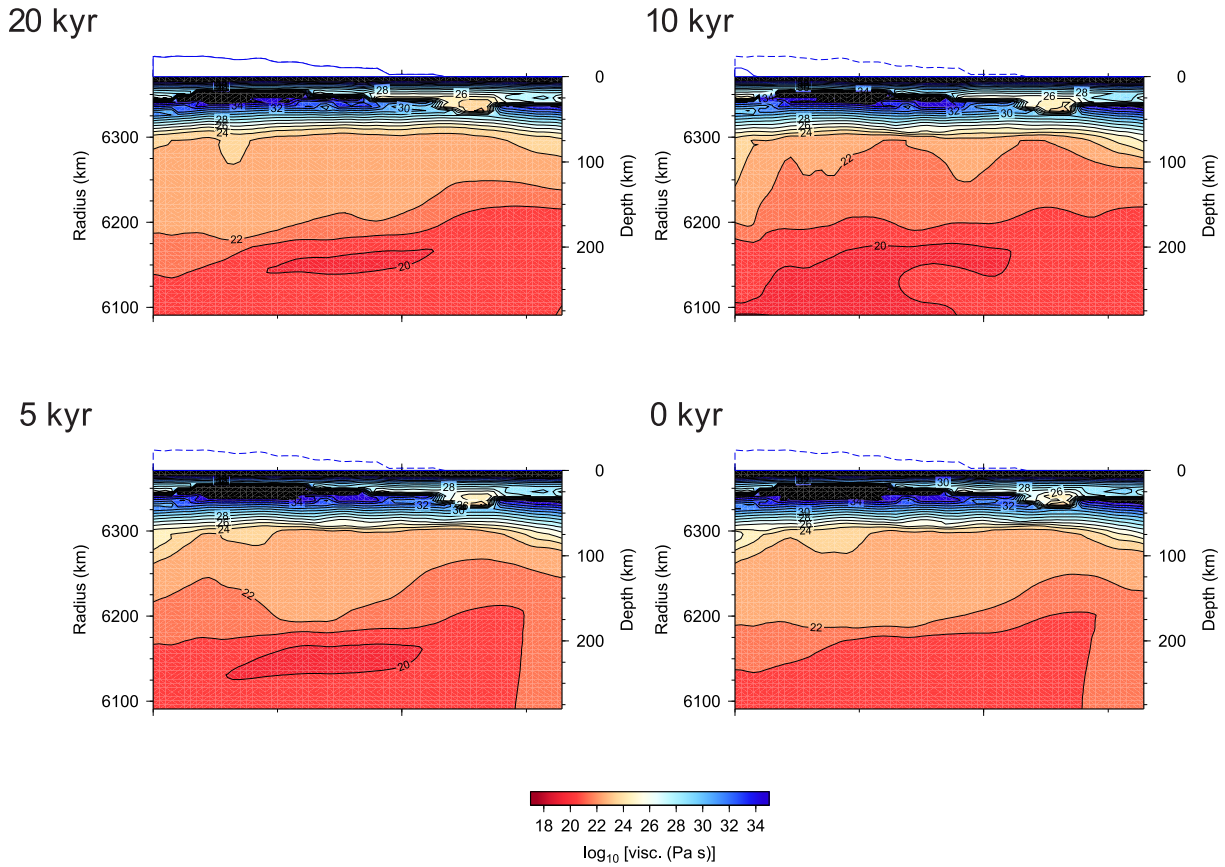

Fig. 2.: Effective viscosity at 20, 10, 5 and 0 ka before present day. Blue line at top shows the current extension of the ice sheet and the dashed line shows the extension at last glacial maximum.

References

Klemann, V., Martinec, Z. & Ivins, E. R. (2008). Glacial isostasy and plate motions, J. Geodyn., 46, 95–103, doi:10.1016/j.jog.2008.04.005.

Martinec, Z. (2000). Spectral–finite element approach for three-dimensional viscoelastic relaxation in a spherical earth, Geophys. J. Int., 142, 117–141, doi:10.1046/j.1365-246x.2000.00138.x.

Tesauro, M., Audet, P., Kaban, M. K., Bürgmann, R. & Cloetingh, S. (2012). The effective elastic thickness of the continental lithosphere: Comparison between rheological and inverse approaches, Geochem. Geophys. Geosyst., 13, 18, doi:10.1029/2012GC004162.

The 3D density and temperature distribution in an intracratonic basin setting: The Barents Sea and Kara Sea region

Peter Klitzke[1,2], Jan Inge Faleide[3], Judith Sippel[1], Magdalena Scheck-Wenderoth[1,2]

[1] *Helmholtz Centre Potsdam, GFZ German Center for Geosciences, Potsdam, Germany*
[2] *RHTW Aachen, Aachen, Germany*
[3] *Department of Geosciences, University of Oslo, Oslo, Norway*
e-mail: *klitzke@gfz-potsdam.de*
session: *Geodynamics*

Introduction

The Barents Sea and Kara Sea region as part of the European Arctic shelf is located in an intracratonical setting between the Proterozoic East-European Craton in the south and young Cenozoic passive margins in the north and the west. The region amalgamated during three major orogenies from latest Precambrian to late Paleozoic times (Breivik et al., 2002; Cocks and Torsvik, 2005; Gee et al., 2006; Gudlaugsson et al., 1998; Otto and Bailey, 1995; Puchkov, 2009; Ritzmann and Faleide, 2007; Roberts and Siedlecka, 2002) and subsequently, underwent multiple phases of locally varying subsidence (Breivik et al., 1998; Clark et al., 2013; Faleide et al., 1993; Gudlaugsson et al., 1998; Henriksen et al., 2011; Johansen, 1992). The present-day architecture of the sedimentary cover indicates different underlying crustal and lithospheric terranes and the influence of locally diverse causative geological processes. We assess how the density and temperature varies in response to the heterogeneous composition of the crystalline crust and the deeper lithosphere.

Therefore, a 3D structural model was developed resolving the sedimentary configuration, the crystalline crust and the lithospheric mantle. The sedimentary part is composed of four megasequences boundaries (pre-mid-Permian, mid-Jurassic, mid-Cretaceous and earliest Eocene. The geometries of the final 3D-structural model are well constrained as they are consistent with interpreted seismic refraction and reflection data, geological maps and previously published 3D-models.

The thickness distribution of each sedimentary megasequence varies strongly across the shelf indicating locally different development of the corresponding basins. The southwestern Barents Sea is characterized by narrow and elongated megasequence thickness maxima. Thereby, the distribution of sediment maxima indicates that the locus of major subsidence shifted towards the present-day continent-ocean boundary, thereby forming a fan-shaped basin system. The East Barents Sea Basin and the South Kara Sea Basin reveals a thick mid-Permian to mid-Jurassic megasequence indicating major subsidence back then. The overlying thinner sedimentary megasequences reveal that subsidence continued to early Cenozoic times in these two basins.

While the crystalline crust is thinned beneath regions where preserved sediments are thickest, the lithosphere-asthenosphere boundary (LAB) does not show any clear correlation with the sedimentary megasequences nor with the subsedimentary crust. Instead, the LAB as the base of the structural model, reveals a step-wise deepening structure towards the east. Thereby, levels of similar depths exhibit a clear correlation with the outline of sub-sedimentary crustal terranes

as defined by Marello et al. (2013).

The shallow LAB beneath the western Barents Sea (−60 km to −105 km) coincides with Caledonian Basement (southwest) and the Barentsia crustal block (northwest). Thereby, the local LAB depth configuration does not allow a clear differentiation of these two terranes. Late Cenozoic volcanism in the NW Barents Sea may have overprinted structural imprints of a Barentsia block. The eastern Barents Sea is underlain by LAB depths of about −150 km which widely correlates with the Timanian basement (Marello et al., 2013). The west coast of Novaya Zemlya exhibits the transition to the Uralian domain as observable by a major thickening of the lithosphere.

To extend the structural analysis in particular towards the composition of the subsiding crystalline crust we performed 3D gravity modelling. Therefore, the sedimentary units were assigned lithology-dependent matrix densities and porosities to calculate bulk densities which consider the effects of erosion, compaction as well as the maximum thickness of the late Cenozoic ice sheet. For the mantle (down to 250 km depth), we implemented a published velocity-density model (Levshin et al., 2007). To calculate an initial density configuration of the crystalline crust, the concept of Pratt's isostasy is applied and the resulting density distribution is used to define an upper and lower crust.

The obtained gravitational response of the parameterized 3D-structural model is compared with the observed gravity field to further investigate the composition of the lithosphere and particularly to define the extent of possible high-density bodies in the crystalline crust. To assess the major controlling factors of the thermal field, the obtained 3D-density model is used to calculate the lithosphere-scale 3D conductive thermal field of the Barents Sea and Kara Sea region. Consequently, the predicted thermal field is validated with measured borehole temperatures. Highest temperature are calculated for the westernmost Barents Sea, which is in accordance with the local rifting history (Fig. 1). Additionally, regions which are known to have experienced strong late Cenozoic uplift and erosion such as the NW Barents Sea and Svalbard reveal higher temperatures (Fig. 1). Beneath the remaining shelf areas minor positive temperature anomalies delineate the geometry of sedimentary basins (Fig. 1). Lowest continental temperatures occur beneath the mainland due to a lack of a thicker sedimentary coverage (Fig. 1).

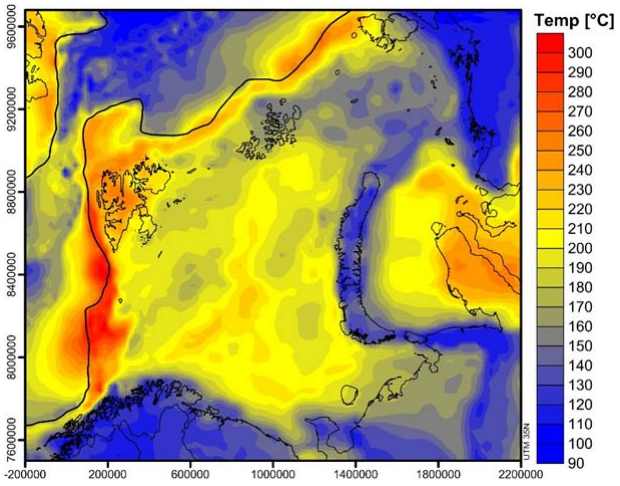

Fig. 1.: Temperature distribution @ −7 km depth.

The developed present-day 3D model provides an ideal base to reconstruct the subsidence/uplift history of the Barents Sea and Kara Sea region through time by considering also the compositional heterogeneities of the crystalline crust and the deeper lithosphere.

References

Breivik, A.J., Faleide, J.I., Gudlaugsson, S.T., 1998. Southwestern Barents Sea margin: late Mesozoic sedimentary basins and crustal extension. Tectonophysics 293, 21–44.

Breivik, A.J., Mjelde, R., Grogan, P., Shimamura, H., Murai, Y., Nishimura, Y., Kuwano, A., 2002. A possible Caledonide arm through the Barents Sea imaged by OBS data. Tectonophysics 355, 67–97.

Clark, S. a., Glorstad-Clark, E., Faleide, J.I., Schmid, D., Hartz, E.H., Fjeldskaar, W., 2013. Southwest Barents Sea rift basin evolution:

comparing results from backstripping and time-forward modelling. Basin Res.

Cocks, L.R.M., Torsvik, T.H., 2005. Baltica from the late Precambrian to mid-Palaeozoic times: The gain and loss of a terrane's identity. Earth-Science Rev. 72, 39–66.

Faleide, J.I., Vågnes, E., Gudlaugsson, S.T., 1993. Late Mesozoic-Cenozoic evolution of the south-western Barents Sea in a regional rift-shear tectonic setting. Mar. Pet. Geol. 10, 186–214.

Gee, D., Bogolepova, O.K., Lorenz, H., 2006. The Timanide, Caledonide and Uralide orogens in the Eurasian high Arctic, and relationships to the palaeo-continents Laurentia, Baltica and Siberia. Geol. Soc. London, Mem. 32, 507–520.

Gudlaugsson, S., Faleide, J.I., Johansen, S.E., Breivik, A.J., 1998. Late Palaeozoic structural development of the South-western Barents Sea. Mar. Pet. Geol. 15, 73–102.

Henriksen, E., Ryseth, a. E., Larssen, G.B., Heide, T., Ronning, K., Sollid, K., Stoupakova, a. V., 2011. Chapter 10 Tectonostratigraphy of the greater Barents Sea: implications for petroleum systems. Geol. Soc. London, Mem. 35, 163–195.

Johansen, S.E.., 1992. Hydrocarbon potential in the Barents Sea region: play distribution and potential. Arct. Geol. Pet. Potential 2, 273–320. Marello, L., Ebbing, J., Gernigon, L., 2013. Basement inhomogeneities and crustal setting in the Barents Sea from a combined 3D gravity and magnetic model. Geophys. J. Int. 193, 557–584.

Levshin, A.L., Schweitzer, J., Weidle, C., Shapiro, N.M., Ritzwoller, M.H., 2007. Surface wave tomography of the Barents Sea and surrounding regions. Geophys. J. Int. 170, 441–459.

Marello, L., Ebbing, J., Gernigon, L., 2013. Basement inhomogeneities and crustal setting in the Barents Sea from a combined 3D gravity and magnetic model. Geophys. J. Int. 193, 557–584.

Otto, S., Bailey, R., 1995. Tectonic evolution of the northern Ural Orogen. J. Geol. Soc. London. 152, 903–906.

Puchkov, V.N., 2009. The evolution of the Uralian orogen. Geol. Soc. London, Spec. Publ. 327, 161–195.

Ritzmann, O., Faleide, J.I., 2007. Caledonian basement of the western Barents Sea. Tectonics 26, 1–20.

Roberts, D., Siedlecka, a., 2002. Timanian orogenic deformation along the northeastern margin of Baltica, Northwest Russia and Northeast Norway, and Avalonian–Cadomian connections. Tectonophysics 352, 169–184.

The effect of melting and crustal production on plate tectonics on terrestrial planets

Diogo L. Lourenço, Paul J. Tackley

Institute of Geophysics, Department of Earth Sciences, ETH Zürich, Switzerland
e-mail: *diogo.lourenco@erdw.ethz.ch*
session: *Geodynamics*

Within the Solar System, Earth is the only planet to be in a mobile-lid regime, whilst it is generally accepted that all the other terrestrial planets are currently in a stagnant-lid regime, showing little or no surface motion. A transitional regime between these two, showing episodic overturns of an unstable stagnant lid, is also possible and has been proposed for Venus (Armann and Tackley, JGR 2012).

Using plastic yielding to self-consistently generate plate tectonics on an Earth-like planet with strongly temperature-dependent viscosity is now well-established, but such models typically focus on purely thermal convection, whereas compositional variations in the lithosphere can alter the stress state and greatly influence the likelihood of plate tectonics. For example, Rolf and Tackley (GRL, 2011) showed that the addition of a continent can reduce the critical yield stress for mobile-lid behaviour by a factor of around 2. Moreover, it has been shown that the final tectonic state of the system can depend on the initial condition (Tackley, G3 2000 – part 2); Weller and Lenardic (GRL, 2012) found that the parameter range in which two solutions are obtained increases with viscosity contrast.

We can also say that partial melting has a major role in the long-term evolution of rocky planets: (1) partial melting causes differentiation in both major elements and trace elements, which are generally incompatible (Hofmann, Nature 1997). Trace elements may contain heat-producing isotopes, which contribute to the heat loss from the interior; (2) melting and volcanism are an important heat loss mechanism at early times that act as a strong thermostat, buffering mantle temperatures and preventing it from getting too hot (Xie and Tackley, JGR 2004b); (3) mantle melting dehydrates and hardens the shallow part of the mantle (Hirth and Kohlstedt, EPSL 1996) and introduces viscosity and compositional stratifications in the shallow mantle due to viscosity variations with the loss of hydrogen upon melting (Faul and Jackson, JGR 2007; Korenaga and Karato, JGR 2008).

We present a set of 2D spherical annulus simulations (Hernlund and Tackley, PEPI 2008) using StagYY (Tackley, PEPI 2008), which uses a finite-volume scheme for advection of temperature, a multigrid solver to obtain a velocity-pressure solution at each timestep, tracers to track composition, and a treatment of partial melting and crustal formation. We address the question whether melting-induced crustal production changes the critical yield stress needed to obtain mobile-lid behaviour as a function of governing parameters.

Our results show that melting and crustal production strongly influence plate tectonics on terrestrial planets. For the same parameters the use of a treatment for melting and crustal production facilitates breaking the stagnant-lid, replacing it with episodic-lid; however, a smoothly evolving mobile lid can also be replaced by episode-lid. Several factors can play a role on these, namely lateral heterogeneities, differences in the lid thickness and internal planetary temperatures induced by melting and crustal production.

3-D numerical modelling of subduction initiation at curved passive margins

F. O. Marques, F. R. Cabral, T. V. Gerya, G. Zhu, D. A. May

Department of Earth Sciences, Swiss Federal Institute of Technology (ETH Zurich), CH-8092 Zurich, Switzerland
e-mail: *fomarques@fc.ul.pt*
session: *Geodynamics*

Subduction initiation at straight passive margins can be investigated with 2-D numerical models, because the geometry is cylindrical (Fig. 1B).

However, on Earth, straight margins rarely occur. The construction of 3-D models is therefore critical in the modelling of spontaneous subduction initiation at realistic, curved passive margins (Fig. 1A).

Here we report on the results obtained from gravitationally driven, 3-D thermomechanical numerical models using a visco-plastic rheology and a passive margin with a single curved section in the middle. The models show that the curvature angle β (Fig. 1A) can control subduction initiation: the greater β is, the more difficult subduction initiation becomes (Figs. 1–3).

The 3-D thermomechanical models provide an in-depth physical understanding of the processes (Figs. 4–6). Temperature is a critical parameter because it controls density, thus affecting stresses and pressure gradients. In the initial stage, isotherms are horizontal, but this configuration rapidly changes with deformation (Fig. DR1). If subduction initiation is fast, as in models 1 and 2, then thermal re-equilibration of the sinking slab with the surrounding mantle is delayed. Hence, the slab remains cold to great depths, the density contrast with the mantle is maintained (cold slab in hot mantle), and the oceanic slab thus sinks rapidly. There is, therefore, a positive feedback between temperature and the sinking velocity of the oceanic slab (e. g., McKenzie, 1977), which can be further enhanced if the cold oceanic slab

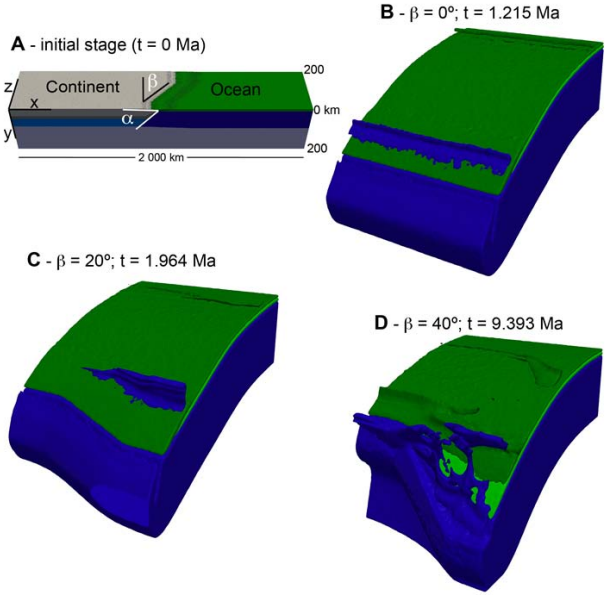

Fig. 1.: Initial stage (A) and final results (B–D) of modelling. The initial stage shows a zig-zag structure to simulate a curved margin, lengths of continent and ocean, and angles α and β. α is the dip of continent-ocean lithospheric boundary surface, and is $45°$ for all models; β is the angle between the trace of the curved section of the margin at the Earth's surface and the z-axis, and is $0°$ (model 1 in B), $20°$ (model 2 in C), or $40°$ (model 3 in D). t – time to subduction initiation

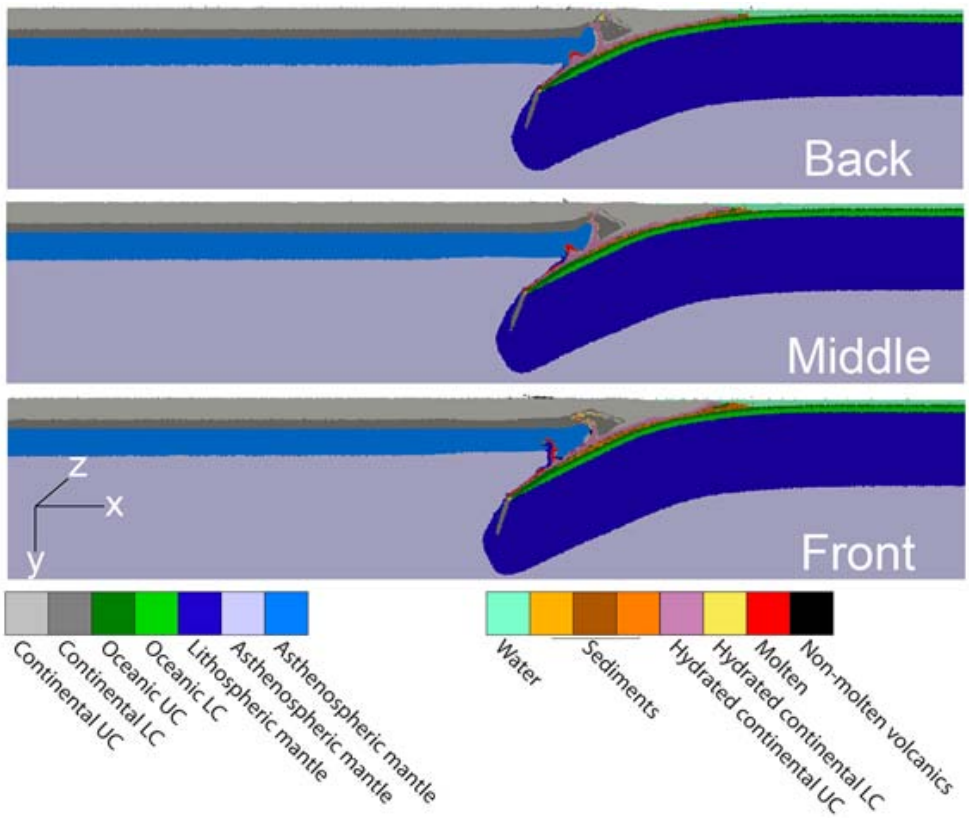

Fig. 2.: Sections through the end result (at $1.964\,\mathrm{Ma}$) of model 2 with $\beta = 20°$, at $z = 0\,\mathrm{km}$ (front wall), $z = 100\,\mathrm{km}$ (middle), and $z = 200\,\mathrm{km}$ (back wall). Note that the oceanic slab reaches $200\,\mathrm{km}$ depth (subduction proper) faster in the front than in the back. UC – upper crust; LC – lower crust.

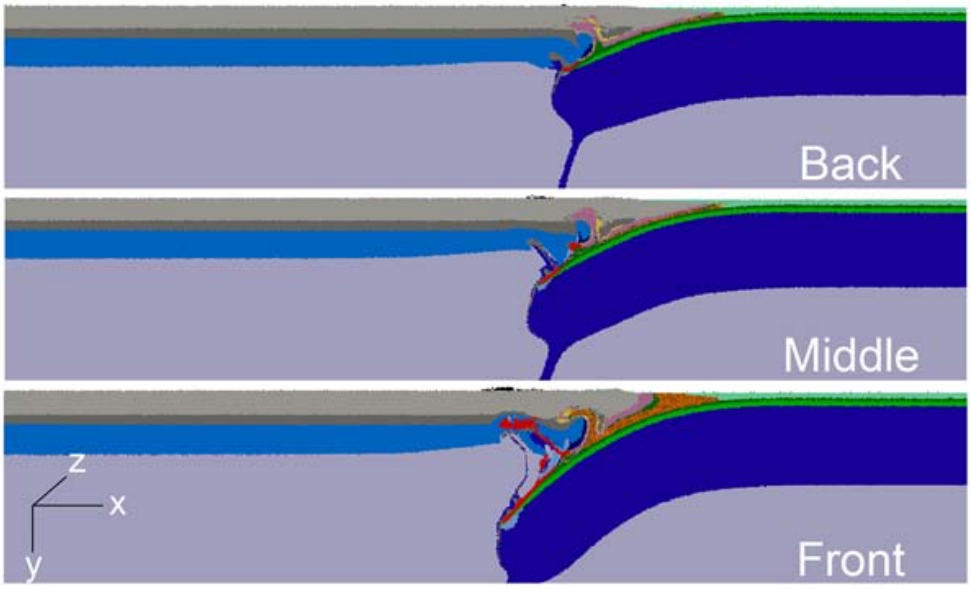

Fig. 3.: Sections through the end result (at $9.393\,\mathrm{Ma}$) of model 3 with $\beta = 40°$, at $\beta = 20°$, at $z = 0\,\mathrm{km}$ (front wall), $z = 100\,\mathrm{km}$ (middle), and $z = 200\,\mathrm{km}$ (back wall). Note that the oceanic slab reaches $200\,\mathrm{km}$ depth (subduction proper) in the front of the model, but not in the back. Colours as in Fig. 2.

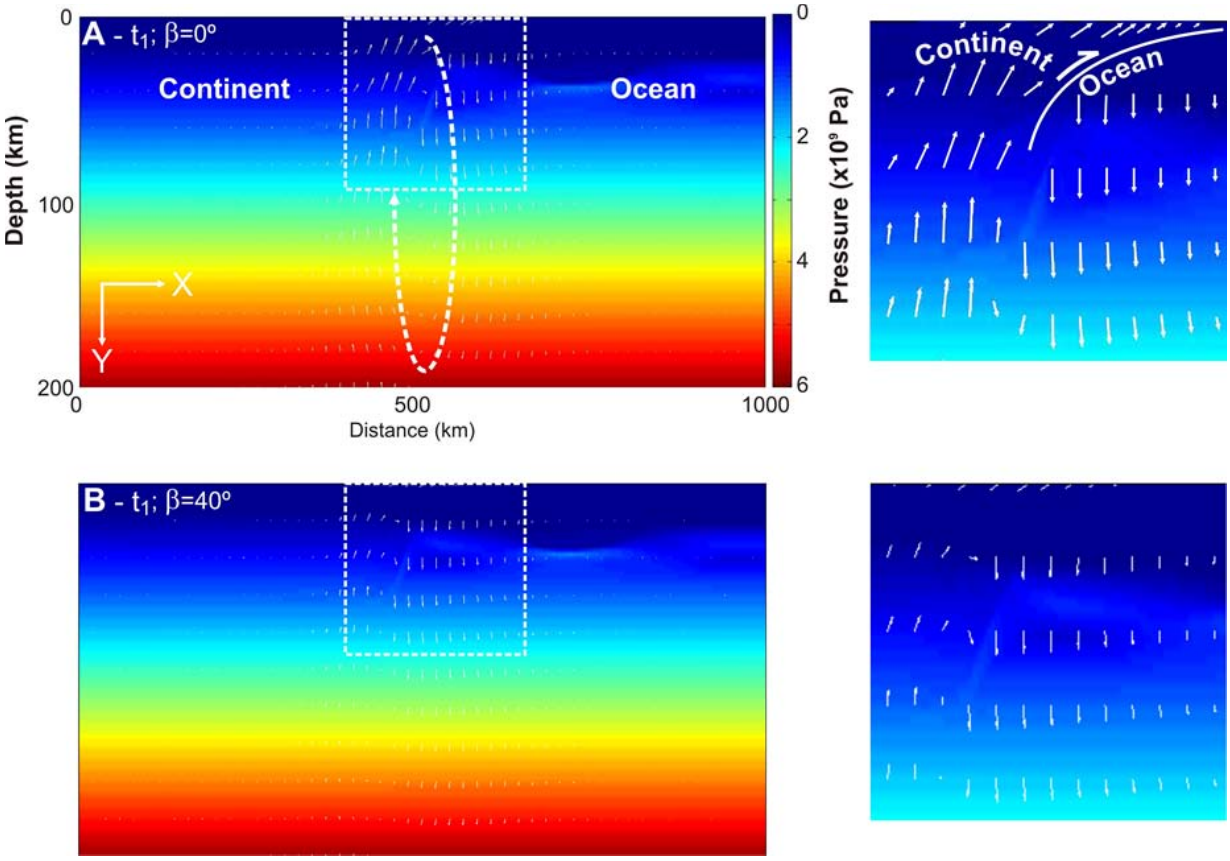

Fig. 4.: Velocity vectors (white arrows) overlain on pressure maps (coloured). The difference in the size of velocity vectors in A (bigger) and B (smaller) indicates why an increase in β hampers subduction initiation. Insets on right are close-ups of the dashed square areas marked in A and B.

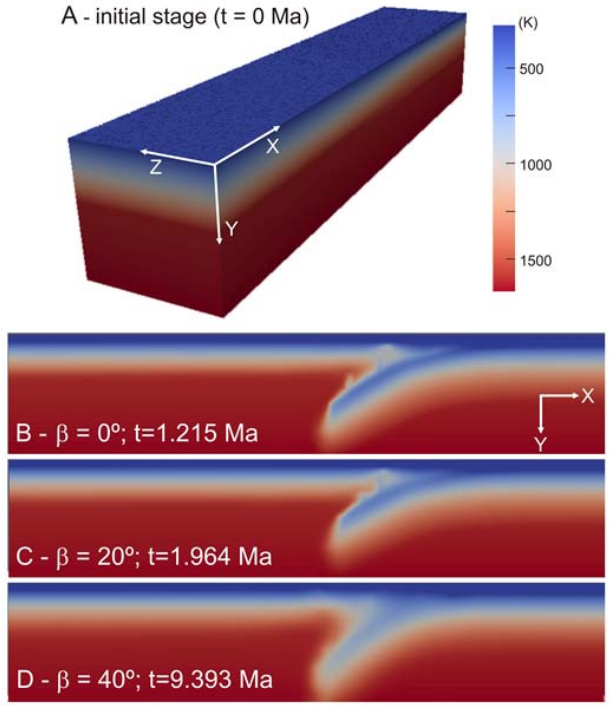

Fig. 5.: Color maps representing the model temperatures in the initial stage (A), and at the front wall in the last stage of Models 1, 2 and 3. Note the higher temperature, from B to D, in the core of the sinking slab.

transforms into high-density eclogite (not modelled).

Specifically, we find that pressure gradients (Fig. 4), arising from density differences between oceanic and continental rocks, drive subduction initiation, and strongly influence the timing. The main difference between straight (cylindrical) and curved margins is that the orientation of the pressure gradient in 3-D is no longer constant, thus producing a horizontal, along-margin component of flow (Fig. 6). We thus conclude that the reason for the impedance of subduction initiation is the result of partitioning of the vertical velocity component into a horizontal component, which therefore decreases the effective slab pull.

We infer that, although favourable for subduction initiation in a 2-D model, because the estimated force balance is adequate, the pronounced curvature in the southeast Brazilian margin is a likely explanation why subduction initiation is hampered there.

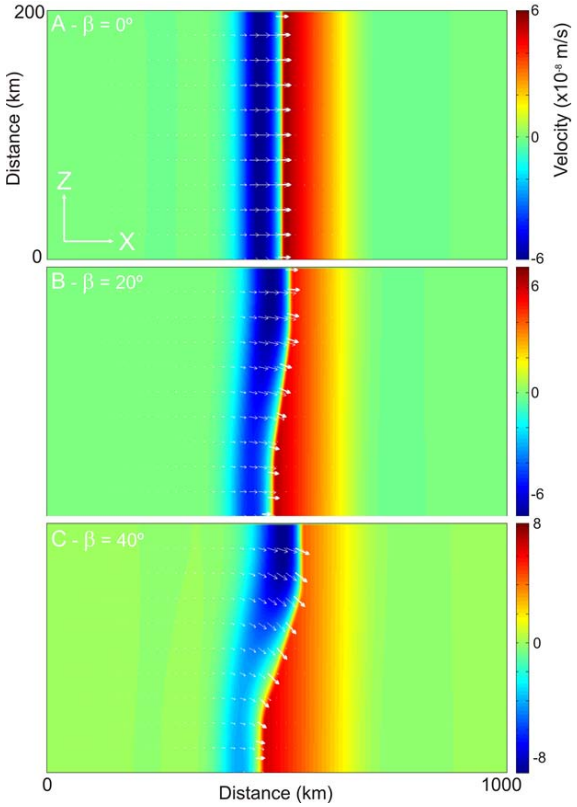

Fig. 6.: XZ plots of the velocity field. In color the Y component, and as vectors (white arrows) the XZ component. A, B and C for Models 1, 2 and 3 respectively. Note the great incorporation of the Z component, towards the front wall (bottom), from A to C. Zero in A, as expected for a 2D equivalent model, and maximum in C. Positive and negative values in the scale bar mean downward and upward flows, respectively.

Crustal deformation and magmatism at the transition between subduction and collisional domains: insight from 3D numerical modeling

Armel Menant[1,2,3], Pietro Sternai[1,2,3], Laurent Jolivet[1,2,3], Laurent Guillou-Frottier[2,1,3], Taras Gerya[4]

[1] *Université d'Orléans, ISTO, UMR 7327, Orléans, France*
[2] *BRGM, ISTO, UMR 7327, 45060 Orléans, France*
[3] *CNRS/INSU, UMR 7327, 45071 Orléans, France*
[4] *Swiss Federal Institute of Technology (ETH), Zurich, Switzerland*
e-mail: *armel.menant@cnrs-orleans.fr*
session: *Geodynamics*

Geodynamic evolution of subduction zones is often complex, due to the variable nature and rheology of interacting lithospheres, 3D slab geometry and related mantle flow. In order to understand the temporal evolution of this dynamics, the long-term geological record should be considered, including the present-day kinematics, the long-term history of deformation and magmatism within the upper plate. This leads to conceptual models that imply complex physical processes that can be tested through numerical modeling.

In this study, we focus on the eastern Mediterranean region where a long-lived subduction zone has been active since the Mesozoic. In this region, the Tethyan active margin is characterized by successive subductions of oceanic and continental ribbons, slab retreat episodes and possible slab tearing processes, notably interpreted from tomographic models showing low-velocity anomaly below Anatolia [Ricou et al., 1986; Piromallo and Morelli, 2003; van Hinsbergen et al., 2005a; Jolivet et al., 2013].

Using G-Plates software, we first modeled the kinematic evolution of the eastern Mediterranean in the last 100 Myrs, accounting for a large number of geological data, including the magmatic occurrences (figure 1). Since 35-30 Ma, the geodynamics of this region has been dominated by the subduction and collision of Arabia with Eurasia and with the development of a large back-arc domain in the Aegean region, resulting from an increase of the rate of slab retreat. This slab retreat is associated with the southward migration of high-potassic magmatism in the back-arc domain with time, and with the southwest fast migration of the Aegean plutons during the middle Miocene from the Menderes to the Cyclades (figure 1).

In addition, a major change occurred in the dynamics of the back-arc opening in the middle Miocene (figure 1) with a new increase of the rate of trench retreat and large-scale block rotations on the edge of this extensional domain in the Hellenides and in western Anatolia [Kissel and Laj, 1988; van Hinsbergen et al., 2005b]. This kinematic change is coeval with the southwest migration of the back-arc plutons and with the increase of their mantle component compared to their crustal component from east to west [Altherr and Siebel, 2002]. Finally, sparse alkaline volcanism emplaced in the Aegean and western Anatolia since ~15 Ma with the same westward migration trend, indicating a hot asthenospheric upwelling associated with a low rate of partial melting [Dilek and Altunkaynak, 2009].

Using high-resolution 3D thermo-mechanical

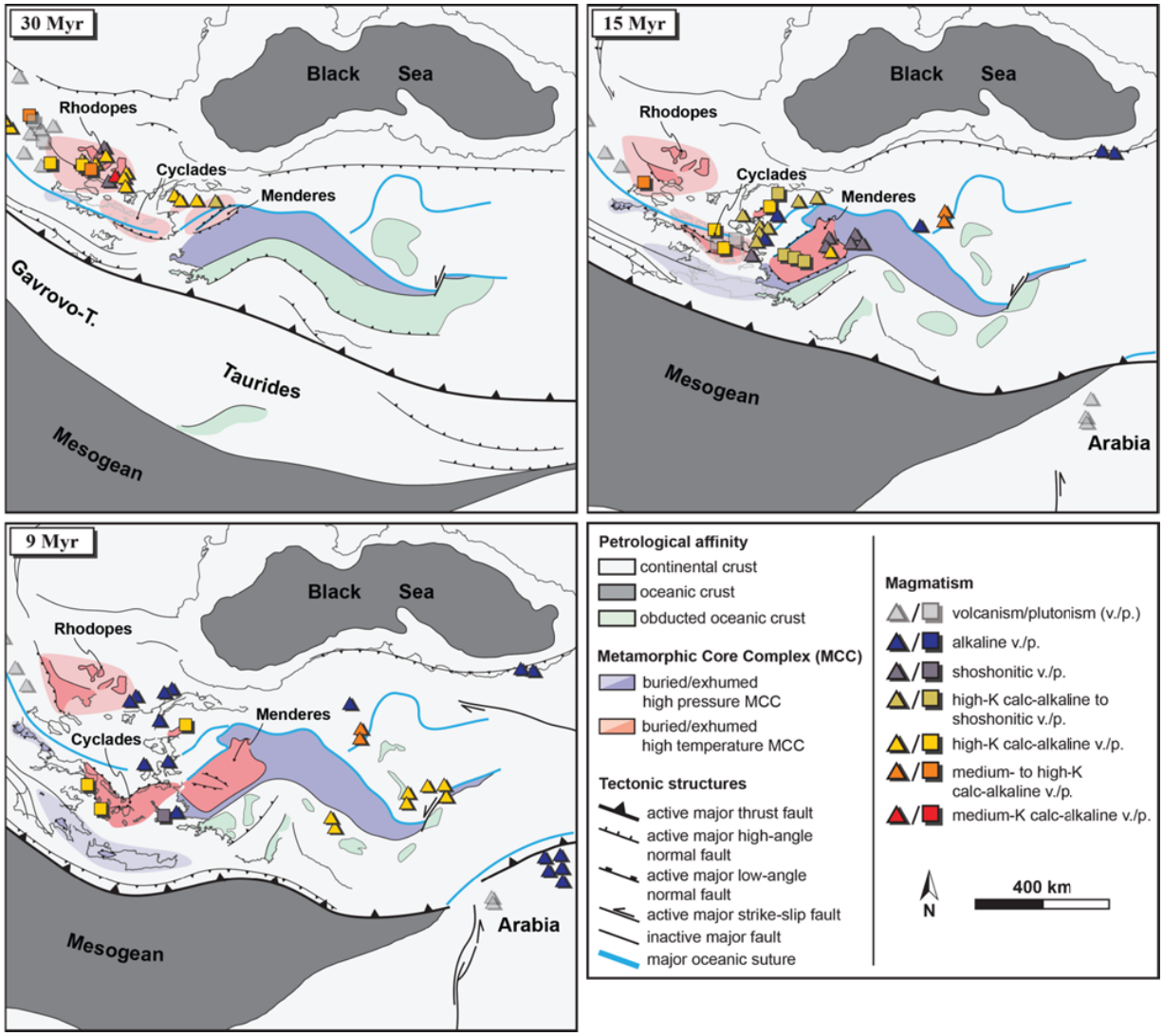

Fig. 1.: Kinematic reconstructions of eastern Mediterranean region at 30, 15 and 9 Ma, highlighting the main metamorphic, tectonic and magmatic features.

numerical modeling, we reproduce a relatively simple model of retreating subduction neighboring a collisional domain that we compare with these geological observations. These numerical experiments are performed with the code I3ELVIS, considering non-newtonian visco-plastic rheologies and notably integrating partial melting and melt extraction processes as well as fluid and melt transport mechanism [Gerya and Yuen, 2003; Zhu et al., 2013]. The resolved grid has a resolution of 3.4, 2.5 and 4.4 km in the x, y and z dimensions respectively and ~130 millions additional randomly distributed moving markers.

The initial model setup shows an oceanic lithosphere and a continental plate (considered as Arabia) converging toward a continental upper plate (considered as Eurasia) (figure 2a). The evolution of the model shows first the subduction of the oceanic crust then of the continental crust below the upper plate margin that is stretched as a result of the trench retreat (figure 2b). When the contient buoyancy and the slab pull forces overstep the strength of the lithosphere, the slab is torn first horizontally then vertically along the subducted continental margins (figure 2c). The slab tear results in the exhumation and the re-

bound of the subducted continental crust and the establishing of a collisional regime (figure 2c). Aside of the collisional domain, the oceanic subduction protracts for longer and slab roll-back and trench retreat occur as faster rates since the slab tearing reduced the along-strike dimension of the slab (figure 2c). Consequently, the upper plate extension rates increase and strike-slip deformation accommodates the rotation of crustal blocks.

The rebound of the subducted continental crust following the slab tearing, combined with 3D mantle flow, carries partially molten mantle wedge toward the base of the stretched upper continental plate (figure 3a). This material then migrates progressively toward the subducting oceanic plate replacing progressively the partially hydrated and molten crustal material previously developed in the back-arc region (figures 3b and 3c). Finally, asthenospheric material rises at the base of the crust, undergoing a possible adiabatic partial melting inducing the development of an alkaline volcanism at the surface (figure 3).

Results from these numerical experiments show a tectonic and magmatic evolution that can be compared to the geological observations across the eastern Mediterranean region. This exercise shows the potential of this double-sided approach involving an independent reconstruction of the long-term evolution of subduction zones based on kinematic reconstructions and 3D thermomechanical numerical modeling to investigate the complex interactions between slab behavior, magmatic history, mantle flow and crustal deformation.

References

Altherr, R., and W. Siebel (2002), I-type plutonism in a continental back-arc setting: Miocene granitoids and monzonites from the central Aegean Sea, Greece, Contributions to Mineralogy and Petrology, 143(4), 397–415, doi:10.1007/s00410-002-0352-y.

Dilek, Y., and S. Altunkaynak (2009), Geochemical and temporal evolution of Cenozoic magmatism in western Turkey: mantle response to collision, slab break-off, and lithospheric tearing in an orogenic belt, Geological Society, London, Special Publications, 311(1), 213–233, doi:10.1144/SP311.8.

Gerya, T. V., and D. A. Yuen (2003), Characteristics-based marker-in-cell method with conservative finite-differences schemes for modeling geological flows with strongly variable transport properties, Physics of the Earth and Planetary Interiors, 140(4), 293–318, doi:10.1016/j.pepi.2003.09.006.

Jolivet, L. et al. (2013), Aegean tectonics: Strain localisation, slab tearing and trench retreat, Tectonophysics, 597-598, 1–33, doi:10.1016/j.tecto.2012.06.011.

Kissel, C., and C. Laj (1988), The Tertiary geodynamical evolution of the Aegean arc: a paleomagnetic reconstruction, Tectonophysics, 146(1-4), 183–201, doi:10.1016/0040-1951(88)90090-X.

Piromallo, C., and A. Morelli (2003), P wave tomography of the mantle under the Alpine-Mediterranean area, Journal of Geophysical Research, 108(B2), doi:10.1029/2002JB001757.

Ricou, L. E., J. Dercourt, J. Geyssant, C. Grandjacquet, C. Lepvrier, and B. Biju-Duval (1986), Geological constraints on the alpine evolution of the Mediterranean Tethys, Tectonophysics, 123(1-4), 83–122, doi:10.1016/0040-1951(86)90194-0.

van Hinsbergen, D. J. J., E. Hafkenscheid, W. Spakman, J. E. Meulenkamp, and R. Wortel (2005a), Nappe stacking resulting from subduction of oceanic and continental lithosphere below Greece, Geology, 33(4), 325, doi:10.1130/G20878.1.

van Hinsbergen, D. J. J., C. G. Langereis, and J. E. Meulenkamp (2005b), Revision of the timing, magnitude and distribution of Neogene rotations in the western Aegean region, Tectonophysics, 396(1-2), 1–34, doi:10.1016/j.tecto.2004.10.001.

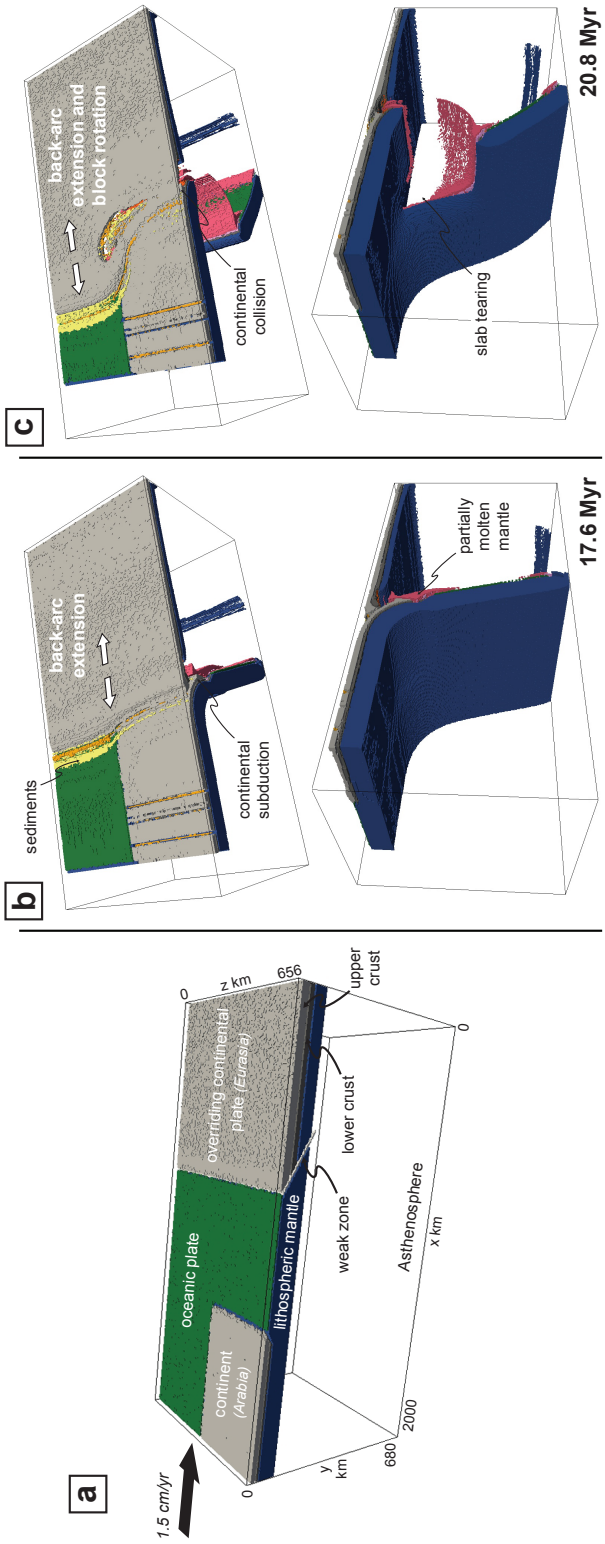

Fig. 2.: 3D thermo-mechanical modeling of retreating subduction neighboring a collisional domain. (a) Initial setup of the 3D model domain with colors showing different rock types. (b, c) Evolution of the reference model at 17.6 and $20.8\,\mathrm{Ma}$. The top layer ("sticky air", $y < 12\,\mathrm{km}$) and the asthenosphere are cut off for clarity.

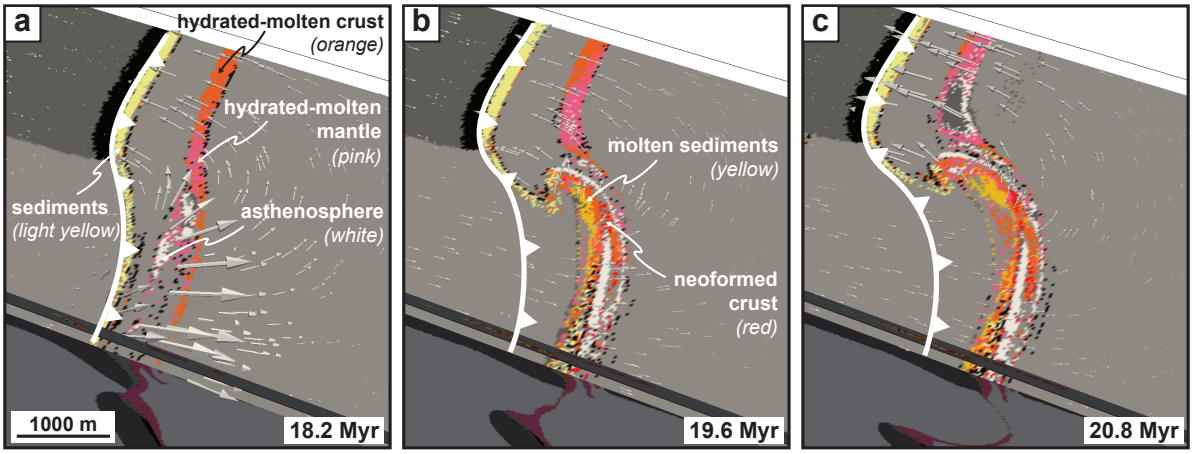

Fig. 3.: 35 km-depth horizontal cross-section of the reference model, corresponding to the base of the stretched continental crust, highlighting the different hydrated and partially molten phases. (a, b, c) Evolution of the model at 18.2, 19.6 and .20.8 Myr.

Zhu, G., T. V. Gerya, P. J. Tackley, and E. Kissling (2013), Four-dimensional numerical modeling of crustal growth at active continental margins, Journal of Geophysical Research: Solid Earth, 118(9), 4682–4698, doi:10.1002/jgrb.50357.

Segregation, Accumulation, and Entrainment of the Oceanic Crust in the Lowermost Mantle: Exploring the Range of Governing Parameters with Numerical Modelling

Elvira Mulyukova[1], Bernhard Steinberger[1,2], Marcin Dabrowski[2,3], Stephan V. Sobolev[1]

[1] *GFZ German Research Center for Geosciences, Physics of the Earth, Potsdam, Germany*
[2] *Physics of Geological Processes, University of Oslo, Oslo, Norway*
[3] *Computational Geology Laboratory, Polish Geological Institute - National Research Institute, Wroclaw, Poland*
e-mail: *mulyukov@gfz-potsdam.de*
session: *Geodynamics*

Introduction

One of the most robust results from tomographic studies is the existence of two antipodally located Large Low Shear Velocity Provinces (LLSVPs) at the base of the mantle, which appear to be chemically denser than the ambient mantle. Results from reconstruction studies (Torsvik et al., 2006) infer that the LLSVPs are stable, long-lived, and are sampled by deep mantle plumes that rise predominantly from their margins.

The amount of the anomalous LLSVP-material that gets entrained into the rising plumes poses a constraint on the survival time of the LLSVPs, as well as on the plume buoyancy, on the lithospheric uplift associated with plume interaction, and geochemical signature of the erupted lavas observed at the Earth's surface. Recent estimates for the plume responsible for the formation of the Siberian Flood Basalts give about 15 % of entrained dense recycled oceanic crust, which made the hot mantle plume almost neutrally buoyant (Sobolev et al., 2011). In order for the entrainment to take place, the destabilizing viscous stresses acting on a volume of anomalously dense material at the CMB must exceed the gravitationally stabilizing stresses associated with its buoyancy. At what conditions are these criteria met in a dynamically active deep mantle?

While hot rising plumes may act as a sink that entrains the dense material away from the CMB, the subducting slabs that bring compositionally dense oceanic crust (OC) into the lowermost mantle, may act as a source of the dense material. A key questions is: at what conditions can a relatively thin (~ 6 km) layer of OC-material segregate at the CMB and contribute to, or even form, the large-scale compositional anomaly?

To investigate this question, we perform high-resolution numerical simulations of thermochemical convection in 2D domains: both Cartesian and hollow cylinder. For this purpose, we have developed a FEM code with particle-in-cell methodology, building on efficient solvers MILAMIN (Dabrowski et al., 2008), together with packages MUTILS (Krotkiewski and Dabrowski, 2013), and Triangle (Shewchuk, 1996) .

Results

In agreement with other studies, we find that the parameters that govern segregation, accumulation, and entrainment of compositional anomalies are the buoyancy ratio (chemical to thermal, where the latter is computed for the temperature difference across the whole layer), as well as the thermally and compositionally induced viscosity variations. An illustrative result of our simulations is presented in Figures 1–3, where the

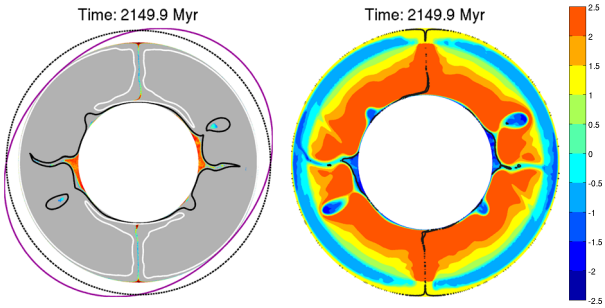

Fig. 1.: Snapshot from one of the simulations to explain the set-up of numerical experimets of segregation of subducted oceanic crust (OC). Left plot: Color-field in the cylinder interior represents the fraction of OC material (computed for each grid-element) – red means pure OC-material. Regions where OC-fraction is less than 0.2 are colored gray. The black and white lines are hot ($T^* = 0.6$) and cold ($T^* = 0.3$) isotherms, respectively (where T^* is the nondimensional temperature). The purple line on the exterior illustrates the direction of the imposed angular velocity boundary conditions (negative means clockwise) – black dashed line indicates the zero angular velocity value. Right plot: Base ten logarithm of viscosity, according to the applied depth- and temperaure-dependent viscosity-profile from (Steinberger & Calderwood, 2006). The black contours represent the OC-fraction value of 0.5. The compositional density anomaly in the presented case is ~1.8 %, corresponding to a buoyancy ratio of ~0.57.

effect of buoyancy ratio of the OC-material on the thermochemical evolution is demonstrated.

The results of our numerical models illustrate that there is both thermal and mechanical feedback between the compositionally distinct materials. The amount of basal heat that flows into the ambient material, and provides the excess buoyancy to drive the convective flow, depends on the volume, or topography, of the anomalously dense material at the CMB. This is largely due to the thermally insulating effect of the latter. The topography of the compositionally dense material, in turn, depends on the flow of the ambient material: the dense material is thickened beneath the upwelling flow, and thinned, or absent, beneath the downwelling flow. The amount of thickening or thinning of the dense basal material is proportional to the strength of the ambient flow.

In cases when the anomalouly dense OC-material manages to accumulate at the CMB, the resulting piles are typically comprised of a mixture of both materials, rather than pure OC-material (based on simulations with two materials: OC and ambient mantle). This is due to two processes. First, the OC-material is introduced into the lowermost mantle as a very thin layer, incapable of complete segregation from its surrounding ambient material. It is, however, capable of slightly reducing the upward flow in its vicinity, albeit on a larger lengthscale. Thus, by retarding its own ascent into the rising plumes, it retards the ascent of the ambient material to which it is viscously coupled, thus both materials end up constituting the piles. The second process that influences the compositional mixture of the dense piles is the convective flow that may develop in the piles interior. This can lead to entrainment of the ambient material into the dense pile-material, further diluting the mixture. The process of convective flow in the dense pile interior leads to a decrease of the piles effective buoyancy ratio over time, increasing its topography and facilitating its entrainment into plumes. The efficiency of this process, compared to the efficiency with which new dense material gets added to the pile, determines the piles survival-time.

References

M. Dabrowski, M. Krotkiewski, and DW Schmid. MILAMIN: MATLAB-based finite element method solver for large problems. Geochemistry Geophysics Geosystems, 9(4):Q04030, 2008. ISSN 1525-2027.

M. Krotkiewski and M. Dabrowski. Mutils - a set of efficient modeling tools for multi-core CPUs implemented in mex. In EGU General Assembly Conference Abstracts, volume 15, page 7877, 2013.

J. Shewchuk. Triangle: Engineering a 2d quality mesh generator and delaunay triangulator. Applied computational geometry towards geometric engineering, pages 203–222, 1996.

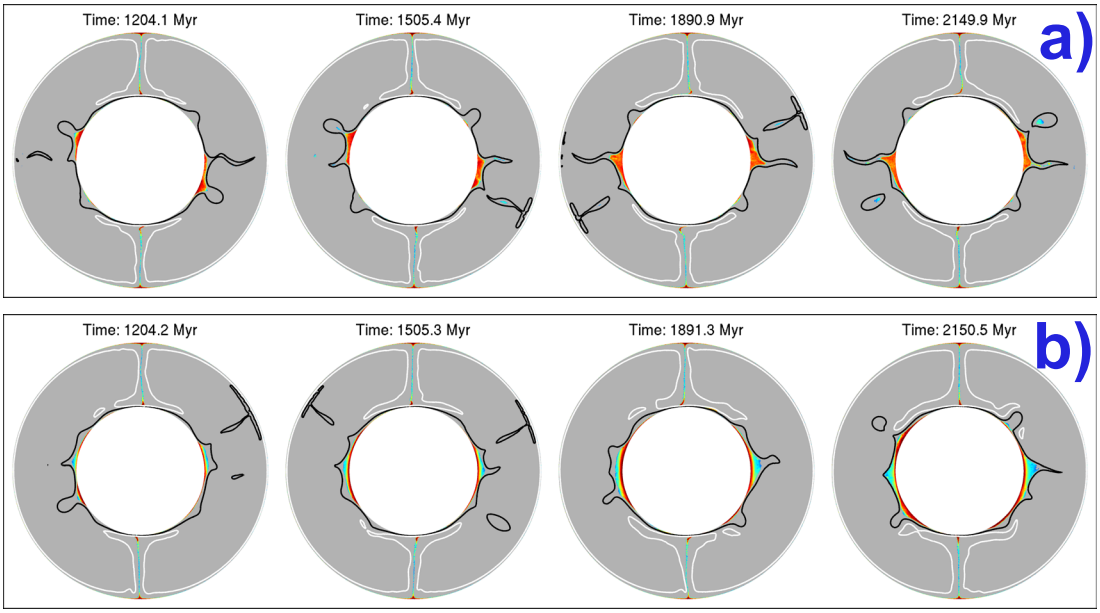

Fig. 2.: Snapshots from the results of two numerical experimets of segregation of subducted oceanic crust (OC), for two different buoyancy ratios (Br). The compositional density anomaly of OC-material is ~1.8 % (Br ~0.57) in the simulation presented in the top row, and ~3.6 % (Br ~1.14) in the bottom row. Explanation of the colors and the set-up is presented in Figure 1. Dense piles of accumulated OC-material formed in case a) have a smaller lateral extent than the piles formed in case b). Further, piles in case a) are constituted by a more homogeneous mixture of OC- and the ambient materials, compared to case b) – where a vertical gradient of the fraction of OC-material within the pile can be observed.

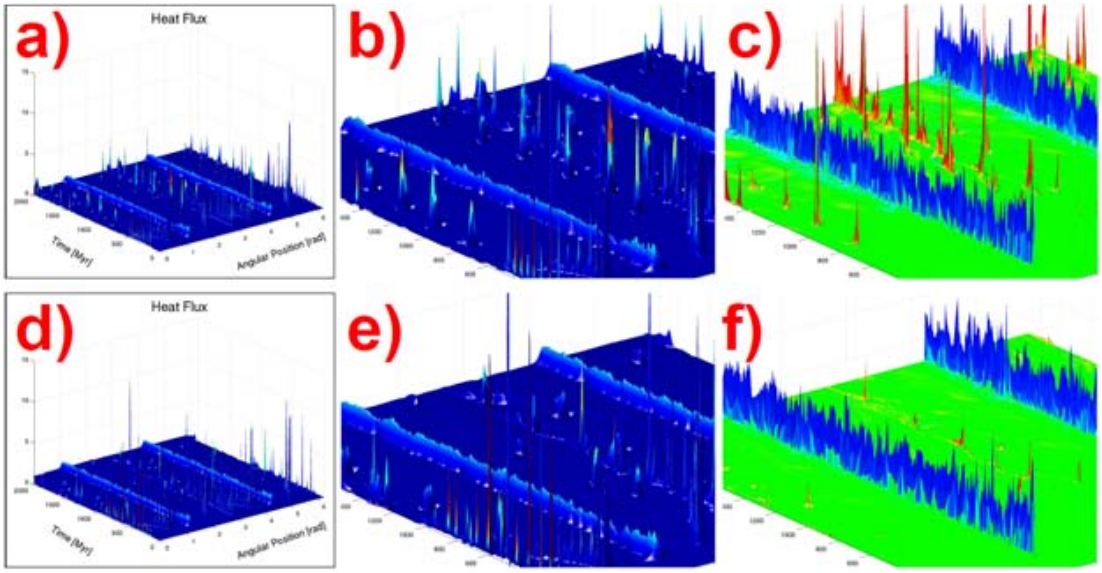

Fig. 3.: Heat (a), b), d), e)) and OC-material (c) and f)) flux over time, measured at mid-depth, for the two simulations presented in Figure 2. Plots b) and e) are zoom-ins on plots a) and d). All values are nondimensional, and scaled to the values measured at the downwelling regions. In plots c) and f) – blue means OC-material flows downwards – towards the CMB, and red means it flows upwards (due to entrainment by rising plumes). Higher heat flux and more efficient entrainment of dense material by plumes can be observed for the simulation with lower buoyancy ratio (case a) in Figure 2).

S.V. Sobolev, A.V. Sobolev, D.V. Kuzmin, N.A. Krivolutskaya, A.G. Petrunin, N.T. Arndt, V.A. Radko, and Y.R. Vasiliev. Linking mantle plumes, large igneous provinces and environmental catastrophes. Nature, 477(7364):312–316, 2011.

T.H. Torsvik, M.A. Smethurst, K. Burke, and B. Steinberger. Large igneous provinces generated from the margins of the large low-velocity provinces in the deep mantle. Geophysical Journal International, 167(3):1447–1460, 2006. ISSN 1365-246X.

Role of extensional strain-rate on lithosphere necking architecture during continental rifting

Nestola, Y.,[1], F. Storti[1], C. Cavozzi[1]

[1]*NEXT – Natural and Experimental Tectonics Research Group, Physics and Earth Science Dept., Università degli Studi di Parma*
e-mail: *yago.nestola@gmail.com*
session: *Geodynamics*

The evolution of lithosphere necking is a fundamental parameter controlling the structural architecture and thermal-state of rifted margin. Among others, parameters such as extensional strain-rate and thermal layering of the lithosphere exert a fundamental control on necking shape and evolution. Despite a large number of analogue and numerical modelling studies on lithosphere extension are available in the literature, a quantitative description of lithosphere necking evolution is still lacking.

We simulated by physical models the progression of lithosphere thinning and necking during orthogonal rifting at different extensional strain-rates. Our models involve a continental 4-layer mechanical lithosphere, which rests on a glucose syrup asthenosphere. Both the topography and the lithosphere base were monitored by time-lapse laser scanning. At the end of deformation, we remove each of the four layers and acquired the surface shape of the underlying ones by laser scanning. This technical approach allowed us to quantify the evolution in space and time of the thinning factors for the crust, mantle, and lithosphere as a whole. Laser-scanning monitoring provided also a detailed picture of the neck shape evolution, which shows a strong dependency on the strain-rate. At low strain-rates, necking is "boxed" with steep flanks and aflat-lying roof. Few deep basins develop at surface. At high strain-rates, more distributed thinning occurs isolating portions of less deformed mantle.A more distributed deformation affects the model topography. Despite large differences in shape, the aspect ratio (height/amplitude) of the necks converge towards very similar values at the end of the experiments.

The significant differences and evolutionary pathways produced by the plate divergence rate on the lithosphere necking profile, suggest that this parameter can exert a fundamental control on the time and space distribution of heat flow during rifting. Following up on this we can speculate on the location and timing of synrift magmatism, which is expected to be preferentially produced on one shoulder for slow plate divergence rate, and more widely distributed and delayed at fast divergence rates.

Toroidal, counter-toroidal, and poloidal flows of the Rivera and Cocos plates

Florian Neumann[1], Alberto Vazquez[2], Gustavo Tolson[3], Juan Contreras[1]

[1] *Graduate School of Earth Sciences, CICESE, Ensenada BC, Mexico*
[2] *Graduate School of Earth Sciences, Institute of Geology, UNAM, Mexico*
[3] *Geology Department, Institute of Geology, UNAM, Mexico*
e-mail: *fneumann@cicese.edu.mx*
session: *Rheology*

Laboratory modeling at a scale 1:4,000,000 was carried out to understand the mantle flow patterns under the Jalisco and Michoacan blocks of the Northern Middle American subduction zone. Scaled model consists of two polyethylene strips that are forced into a tank filled with corn syrup. One of the strips dips 60^{circ} and moves at a velocity of 25 mm/min simulating the Rivera plate. The other one dips 45^{circ}, moves at 75 mm/min and represents the Cocos plate. An acrylic plate 3-mm thick simulates the continental crust of western Mexico. Analysis of pathlines described by embedded markers in the syrup reveal complex, three-dimensional flow patterns in the simulated subduction zone.

The differential motion of the slabs creates a shallow counter-toroidal rotation flow in the simulated mantle wedge from the slow Rivera plate to the fast moving Cocos plate. Similarly, the differential motion gives rise to a deep toroidal flow asthenospheric mantle around the edges of the Rivera slab. Moreover, a hydraulic jump develops in the deep portion of the slow moving strip representing the Rivera slab that causes upwelling poloidal flow under the acrylic plate representing western Mexico. The upwelling eventually merges with the shallow counter-toroidal and poloidal flow of the simulated Cocos slab. Model results are in excellent agreement with seismic anisotropy studies and geochemistry of lavas erupted in the Jalisco and Michoacan blocks. Our results indicate that mantle mixing in the mantle wedge of the Rivera slab is an ongoing process driven by the differential motion between subducting slabs. Rollback of the Rivera plate, if any, likely is a second order effect.

Sponsored by Conacyt

References

Pardo, M. and Suarez, G.. 1995. Shape of the subducted Rivera and Cocos plates in southern Mexico: Seismic and tectonic implications. Journal of Geophysical Research, 100, 357-374.

Soto, L.G. and Ni, J.F. and Grand, S.P. and Sandvol, E. and Valenzuela, R.W. and Guzman-Speziale, M. and Gomez-Gonzalez, J.M. and Dominguez-Reyes. 2009. Mantle flow in the Rivera–Cocos subduction zone. Geophysical Journal International, 179, 1004-1012.

Stubailo, I. and Beghein, C. and Davis, P. M. 2013. Structure and anisotropy of the Mexico subduction zone based on Rayleigh-wave analysis and implications for the geometry of the Trans-Mexican Volcanic Belt. Journal of Geophysical Research, 117, 1–16.

Yang, T. and Grand, S.P. and Wilson, D. and Guzman-Speziale, M. and Gomez-Gonzalez, J.M. and Dominguez-Reyes, T. and Ni, J. 2009. Seismic structure beneath the Rivera subduction zone from finite-frequency seismic tomography. Journal of Geophysical Research 114, 1–12.

Estimating Crustal Thickness of Iran Using Euler Deconvolution Method and EIGEN-GL04C Geopotential Model

Soran Parang

Department of Surveying and Geomatics Engineering, College of Engineering, University of Tehran, Tehran, Iran
e-mail: *soran_parang@ut.ac.ir*
session: *Geodynamics*

The Moho is the boundary between Earth's crust and the mantle. Moho depth is an important parameter in identification of crustal structure and it is also related to geological and tectonic evolution of each zone. The crustal thickness model and Moho depth may be used for studying the state of local and regional isostasy, hence assisting in the characterization of vertical stresses in the lithosphere. These horizontal and vertical stresses are factors that clearly contribute to the seismicity in the upper-to-mid crust. Crustal thickness models are also useful for mineral and geothermal exploration, as areas of thinned crust are sites where the hotter mantle is closer to the Earth's surface. This can result in enhanced plutonic and volcanic activities in the region. In this research, Moho depth is determined according to geopotential models and 3D Euler Deconvolution method. Euler Deconvolution method is not dependent on an initial depth or density limitations. This method is generally used in determining source position and estimating magnetic and gravity anomalies and it is proper to determine depth of vertical and horizontal contacts so it can be used in estimating crust-mantle boundary (Moho depth). In Euler Deconvolution method, Structural index and window size of estimator are important parameters which affect solution very strongly. To estimate crustal thickness using Euler Deconvolution method it is assumed that crust-mantle boundary is a horizontal sheet or it has sill type anomaly which can be expressed in an infinite 2D space. Data used to estimate Moho depth are free air gravity anomaly resulted from expansion of spherical harmonic coefficients of EIGEN-GL04C model (Figure 1), after comparing this model to GPS leveling data, it has been chosen as the most precise model in Iran. In this study Moho depth was estimated for various structural indices and window sizes, in this way the best structural index and window size in the studied region (Iran) and in structural zones of Iran were determined by comparing Moho depth estimated from Euler Deconvolution method and Moho depth calculated by receiver function method in 91 seismic stations of studied region. The results show that for a window size of 45 km and structural index of 0.5 the best Moho depth is estimated for the region, finally the results were also compared to CRUST 2.0 model. Figures 3 to 9 show results of Moho depth estimation using Euler Decovolution method for window sizes of 15 km to 30 km and structural index of 0.5, along 7 profiles in Figure 2.

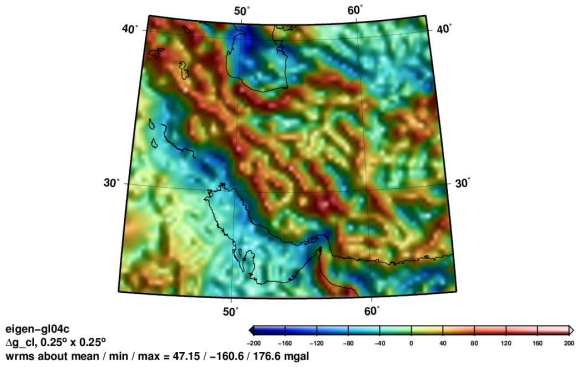

Fig. 1.: Free air gravity anomaly resulted by EIGEN-GL04C model

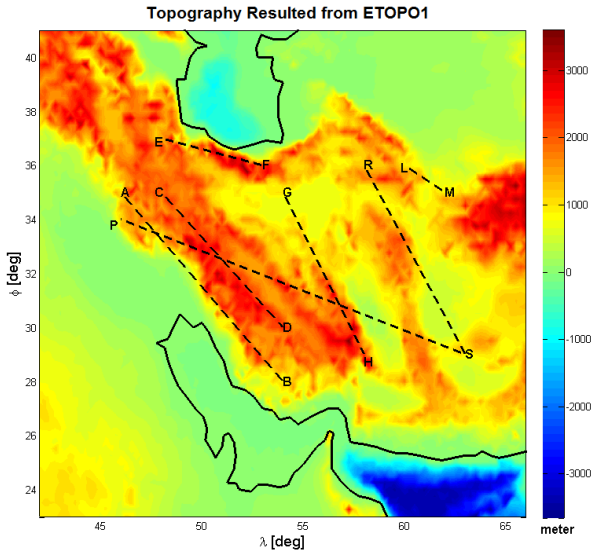

Fig. 2.: Seven considered profiles in Iran

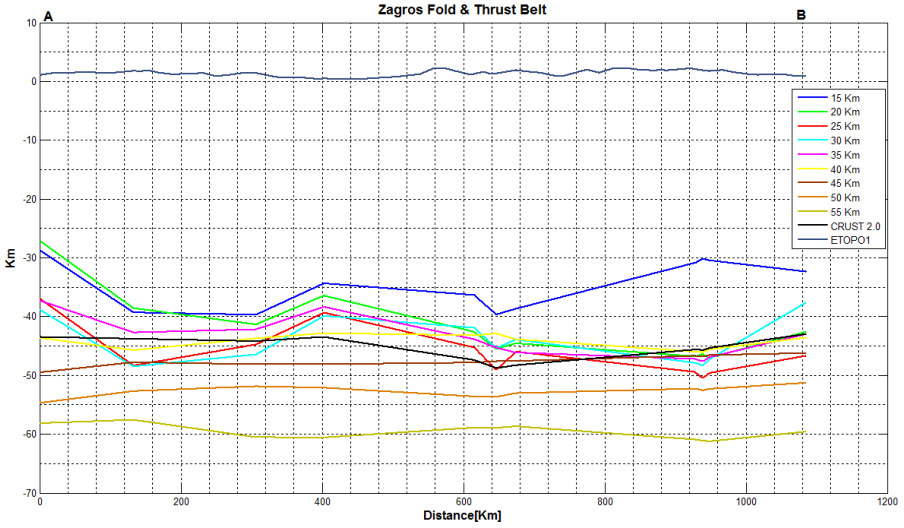

Fig. 3.: Moho depth variation along AB profile located in the Zagros fold & thrust belt

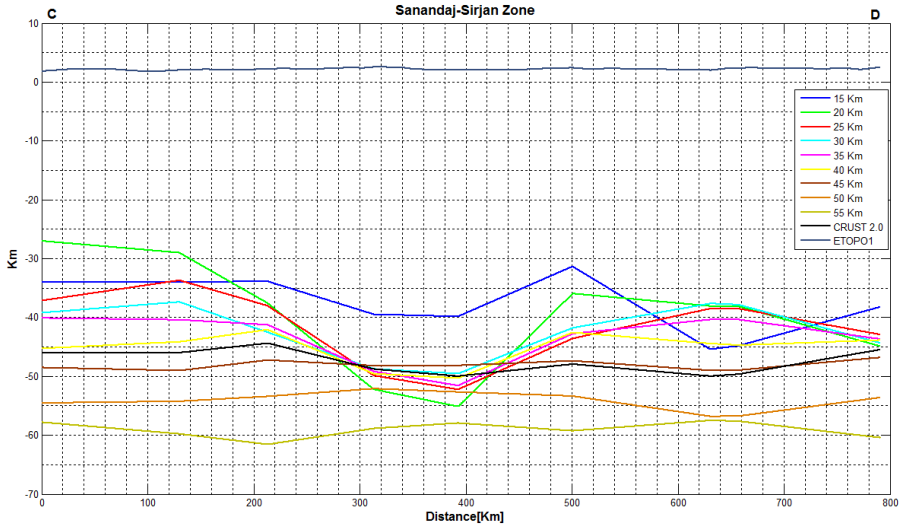

Fig. 4.: Moho depth variation along CD profile located in the Sanandaj-Sirjan zone

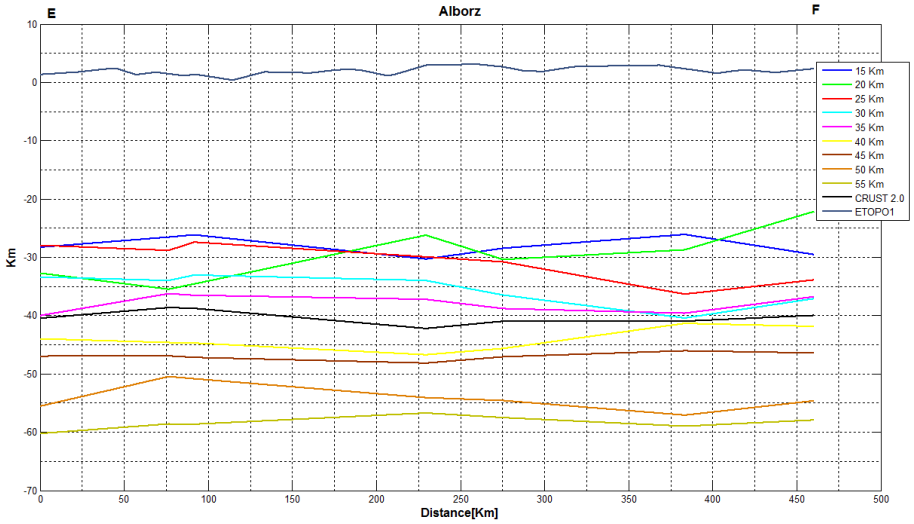

Fig. 5.: Moho depth variation along EF profile located in the Alborz zone

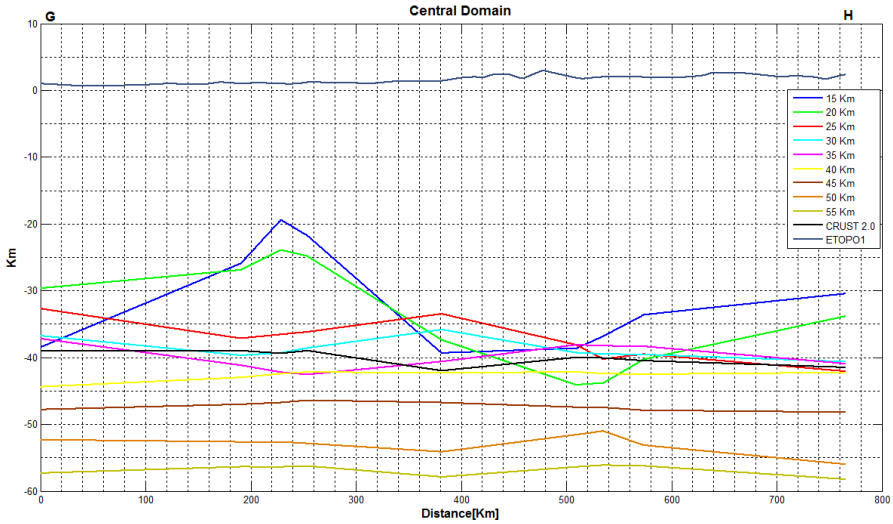

Fig. 6.: Moho depth variation along GH profile located in the Central domain

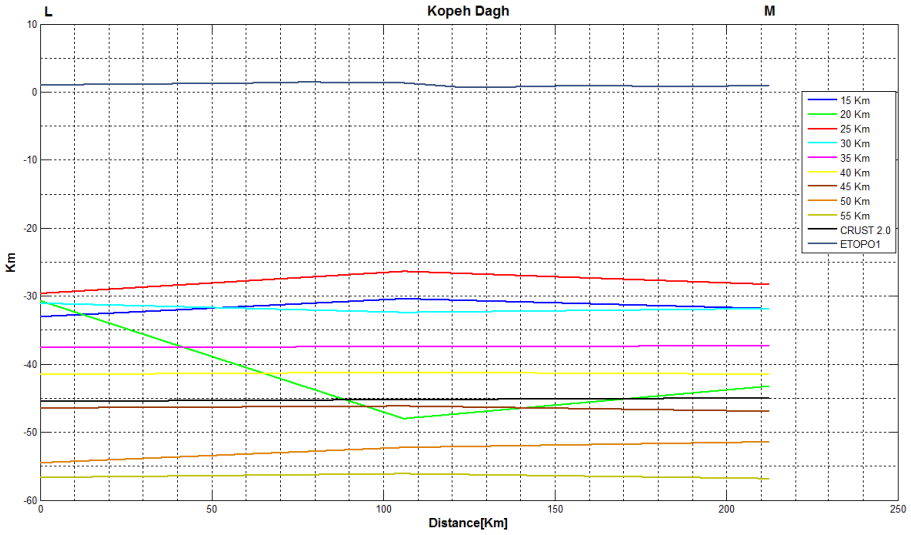

Fig. 7.: Moho depth variation along LM profile located in the Kopeh Dagh zone

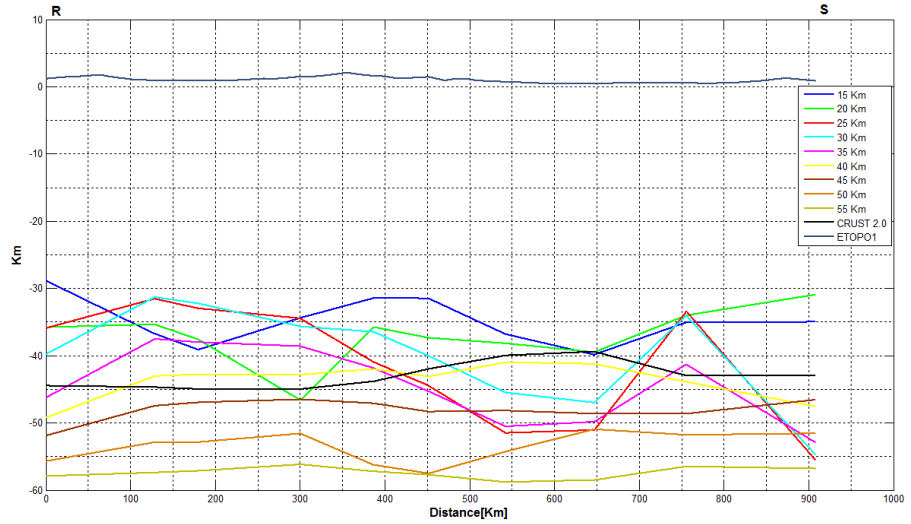

Fig. 8.: Moho depth variation along RS profile

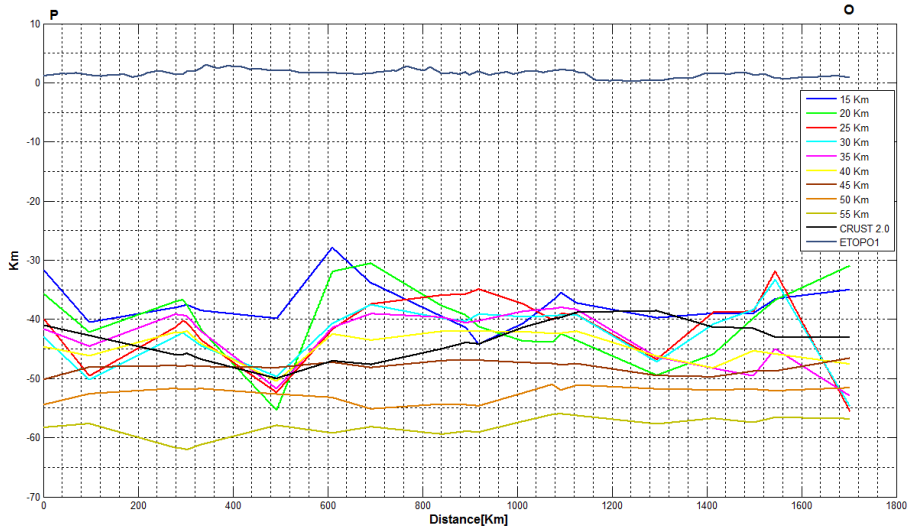

Fig. 9.: Moho depth variation along PS profile

How do weak plate boundaries affect the dynamic topography and geoid?

Alexey G. Petrunin[1], Mikhail K. Kaban[1], Bernhard Steinberger[1], Harro Schmeling[2]

[1] *Helmholtz Centre Potsdam GFZ German Research Centre for Geosciences, Telegrafenberg, D-14473 Potsdam, Germany*
[2] *Goethe-University, D-60323 Frankfurt M, Germany*
e-mail: *alexei@gfz-potsdam.de*
session: *Geodynamics*

The density and viscosity are two major factors controlling mantle dynamics. The geoid, being extremely sensitive to both of them, is a perfect tool reflecting mantle structure. That is why many researchers use the geoid inversion problem to reveal the viscosity-density structure of the lithosphere since decades. The spectral method for solving Navier-Stokes and Poisson equations remains most common technique for such type of problem so far (e. g., Hager and O'Connel, 1981). This method is based on spherical harmonics decomposition of physical fields (e. g., viscosity, density, etc.) that allows obtaining a semi-analytical solution for stress, velocity and gravitational potential with high computational efficiency and preciseness. In its classical formulation, this technique considers the viscosity structure as a number of laterally uniform layers, representing its averaged value for each depth. Most solutions assessing only radial viscosity structure for the mantle that have good fit to the observed geoid, show considerably low value of 1×10^{22} Pa s to 6×10^{22} Pa s for the lithosphere that is too low for the lithospheric plates, and thus do not able to reproduce a plate-like dynamics. Introducing of weak boundaries, dividing strong plates will lead to severe changes in the plate dynamics and, as consequence, in both the geoid and dynamic topography.

So far, most of the studies including strong variation of viscosity have been performed with finite differences (FD)/elements (FE)/volume (FV) methods (e. g. Ratcliff et al., 1997; Yoshida et al., 2001; Tackley, 2008). Using the spectral method on the sphere, we developed the ProSpher code that implies advantages of both spectral-based and FD numerical methods, taking into account strong lateral variations of viscosity, self-gravitation and compressibility, and demonstrates high computational performance and preciseness under high resolution and strong lateral viscosity contrasts (see Petrunin et al., 2013 for more details).

In this study, we intend to determine a pure impact of weak plate boundaries (WPB) on the dynamic topography and geoid. Our numerical experiments assume lateral viscosity variations (LVV) across WPB in uppermost 150 km of the upper mantle only, and only because of effective viscosity decrease along tectonically active plate boundaries (Fig. 1a). In this study we do not intend to construct a self-consistent global model of the mantle, which would require a more extensive work on a joint interpretation of various fields.

To determine a 3D density structure we apply widely-used method connecting shear wave seismic velocity anomalies with density anomalies using standard scaling-factor approach, which has been applied to S40RTS tomography model

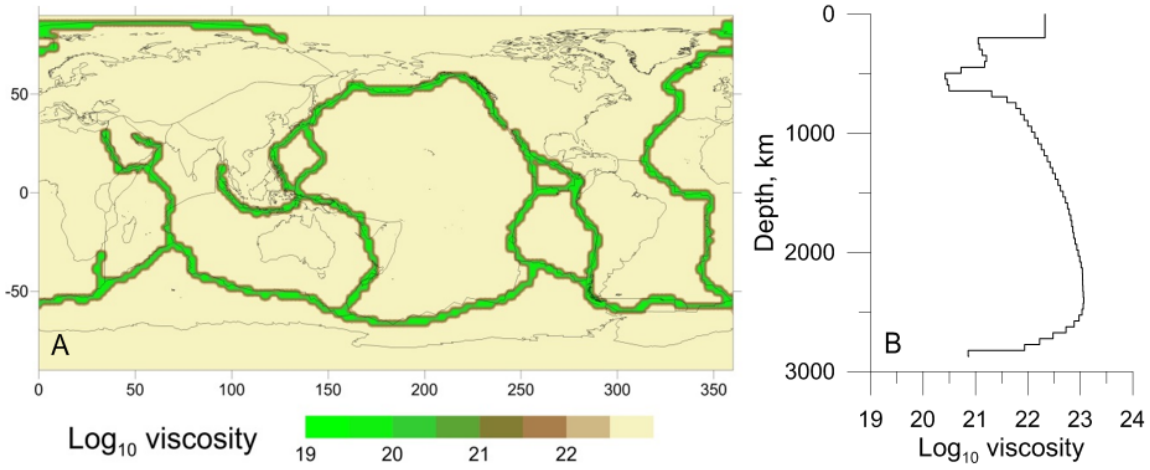

Fig. 1.: WPB based on an integrated global model of plate boundary deformations GSRM (Kreemer et al., 2003); B: radial viscosity model of the mantle (based on Steinberger and Calderwood, 2006)

(Ritsema et al., 2011) as follows:

$$\delta\rho\left(r,\theta,\phi\right) = \alpha\frac{\delta V_{\mathrm{s}}\left(r,\theta,\phi\right)}{V_{\mathrm{s}}\left(r,\theta,\phi\right)}\rho\left(r\right), \qquad \alpha = \frac{d\ln\left(\delta\rho\left(r\right)\right)}{d\ln V_{\mathrm{s}}\left(r,\theta,\phi\right)} \tag{1}$$

where (r,θ,ϕ) are spherical coordinates (radius, latitude and longitude, correspondingly), $\delta\rho$– is density variation, α– is scaling factor and $\frac{\delta V_{\mathrm{s}}(r,\theta,\phi)}{V_{\mathrm{s}}(r,\theta,\phi)}$ is relative shear-wave velocity perturbation. The radial density $\rho\left(r\right)$ profile is obtained from the PREM model (Dzewonski and Anderson, 1981). Taking into account that the presence of WPB changes an average radial viscosity value, that itself affects geoid, we use an algorithm that allows keeping the mean radial viscosity profile unchanged within all models.

The modeling results show that the effect of WPB is significant and may remarkably modify the dynamic topography (Fig. 2) and geoid (Fig. 3). The amplitude of the geoid perturbations reaches -40 m to 70 m with RMS $\sim$20 m. The maximum changes are found around the big subduction zones at the western margin of South America and over the Southwestern Pacific. The maximum of the observed geoid around South America can be explained by introducing a weak zone separating the Nazca and South American plates. The negative changes of the dynamic geoid are mainly associated with mid-oceanic ridges. Geoid perturbations mainly result from changes of the dynamic topography, which are about -300 m to 400 m.

The amplitude of the geoid undulations grows with increasing of the viscosity contrast between WPB and plates up to values of 2.5–3 orders of magnitude. Further weakening of WPB does not produce significant effect on the geoid. This threshold likely manifests the level when the plates might be considered as decoupled.

The obtained results also show that including WPB may significantly improve the reliability of the global dynamic (snapshot) models and should be considered in future studies.

References

Dziewonski, A.M. & Anderson, D.L. Preliminary Reference Earth Model (PREM), Phys. Earth Planet. Inter. 25, 297-356, (1981).

Hager, B. H. & O'Connell, R. J. A simple global model of plate dynamics and mantle convection. J. Geophys. Res. 86, 4843 (1981).

Kreemer, C., Holt, W. E. & Haines, A. J. An integrated global model of present-day plate motions and plate boundary deformation. Geophys. J. Int. 154, 8–34 (2003).

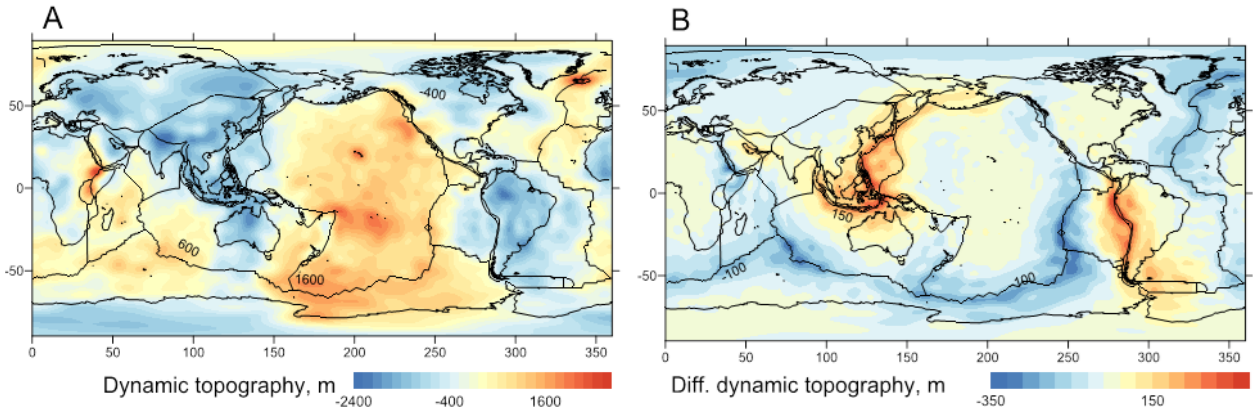

Fig. 2.: A: the calculated dynamic topography for the model with reference radial viscosity profile (Fig. 1b) and plates viscosity of 10^{23}; B: an impact of WPB on the dynamic topography for WPB viscosity contrast of 10^3 with respect to the plate viscosity

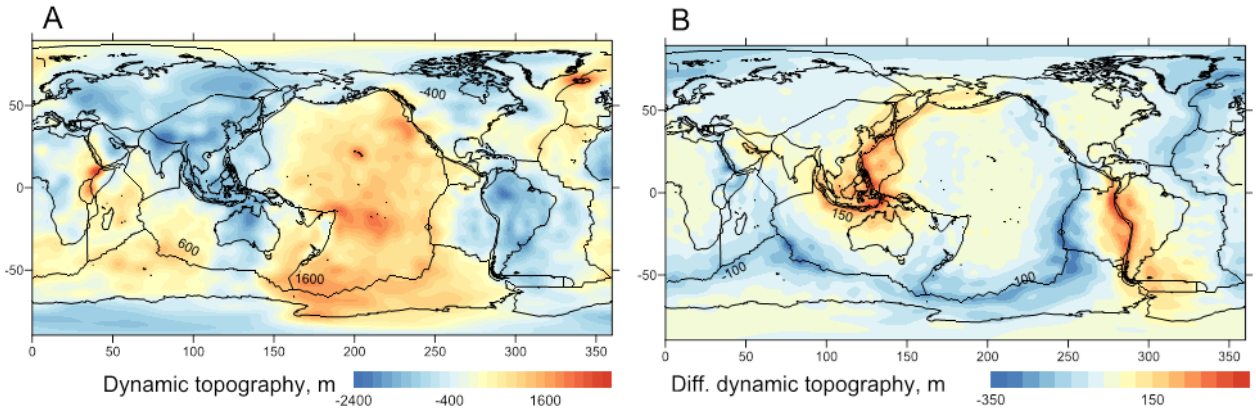

Fig. 3.: A: the resulting geoid for the model with WPB and plate's viscosity of 10^{23}; B: undulations of the geoid as a difference between models with and without WPB. The viscosity at plate boundaries are three orders of magnitude less than the plate's viscosity

Petrunin, A. G., Kaban, M. K., Rogozhina, I. & Trubitsyn, V. Revising the spectral method as applied to modeling mantle dynamics. Geochemistry, Geophys. Geosystems 14, 3691–3702 (2013).

Ratcliff, J. T., Tackley, P. J., Schubert, G. & Zebib, A. Transitions in thermal convection with strongly variable viscosity. Phys. Earth Planet. Inter. 102, 201–212 (1997).

Ritsema, J., Deuss, A., van Heijst, H. J. & Woodhouse, J. H. S40RTS: a degree-40 shear-velocity model for the mantle from new Rayleigh wave dispersion, teleseismic traveltime and normal-mode splitting function measurements. Geophys. J. Int. 184, 1223–1236 (2011).

Steinberger, B. & Calderwood, A. R. Models of large-scale viscous flow in the Earth's mantle with constraints from mineral physics and surface observations. Geophys. J. Int. 167, 1461–1481 (2006).

Tackley, P. J. Modelling compressible mantle convection with large viscosity contrasts in a three-dimensional spherical shell using the yin-yang grid. Phys. Earth Planet. Inter. 171, 7–18 (2008).

Yoshida, M., Honda, S., Kido, M. & Iwase, Y. Numerical simulation for the prediction of the plate motions: Effects of lateral viscosity variations in the lithosphere. Earth, Planets, Sp. 53, 709–721 (2001).

The development of topographic plateaus in an India-Asia-like collision zone using 3D numerical simulations

Adina E. Pusok, Boris Kaus, Anton Popov

Institute of Geosciences, Johannes-Gutenberg University, Mainz, Germany
e-mail: *puesoek@uni-mainz.de*
session: *Geodynamics*

Abstract

The Himalayas and the adjacent Tibetan Plateau represent the most remarkable feature of the Earth's surface as the largest region of elevated topography and anomalously thick crust. Understanding the formation and evolution of the Himalayan-Tibetan region has become of high interest in the scientific community and different models have emerged over the last decades. They range from wholescale underthrusting of Indian lithospheric mantle under Tibet, distributed homogeneous shortening or the thin-sheet model, slip-line field model to the lower crustal flow model for the exhumation of the Himalayan units and lateral spreading of the Tibetan plateau. While some of these models have successfully illustrated some of the basic physics of continental collision, none can simultaneously represent active processes such as subduction, underthrusting, delamination, channel flow or extrusion, which are thought to be important during continental convergence, since these mechanisms require the lithosphere to interact with the underlying mantle.

3D numerical models prove to be powerful tools in understanding the dynamics of coupled systems. However, because of yet recent developments and various complexities, the current 3D models simulating the dynamics of continental collision zones have relied on certain explicit assumptions, either focusing on crustal dynamics or slab-mantle dynamics.

Here, we employ the parallel 3D code LaMEM (Lithosphere and Mantle Evolution Model), using a finite difference staggered grid solver, which is capable of simulating lithospheric deformation while simultaneously taking mantle flow and an internal free surface into account, which allows for the development of topography. We build our model setup to resemble a simplified tectonic map of the India-Asia collision zone and we perform a large number of 3D simulations to investigate the role subduction, continental collision and indentation play on the lithosphere dynamics at convergent margins. The results show that the arrival of a laterally finite continent at the subduction front introduces a strong buoyancy force that changes dramatically the force balance and the dynamics of the system. Trench advance, slab thinning and detachment are processes occurring at the collision zone, while trench retreat, slab roll-back and buckling, coupled with extensive lateral extrusion of material in the upper plate, represent the main processes along the oceanic subduction front. The great variation in slab shape across the subduction-collision zone is consistent with observations from tomographic studies suggesting that 3D models are appropriate to study continental collision settings.

We also analyse the conditions under which large topographic plateaus, such as the Tibetan Plateau can form in an integrated lithospheric and upper-mantle scale model and we discuss the implications these offer for the Asian tectonics. In particular, it has been suggested that slab pull

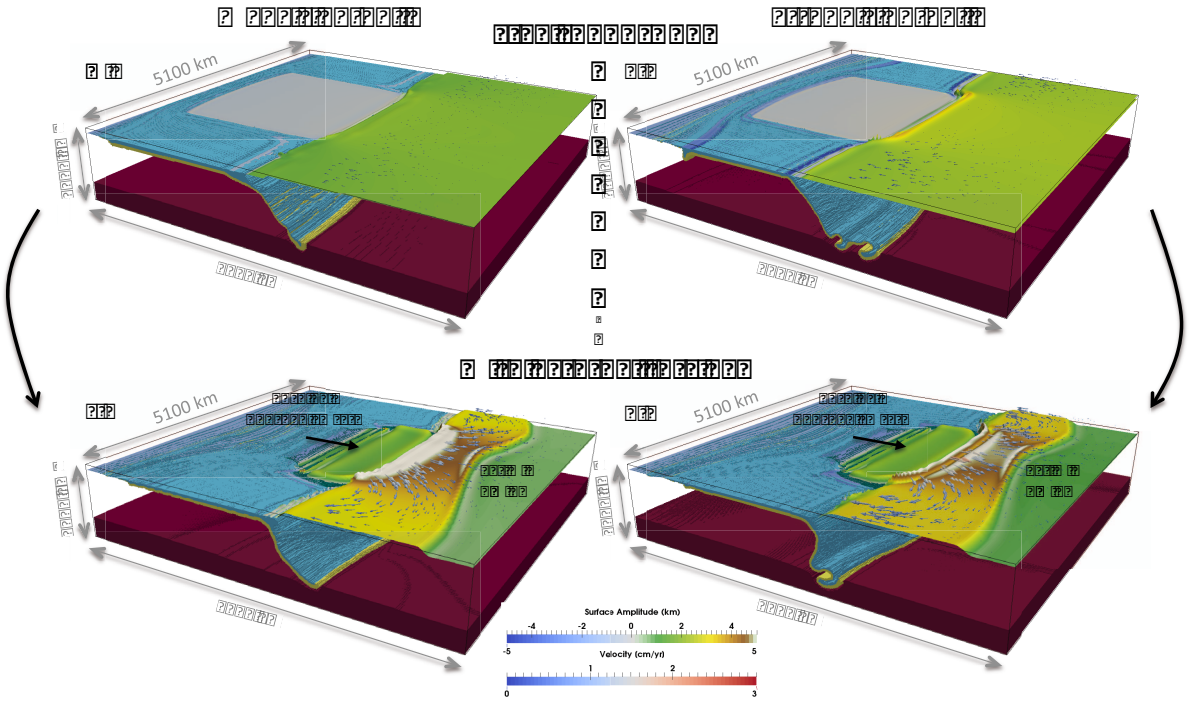

Fig. 1.: The effect of external forcing on upper plate topography in an India-Asia-like setup. (a–b) Simulation results with free subduction after 90 Ma (a) and 70 Ma (b). (c-d) Simulation results with external forcing after 30 Ma. Two additional cases are considered: weak slab-pull (a–c) and strong slab-pull (b-d). External forcing is referred here as an integrated force needed to sustain the present-day convergence of India towards Eurasia ($\sim 5\,\mathrm{cm/a}$) and is implemented numerically as internal Dirichlet boundary conditions. Irregular-shaped crustal blocks such as the Tarim Basin N of the Tibetan Plateau have also been tested (c–d). The subducting slab and the lower mantle are displayed as phases, while topographic maps are shown for the upper plate and continental indentor. Topography has an amplitude exaggeration of x 30 and the velocity arrows represent surface velocity in the upper plate. The results suggest that external forcing and the presence of strong blocks within the Asian lithosphere are necessary to create anomalously high topographic fronts and plateaus, analogous to the Himalayas and the Tibetan Plateau.

is not enough to sustain the on-going convergence of India towards Eurasia, and external forcing, such as ridge push, plume push or slab suction, is important. Furthermore, the presence of strong crustal blocks within the Asian lithosphere such as the Tarim Basin or the Sichuan Basin have also been proposed to be important for the shaping and uplift of the Tibetan Plateau. We test these hypotheses (Figure 1) and show that external factors are necessary to create anomalously high topographic fronts and plateaus, analogous to the Himalayas and the Tibetan Plateau.

Acknowledgements

Funding was provided by the European Research Council under the European Community's Seventh Framework Program (FP7/2007-2013) / ERC Grant agreement #258830. Numerical computations have been performed on MOGON (ZDV Mainz computing center) and JUQUEEN (Jülich high-performance computing center).

Towards quantification of the interplay between strain weakening and strain localisation using analogue models

Malte C. Ritter, Matthias Rosenau, Karen Leever, Onno Oncken

GFZ Potsdam, Lithosphere Dynamics, Potsdam, Germany
e-mail: *malte.ritter@gfz-potsdam.de*
session: *Geodynamics*

Strain weakening is known to be one of the driving factors for the localisation of deformation into discrete faults, entire fault systems and finally into plate boundaries. Nevertheless, the quantitative relationship between weakening and localisation still remains unclear especially when the evolution of whole fault systems is considered. This lack of understanding is at least partly due to the unavailability of geological data with a temporal resolution high enough to image these comparatively fast processes. Physical models using granular materials are able to mimic the process and provide the high temporal and spatial resolution necessary to describe the processes of weakening and localisation with satisfactory precision. Most importantly strain localisation emerges physically self-consistent from simple grain-grain interaction. Physical models therefore seem to be the ideal tool to assess the interplay of both phenomena. However, so far attempts have been made only to quantify either strain weakening (e. g. Lohrmann et al., 2003, using Ring-Shear-Tests) or strain localisation as isolated properties (e. g. Schrank et al., 2008, using the classical Riedel-experiment). While Ring-Shear-Tests are a standard procedure in industry that is correspondingly well developed and yields excellent data on the intrinsic mechanical properties of a granular medium, they do not allow monitoring the process of localisation because of experimental inaccessibility of the shear zone. In Riedel-type strike-slip experiments, on the other hand, no measurements of shear stresses have been available so far. Furthermore, they contain a strong boundary condition in form of a pre-defined linear discontinuity at the base, that might force localisation in otherwise non-localising materials (Schrank et al., 2008).

We developed a new experimental set-up in which deformation of a layer of granular material (sand) in strike-slip mode is driven solely by push from one side and without the need of a basal discontinuity. This is made possible by a layer of low viscosity silicone on which the sand pack rests (cf. fig. 1.) and that reduces the basal drag force to an amount that allows pushing the sand as a rigid block without forming a wedge. The push is applied by a moving indenter, that acts on one half of the sand pack, while the other half is held back by a stationary back wall opposite the indenter, such that in between the two a shear zone forms. The indenter is equipped with a sensor that measures the force integrated over the shear stress along the entire shear zone and the basal drag. The deformation of the sand pack is monitored by a video camera from above. By means of digital image correlation (DIC) displacement- and strain fields can be calculated from the video data, and these in turn can be used to calculate a localisation intensity factor (Schrank et al., 2008). Thus, simultaneous monitoring of shear stress and localisation is possible with this set up.

Here we present data from experiments in this set-up, using materials that show strain weakening to a different amount. These data show a principal pattern of correlated strain weakening and localisation in which overall weakening lags

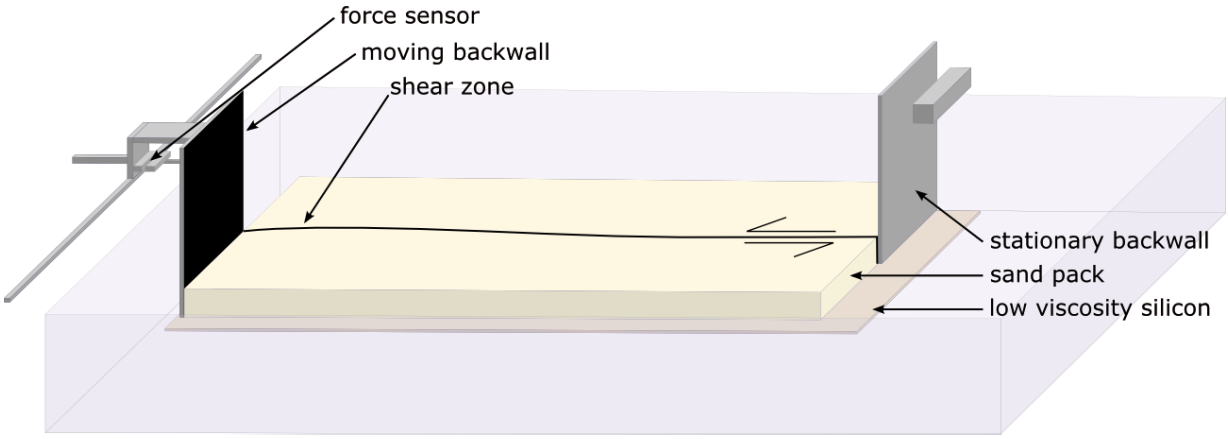

Fig. 1.: Experimental set-up. A sand pack resting on low viscosity silicon is deformed in strike-slip mode by an indenter ("moving back wall") moving against a stationary back wall. The applied integrated shear force is measured by a force sensor connected to the indenter, and the resulting deformation is recorded by a video camera from the top (not shown in figure).

behind the overall localisation (cf. fig. 2). We attribute this lag to the evolution of the fault zone system. More specifically, we hypothesize, that small areas of reduced localisation intensity occurring between adjacent segments of the evolving shear zone act as force bridges that keep up the overall strength, while localisation within the fault segments themselves increases. Only when the bridges rupture, the overall stress decreases, but without a significant increase of overall localisation. Furthermore, we do not measure a direct correlation between the amount of weakening and the amount of localisation, i. e. localisation in the fully evolved shear zone is similar for different materials, independently of the amount of weakening that occurred. The main difference between materials that we observe is the amount of displacement needed to start localisation.

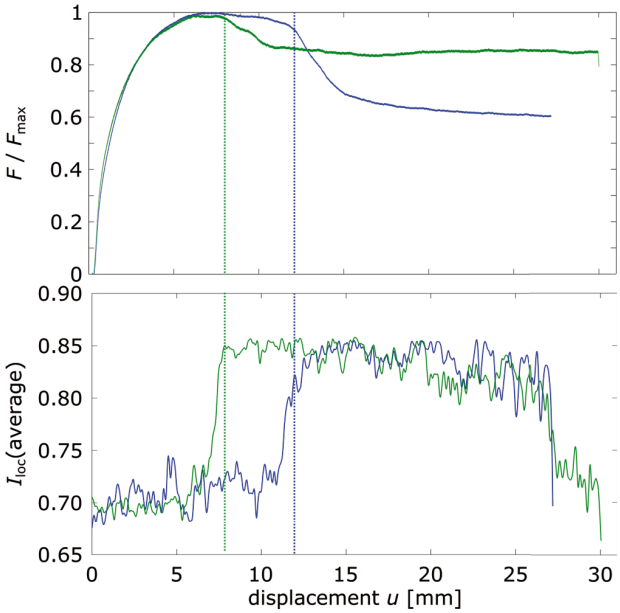

Fig. 2.: Plots showing normalized integrated push force and the amount of localisation (according to Schrank et al., 2008) for two selected experiments, using materials with different strain weakening behaviour (quartz sand, strong weakening, blue, and glass beads, less weakening, green). The amount of localisation is approximately the same, although the amount of weakening is very different. Note the different displacement increments, at which localisation and weakening occur for both materials.

We conclude, that the weakening of lithospheric scale faults strongly depends on their small-scale structural evolution and is to be distinguished from the strain weakening of rock (or sand, in our experiments) as an intrinsic material property. Our experimental set-up, that facilitates simultaneous measurements of force and strain, offers the possibility to evaluate this interplay between lithospheric scale weakening and structural evolution.

References

Lohrmann, J., Kukowski, N., Adam, J., and Oncken, O., 2003, The impact of analogue material properties on the geometry, kinematics, and dynamics of convergent sand wedges: Journal of Structural Geology, v. 25, no. 10, p. 1691–1711, doi: 10.1016/S0191-8141(03)00005-1.

Schrank, C.E., Boutelier, D.A., and Cruden, A.R., 2008, The analogue shear zone: From rheology to associated geometry: Journal of Structural Geology, v. 30, no. 2, p. 177–193, doi: 10.1016/j.jsg.2007.11.002.

Modelling plate kinematics, slabs and LLSVP dynamics – an example from the Arctic and northern Panthalassa

G. E. Shephard, A. L. Bull, C. Gaina

Centre for Earth Evolution and Dynamics (CEED), Department of Geosciences, University of Oslo, Norway
e-mail: *g.e.shephard@geo.uio.no*
session: *Geodynamics*

The Arctic Ocean, one of the world's smallest and shallowest, is also amongst the most tectonically complicated. Bathymetry of the Arctic Ocean is delineated by two major basins, the elongate Eurasia Basin and the larger Amerasia Basin, which are surrounded by extensive continental shelf margins (Figure 1). Our current understanding of its Mesozoic and Cenozoic evolution reveals a history dominated by ocean basin consumption and opening, multiple plate boundary reorganizations and successive magmatic events. While the timing and rates of seafloor spreading within the Eurasia Basin are relatively well constrained, our existing state of knowledge of the evolution of the Amerasia Basin pails in comparison. Some of the most fundamental and outstanding questions about the Amerasia Basin concern the timing of extension and possible seafloor spreading (Jurassic to Cretaceous), style of opening (counter-clockwise, orthogonal or other), location of continental versus oceanic or "transitional" crust, timing of magmatism (High Arctic Large Igneous Province), and quantifying the amount of direction of recent extension (possibly more than 100 %). The opening of the Amerasia Basin is also widely thought to be associated with the closure of an intervening ocean basin, the South Anuyi Ocean, located between Siberia, North America and Panthalassa (Figure 2). Furthermore, considering the Arctic within a global context and with dynamic and connected plate boundaries, demands a consideration of adjacent plate margins, including those within Panthalassa, North America and the nearby Mongol-Okhotsk Ocean.

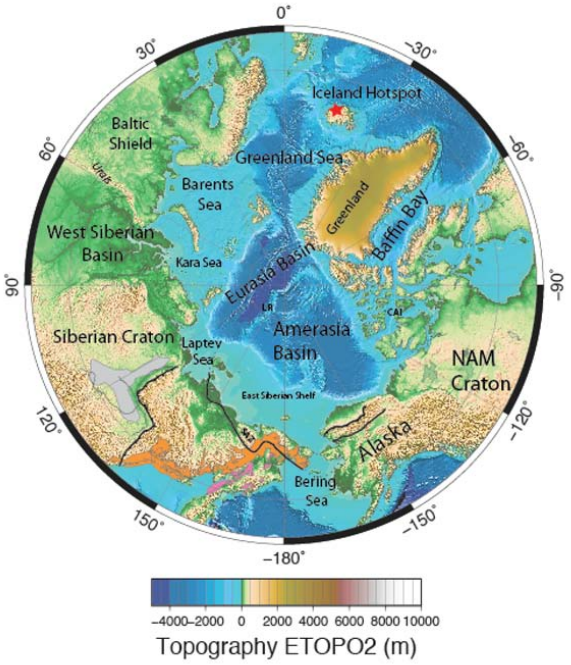

Fig. 1.: Topographic overview of Arctic region with major structural and geographic features labeled.

The onshore geological record and near-surface geophysical data across the circum-Arctic is of variable resolution and coverage, and is compounded by limited accessibility e. g. ice-coverage and expensive reconnaissance and field missions. Ambiguity has permitted a myriad of alternative tectonic scenarios (an example is shown in Figure 2) and there is a need to look to other data-

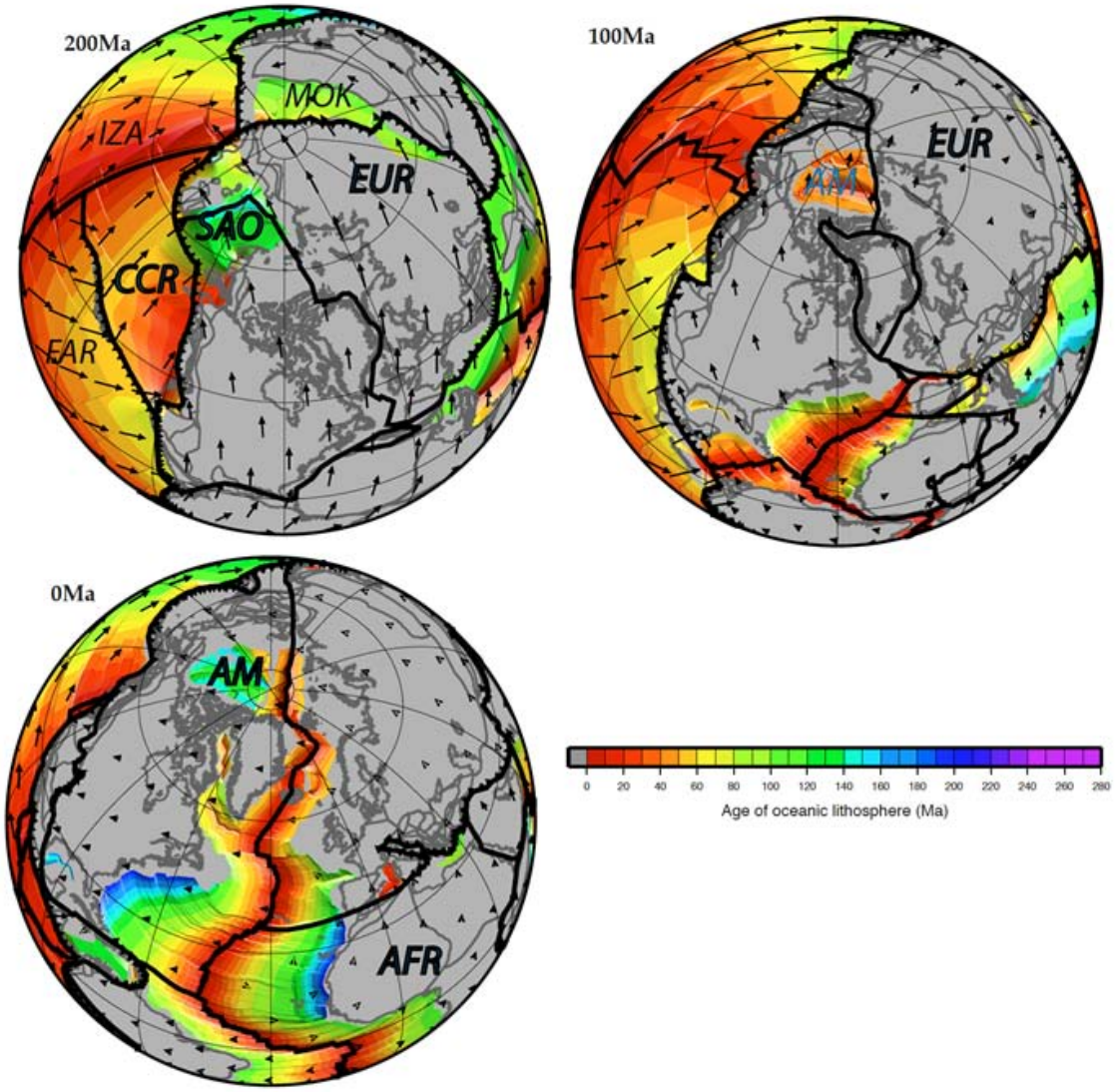

Fig. 2.: Three timesteps from the revised plate reconstruction of the Arctic and Panthalassa region presented in Shephard et al. (2013). Age grid, coloured to age of oceanic lithosphere (Myr), plate velocities in black, continental regions in grey with present-day coastlines in dark grey, plate boundaries in black. Plate and ocean basin acronyms: IZA Izanagi, FAR Farallon, CCR Cache Creek, SAO South Anuyi Ocean, EUR Eurasia, MOK Mongol-Okhotsk, AM Amerasia Basin, AFR Africa.

sets to better constrain surface kinematics and generate refined plate reconstructions. Seismic tomography has the potential to help reveal past kinematic history in regions where subduction processes were sufficiently long-lived to produce considerable amounts of slab that have sunk into the mantle. For example, by assuming vertical sinking of slabs and mantle sinking rates, the location and timing of subduction can be linked to features inferred from seismic tomography (e. g. van der Meer et al., 2012; Sigloch and Mihalynuk 2013, Figure 3). Subduction within the highest Arctic region is suggested to have occurred since at least the Late Jurassic, of which associated slabs can be interpreted to be located under present-day Greenland Siberian Shelf and North America (Shephard et al., 2013; Gaina et al., 2013).

With ever-increasing detail of global plate motion models, advances in numerical modeling and the resolution of seismic tomography, alternative plate reconstructions can now be robustly tested within a geodynamic framework.

Shephard et al. (in press) (Figure 3) compared the spatial and temporal evolution of slabs predicted by two alternative regional reconstructions (Shephard et al., 2013 and Seton et al., 2012) with seismic tomography. While noting an improved match between seismic tomography and a mantle flow model with a refined plate reconstruction, reasonable offsets still remained. Kinematic variability remaining to be further tested includes the timing and location of intra-oceanic and/or continental subduction, subduction polarities, relative plate velocities, convergence and the rate of subduction, age of subducting lithosphere and dip of subducting slabs.

We also present preliminary investigations into the interaction of these regional slabs with the Pacific Large Low Shear Wave Velocity Province (LLSVP). In combination with its antipodal LLSVP located under Africa, these dominant, degree-two features of the lowermost mantle are thought to be of thermochemical origin and have possibly been stable for > 410 Myr (Bull et al., 2014; Torsvik et al., 2008) (Figure 4). However, the specific role of these Arctic and Panthalassa slabs in LLSVP stability and topography as well as plume generation zones and the D" boundaries remains to be further quantified (Bower et al., 2013). By integrating surface kinematics, global mantle flow models and seismic tomography we aim to unravel the complex interaction of surface and mantle dynamics of this region, stretching throughout the Phanerozoic to present-day.

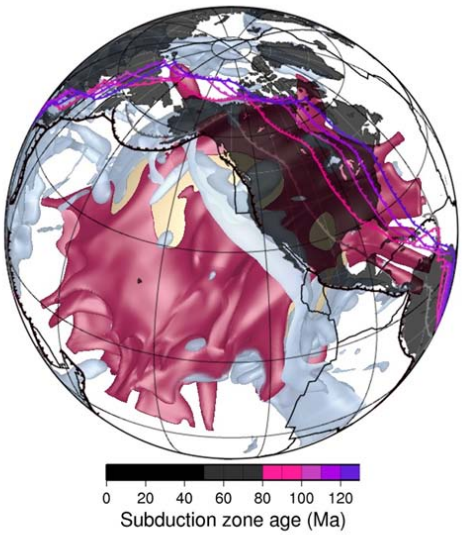

Fig. 4.: Forward modelled mantle structure of Bull et al. (2014) showing residual non-dimensional temperature isosurfaces +/- 0.15 (red/blue respectively) in the lower mantle for the Pacific LLSVP. Present-day coastlines are superimposed in black and reconstructed subduction zones from 0 Ma to 120 Ma shown by coloured lines.

References

Bower, D. J., Gurnis, M. and Seton, M. (2013). Lower mantle structure from paleogeographically constrained dynamic Earth models. Geochemistry, Geophysics, Geosystems v.14 doi:10.1029/2012GC004267

Bull, A.L. Domeier, M., & Torsvik, T.H., (2014). The effect of plate motion history on the longevity of deep mantle heterogeneities. Earth and Planetary Science Letters (in press)

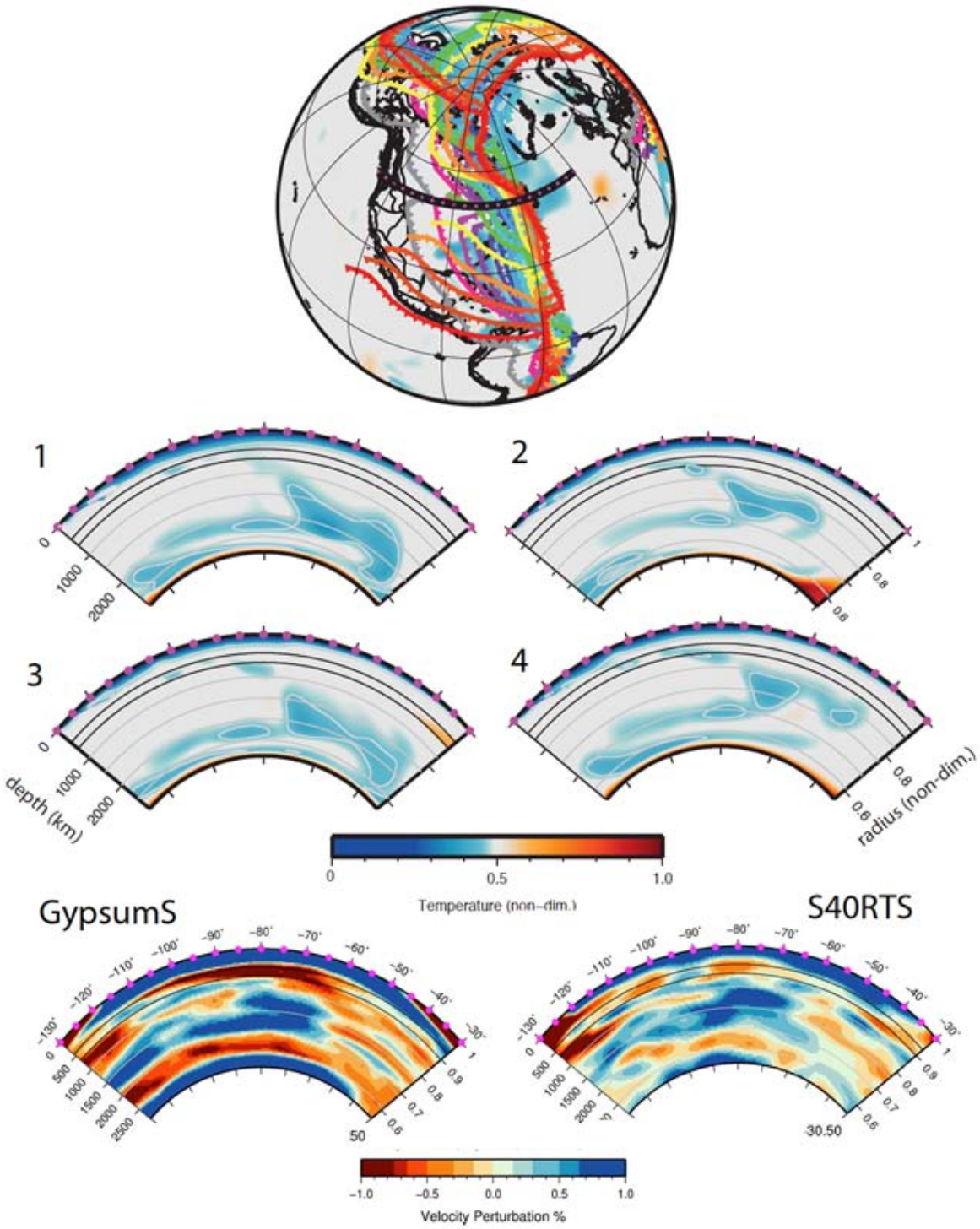

Fig. 3.: Top panel, projection of vertical section, black (50°N, North America) superimposed over reconstructed subduction locations based on Shephard et al., 2013 (230 Ma to 0 Ma). Panels 1–4 forward modeled mantle thermal (slab) structure predicted by four alternative models (differing rheologies). Bottom panels, two seismic tomography models at same vertical section.

Gaina, C., S. Medvedev, T. H. Torsvik, I. Koulakov and S. C. Werner (2013), 4D Arctic: A glimpse into the structure and evolution of the Arctic in the light of new geophysical maps, plate tectonics and tomographic models, Surveys in Geophysics, doi:10.1007/s10712-013-9254-y.

Seton, M., Müller, R.D., Zahirovic, S., Gaina, C., Torsvik, T.H., Shephard, G., Talsma, A., Gurnis, M., Turner, M., Maus, S., Chandler, M. (2012). Global continental and ocean basin reconstructions since 200 Ma. Earth-Science Reviews 113 (3–4), 212–270. doi.org/10.1016/j.earscirev.2012.03.002.

Sigloch, K., and Mihalynuk, M. (2013) Intra-oceanic subduction shaped the assembly of Cordilleran North America. Nature v.496 p.50-56 doi:10.1038/nature12019

Shephard, G.E., Müller, R.D., Seton M., 2013, The tectonic evolution of the Arctic since Pangea breakup: Integrating constraints from surface geology and geophysics with mantle structure. Earth-Science Reviews v.124 p.148-183.

Shephard, G. E., Flament, N., Williams, S., Seton, M., Gurnis, M., and Müller, R.D., In Press. Circum-Arctic mantle structure and long-wavelength topography since the Jurassic. Journal of Geophysical Research

Torsvik, T. H., B. Steinberger, B., L. R. M. Cocks and K. Burke (2008). Longitude: Linking Earth's ancient surface to its deep interior, Earth Planet. Sci. Lett., 276, 273-282, doi:10.1016/j.epsl.2008.09.026

van der Meer, D.G., Torsvik, T.H., Spakman, W., van Hinsbergen, D.J.J. and Amaru, M.L. (2012) Intra-Panthalassa Ocean subduction zones revealed by fossil arcs and mantle structure, Nature Geoscience 5, p. 215-219

Strike-slip movements and Rotation of tectonic blocks in the Kaboodan area, south Khur, Central Iran

Arash Sohrabi, Alireza Nadimi

Department of Geology, Faculty of Science, University of Isfahan, Hazarjirib, P.O.Box 81746-73441, Isfahan, Iran
e-mail: *arashshrbi@yahoo.com*
session: *Geodynamics*

The active tectonics of Iran results from the northward Arabia–Eurasia convergence. At the southwestern and southern boundaries of the Arabia-Eurasia collision zone, the convergence is taken up by the continental collision in the Zagros Mountains, and the active subduction of Makran, respectively. Further north, the northward motion not absorbed by the Makran subduction is expressed as the N-trending right lateral shear between central Iran and Eurasia at a rate of 16 mm/yr (e. g., Regard et al., 2005; Vernant et al, 2004).

The Khur area is located in the central and western part of Central Iran (Stocklin 1968) that characterized by an intricate heterogeneous structures and combination of ancient continental faulty blocks and narrow suture zones. Faults play important role in the tectonic evolution of the area and breaking it into smaller blocks. Major deep and long-lived faults separate structural zones.

Several map-scale NE-SW-trending faults are stretched in the Central Iran. These are Great Kavir, Ordib and Chapedony faults. Ordib fault bounds the Anarak-Khur massif to the southeast. The fault is represented on the surface by a series of sub-parallel vertical reverse faults locally passing into steep thrust dipping to northwest. The width of the fault zone ranges from several hundred meters to 1.5 km to 2 km. The amount of displacement decreases eastward, and the major fault branches out into a series of minor faults which cut practically through all the rock complexes from the Upper Proterozoic to Neogene, even locally through the oldest Quaternary sediments. Many of faults in this zone are accompanied by heavy crushing, schistosity and hydrothermal alteration of the rocks (Aistov, 1984).

It has been recognized that fault blocks in strike-slip tectonic domains must progressively rotate around vertical axes as the overall strike-slip motion continues. Two direct consequences of the deformation mechanism are (1) slip on each of the fault within a domain must be related to the rotation of the blocks bounded by these faults, and (2) the faults themselves must also rotate because they are the boundaries of the blocks (Kissel and Laj 1989). When rotation becomes sufficiently large, slip on the rotating faults ceases because the resolved shear stress on them has decreased and the normal stress has increased to the point where the frictional resistance is too great for further slip. If crustal deformation is to proceed it must be accommodate by a set of new faults, more favorable oriented to the principle direction of the regional stress field (Hogai et al, 1993).

In Kaboodan area the blocks rotated in domino style in different sizes between the strike-slip faults clockwise around vertical axis. These rotations are directly controlled by the orientation of the faults relative to the direction of the principle tectonic shortening.

The following results can be summarized as follows:

1. The Ordib fault and other NE-SW-trending

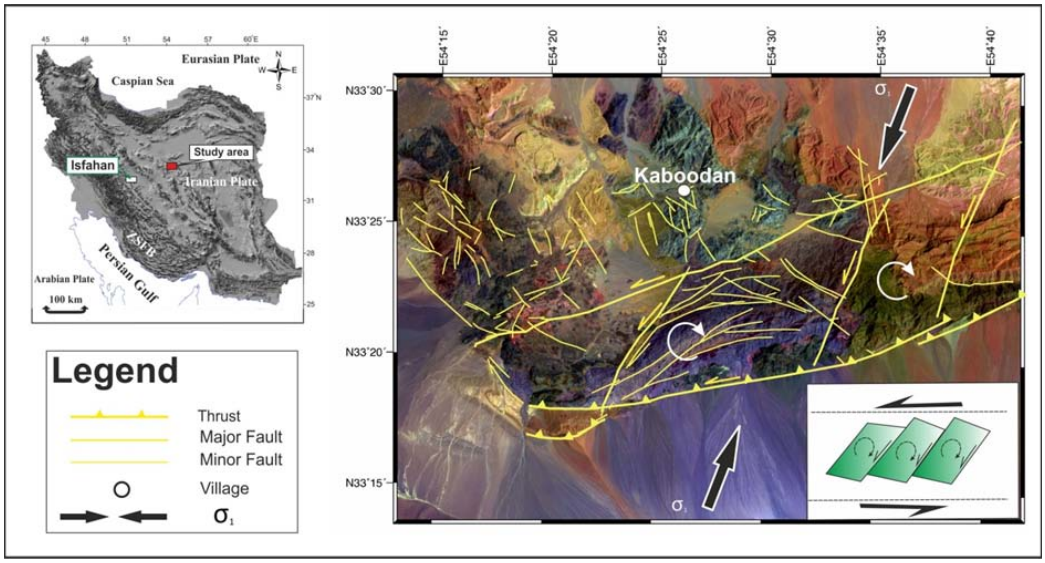

Fig. 1.: Location of the studied area and the Kaboodan structural zones. Fault patterns and the rotated blocks in this area.

faults of the Khur area have important role in tectonic evolution of the Central Iran. Strike-slip movements along the faults have been occurred during northward convergence of the Arabian and Eurasian plates. The movements are created several kinds of smaller faults and have formed different sizes of structural blocks.

2. Clockwise rotation of the structural blocks has been occurred along the major and minor faults of the area.

References

Aistov, L., Melanikov, B., Krivyakin, B., Morozov, L. and Kiristaev, V.(Eds.), (1984) Geology of the Khur Area (central Iran).Explanatory text of the Khur quaderangle map.

Farbod, Y, Bellier, O, Shabanian, E and Abbassi, M.R. (2010) Structural and geomorphic fault segmentations of the Doruneh Fault System, central Iran, Geophysical Research Abstracts, Vol. 12, EGU2010-6576-1.

Hogai, R, Amos, N and Atilla, A (1993) Stress field rotatio or block rotation an example from tha lake mead fault system. J. Geofisica. Vol. XXXVI, N, 2, P. 65-73.

Kisel, C and Laj, C. (1989) Paleomagnetic rotation and continental deformation, Kluwer Academic publishers, 209-228.

Regard, V., Bellier, O., Thomas, J. C., Bourles, D., Bonnet, S., Abbassi, M. R., Braucher, R., Mercier, J., Shabanian, E., Soleymani, S., and Feghhi, K. (2005). Cumulative right-lateral fault slip rate across the Zagros-Makran transfer zone: role of the Minab-Zendan fault system in accommodating Arabia-Eurasia convergence in southeast Iran.Geophysical Journal International 162, 177-203

Stöcklin, J., (1968) Structural history and tectonics of Iran. A review: American Association of Petroleum Geologists Bulletin, v. 52, 7, p. 1229–1258.

Vernant, P., Nilforoushan, F., Hatzfeld, D., Abbassi, M.R., Vigny, C., Masson, F., Nankali, H., Martinod, J., Ashtiani, A., Bayer, R., Tavakoli, F., and Chery, J., 2004. Present-day crustal deformation and plate kinematics in the Middle East constrained by GPS measurements in Iran and northern Oman. Geophysical Journal International, 157, 381–398.

On the relation between plate tectonics, large-scale mantle flow and mantle plumes: Some recent results and many open questions

Bernhard Steinberger[1,2], Rene Gassmoeller[1], Elvira Mulyukova[1], Juliane Dannberg[1], Stephan V. Sobolev[1,3]

[1] *Section 2.5, Geodynamic Modelling, GFZ German Research Centre for Geosciences, Potsdam, Germany*
[2] *Centre for Earth Evolution and Dynamics, University of Oslo, Norway*
[3] *Schmidt Institute of the Physics of the Earth, Russian Academy of Sciences*
e-mail: *bstein@gfz-potsdam.de*
session: *Geodynamics*

Tectonic plate motions are a surface representation of convection in the Earth's mantle. Seismic tomography reveals that most subducted plates eventually sink into the lowermost mantle. Yet the relation of plate tectonics and mantle dynamics remains incompletely understood. The observed stability of the two Large Low Shear Velocity Provinces (LLSVPs) over at least 250 Myr, and possibly much longer, is an important constraint on models of mantle dynamics, and difficult to explain with current models.

Approximately stable LLSVPs that match observed locations and shapes can be reproduced by 3D numerical models with imposed locations and amounts of subduction, as dictated by the plate tectonic reconstructions for the past 250 Myr. In these models, LLSVPs are represented by thermochemically distinct piles, which form when an initially flat and compositionally dense basal layer gets deformed by the ambient mantle flow. The long-term stability of LLSVPs in these models is aided by subduction, which has occurred in similar areas during this period, and mostly stayed away from the LLSVPs; yet it is unclear what could have caused relative stability of subduction zone locations. The fact that the locations of major upwellings (divergent plate tectonic quadrupole; Conrad et al., 2013) have approximately remained stable for the past 250 Myr, but the location of the strongest downwellings (convergent quadrupoles) have moved along the great circle bisecting between the divergent quadrupoles, may suggest that it is the upwellings themselves that maintain stability and orchestrate the global mantle flow. Yet we currently have no dynamically consistent model that explains such behaviour.

Another surface representation of mantle dynamics are hotspots, believed to be caused by mantle plumes. Plumes may interact with spreading ridges, causing increased volcanism and crust production in ridge segments nearby. They may also be instrumental in causing ridge jumps, which may lead to continental fragments in the oceans. Recent results show that plumes and plates also interact at the base of the mantle: the locations and distribution of hotspots can be much better explained with a geodynamic model where plumes are triggered, mainly along the margins of thermochemical piles, by slabs approaching the core-mantle boundary, rather than freely developing (Figure 1).

Important parameters governing the thermochemical evolution of the mantle are buoyancy ratio (chemical vs. thermal), the dependence of viscosity on temperature and chemical compos-

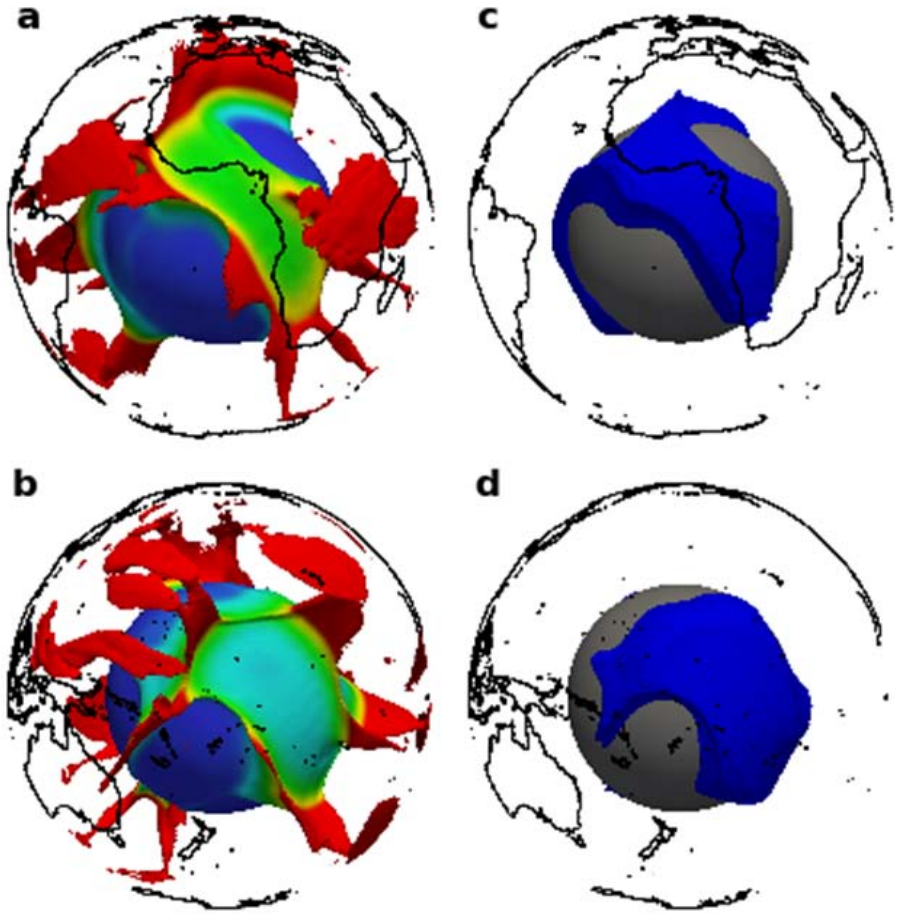

Fig. 1.: Thermo-chemical piles near the core-mantle boundary plotted as chemical isosurface in **c** and **d**, and plumes rising from their margins as isosurface 250 K hotter than the surrounding mantle in **a** and **b**, coloured according to the height above the CMB. The figure shows the model for present-day after 250 Myr of plate motions imposed as surface boundary condition.

ition, as well as the deviation of lower mantle temperature from the adiabatic profile. There is a large uncertainty associated with each of these parameters. For instance, the buoyancy ratio depends on the origin of the chemically anomalous material, which is currently debated. This material, which is responsible for the large scale heterogeneity in the mantle – such as the LLSVPs – may be either primordial, recycled subducted crust, or leaked outer core material – or a combination of these.

Numerical experiments can also show under what circumstances, and to what degree, subducted crust can accumulate in the lowermost mantle, and/or primordial material can remain there for billions of years without being entrained. A modelling result that illustratres how the lower mantle viscosity affects segregation, accumulation, and reentrainment of the subducted oceanic crust is shown in Figure 2.

The behaviour of mantle plumes depends on how much of the chemically different, heavier material is carried upward by them. Numerical models can show under which conditions the low-buoyancy thermochemical plumes could arrive to the lithosphere from the core mantle boundary (Figure 3).

Geodynamic models can be constrained by vari-

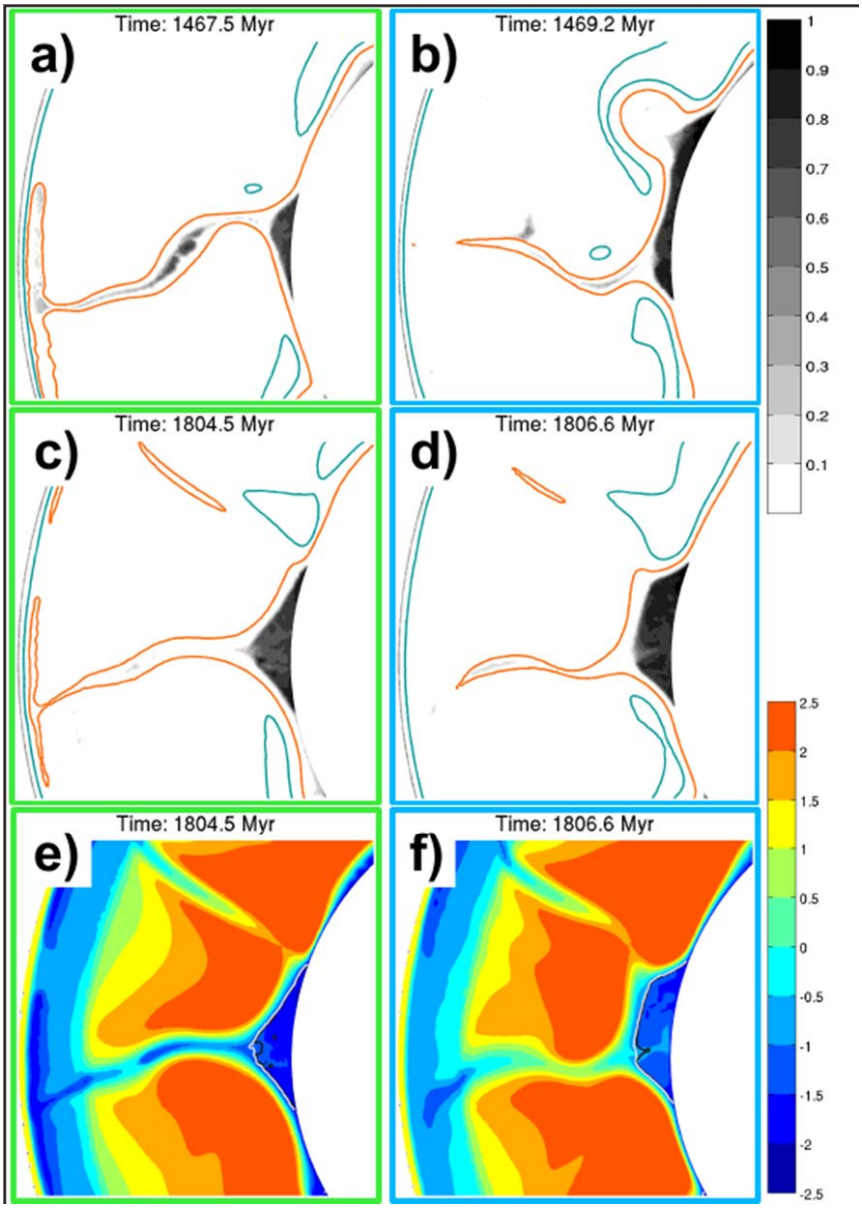

Fig. 2.: Numerical modelling of thermochemical convection in the mantle, illustrating the process of segregation, accumulation, and reentrainment of subducted oceanic crust (OC) for two (subtly) different viscosity-profiles. Left column (figures a), c), and e)) are results obtained with the depth- and temperaure-dependent viscosity-profile from (Steinberger & Calderwood, 2006). Right column (figures b), d), f)) are results obtained with the same profile, but with viscosity lowered by a factor of five in the lowermost $500\,\mathrm{km}$ of the mantle. The top two rows (figures a), b), c) and d)) show the fraction of the OC-material in a small part of the hollow cylinder domain at two different simulation times: $\sim 1.4\,\mathrm{Gyr}$ and $\sim 1.8\,\mathrm{Gyr}$. The red and blue lines are hot ($T^* = 0.6$) and cold ($T^* = 0.4$) isotherms, respectively (where T^* is the nondimensional temperature). The bottom row shows the base ten logarithm of viscosity for the two cases at time $\sim 1.8\,\mathrm{Gyr}$. The black and white lines are isolines for compositional field values 0.6 and 0.4, respectively (where 1 means pure oceanic crust). The main observation is that reducing viscosity in the lower mantle leads to noticably smaller piles, with more ridge-like topography, and composed of a mixture of OC- and ambient material that has a smaller fraction of the OC, compared to the piles produced in a lower mantle with higher viscosity. The compositional density anomaly in both cases is $\sim 1.8\,\%$, corresponding to a buoyancy ratio (chemical to thermal) of ~ 0.57.

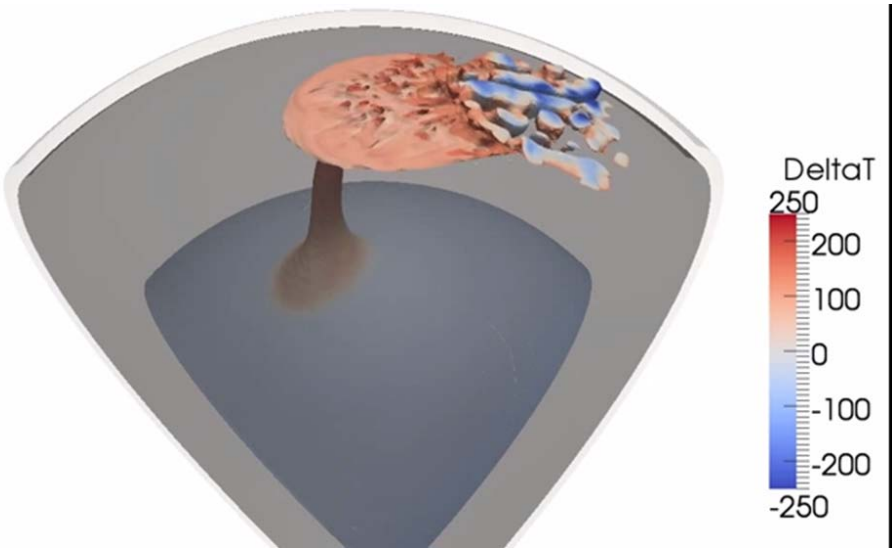

Fig. 3.: A thermo-chemical plume rising from the core-mantle boundary and interacting with an overlying, moving plate. The figure shows the isosurface of the chemical composition (fraction of recycled oceanic crust). The plume is colored by the difference of the local temperature to the adiabatic temperature profile.

ous observations, including geoid, dynamic topography, and lithospheric stresses. Forward model predictions of slabs and plumes can be compared against seismic observations, with the help of recent developments in mineral physics.

The role of crustal thickness and lithospheric rheology on rifted margins width and tectonic subsidence

Anna Eliza Svartman Dias[1,2], Luc. L. Lavier[1,3], Nicholas W. Hayman[1]

[1] *Institute for Geophysics, University of Texas at Austin, USA*
[2] *E&P-EXP, Petrobras, Brazil*
[3] *Department of Geological Sciences, University of Texas at Austin, USA*
e-mail: *annasvartman@gmail.com*
session: *Geodynamics*

Features such as crustal geometry, structural style, amount of magmatism, sedimentary architecture, and subsidence history vary among rifted margins along the world as well as along strike of a single margin. The most variable characteristic is the extent of continental crust deformed by extension. Seismic data from margins around the world exhibit a large variation of the basin width, particularly of the width of a domain where continental crust was thinned to less than 15 km (hyperextended domain), which spans from less than 50 km to more than 150 km in margins such as conjugate Iberia-Newfoundland, the fossil Alpine Tethys, or part of the South Atlantic margin (e. g. Van Avendonk et al., 2006, 2009; Perón-Pinvidic and Manatschal, 2009; Zálan et. al., 2011; Aslanian and Moulin, 2012; Perón-Pinvidic et al, 2013). The South Atlantic Brazilian margin is an extreme example of along strike basin-width variation. The margin width changes from about 600 km in southern Santos Basin to less than 150 km in Camamu Basin (Figure 1). Their hyperextended domains range from 300 km in Santos to about 50 km wide in Camamu Basin. Even though Brazilian margins have features similar to those of the so-called magma-poor conjugate Newfoudland-Iberia, the high volume of early volcanism, especially in Santos and Campos basins, suggest this basins may share some characteristics with magma-rich margins (e. g. Mohriak and Leroy, 2012; Quirk et al., 2013).

Along strike variation in the Brazilian offshore basin-width coincides with changes in the geological provinces in onshore Brazil, from the Ribeira and Araçuaí mobile belts to the São Francisco craton (SFC) (figure 1). The role of initial lithospheric conditions (such as rock rheology and thermal structure) and of the rate of extension on the evolution of rifts and rifted margins have been discussed over the past decades (e. g. Kusznir and Park, 1987; Buck, 1991, 1999; Lavier and Manatschal, 2006; Huismans and Beaumont, 2011). However, the impact of each of these factors on the necking/thinning of the continental crust, particularly on the formation of very wide (> 150 km) asymmetric margins, remains unclear. Therefore, we use numerical experiments to test if there is a physical relationship between initial conditions and the width of the basins; as well as to assess tectonic subsidence histories. We assumed a range of composition (plagioclase, dry or wet quartz dominated crust; and, dry or wet olivine mantle), initial crustal thickness (30 km to 45 km), initial lithosphere thickness (increasing with thermal age varying between 250 Myr and 1 Gyr), initial geotherm (varying with thermal age, crustal thickness and surface heat flow), and velocity of extension (0.5 cm/yr, 1 cm/yr or 2 cm/yr).

We find that small crustal thicknesses (< 35 km) result in narrow margins (< 150 km). Figure 2 a shows the results for a 500 Myr- lithosphere, 30 km crust and strong (dry olivine)

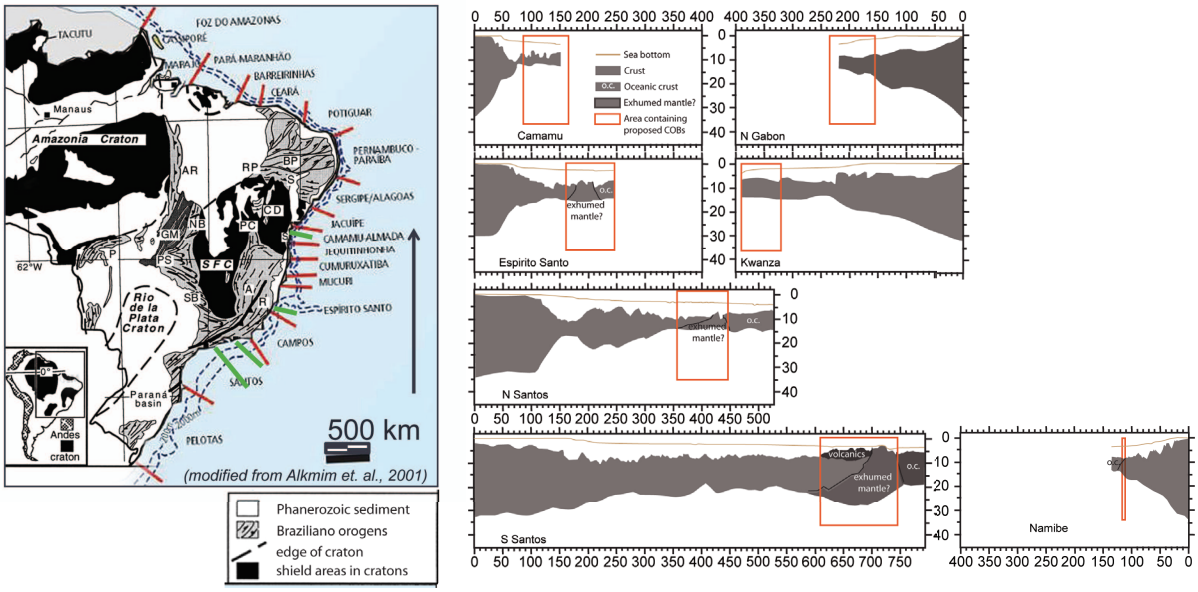

Fig. 1.: On the left, simplified geological map of Brazil depicting the cratonic (black) and mobile belts (grey) domains (modified from Alkimin et al, 2001). Red lines show limits between offshore basins. Green lines show the approximate location of the cross-section of the Brazilian basins displayed on the right. Cross-section cartoons, from bottom to top: Santos Basin and its conjugate at the Namibian margin; Espírito Santo and its conjugate, Kwanza Basin; and, Camamu Basins and its conjugate, Gabon Basin. Orange rectangles encompass various locations proposed for the continent-ocean boundary (COB) in each margin, and interpreted areas of transitional crust or exhumed mantle. Cross-sections and COBs from Sakariasse, (2007), Blaich et al, (2010), Zálan et al. (2011), Heine et al (2013) and references therein.

mantle. Deformation is localized at a narrow area (keystone block H) at the center of the models throughout the rifting process. The thinning and stretching evolution results in a set of narrow conjugate margins (Lavier and Manatschal, 2006; Van Avendonk et al., 2009). Even though there is a delay in thinning the base of the block H in figure 2 a, early crustal necking can occur when the mantle is weak (wet olivine). On the other hand, a wide margin (150 km to $>$ 300 km) can be formed for an initially thick crust ($\geq$ 35 km), a slow rate of extension ($\leq$ 1 cm/yr) and Moho temperatures above 600 °C (figure 2). An initially narrow zone of deformation widens with time and thinning is distributed over a very wide area. The width of the thinning and stretching area also varies with crustal and mantle composition. A wet mantle rheology allows for more widening of the margin than a dry mantle because mantle flow can compensate for crustal thinning and allow for even more distributed deformation even though the mantle is weak (Figure 2 c). The experiment with 45 km crust and a wet olivine upper mantle result in a wide ($>$ 300 km) highly asymmetric lithosphere even for a lithosphere as old as 500 Myr. One margin can be less than one third the width of its conjugate. A young lithosphere/hot geotherm also helps to widen the rift basins. In cold Archean cratonic areas, without significant thickness of ductile lower crust even when the crust is thick, a brittle upper mantle probably controls deformation and early coupling between the crust and mantle forms a block H, leading to a narrow margin. For wide margins, syn-rift subsidence is mostly shallow (300m depth or less), locally reaching 1 km to 1.5 km depths more than 10 Myr after the onset of rifting. For narrow margins, the subsidence curves show a first phase of rapid subsidence during the initiation of block H, followed by a slow uplift accompanying the weakening and deformation of block H (figure 3). However, this uplift alone is

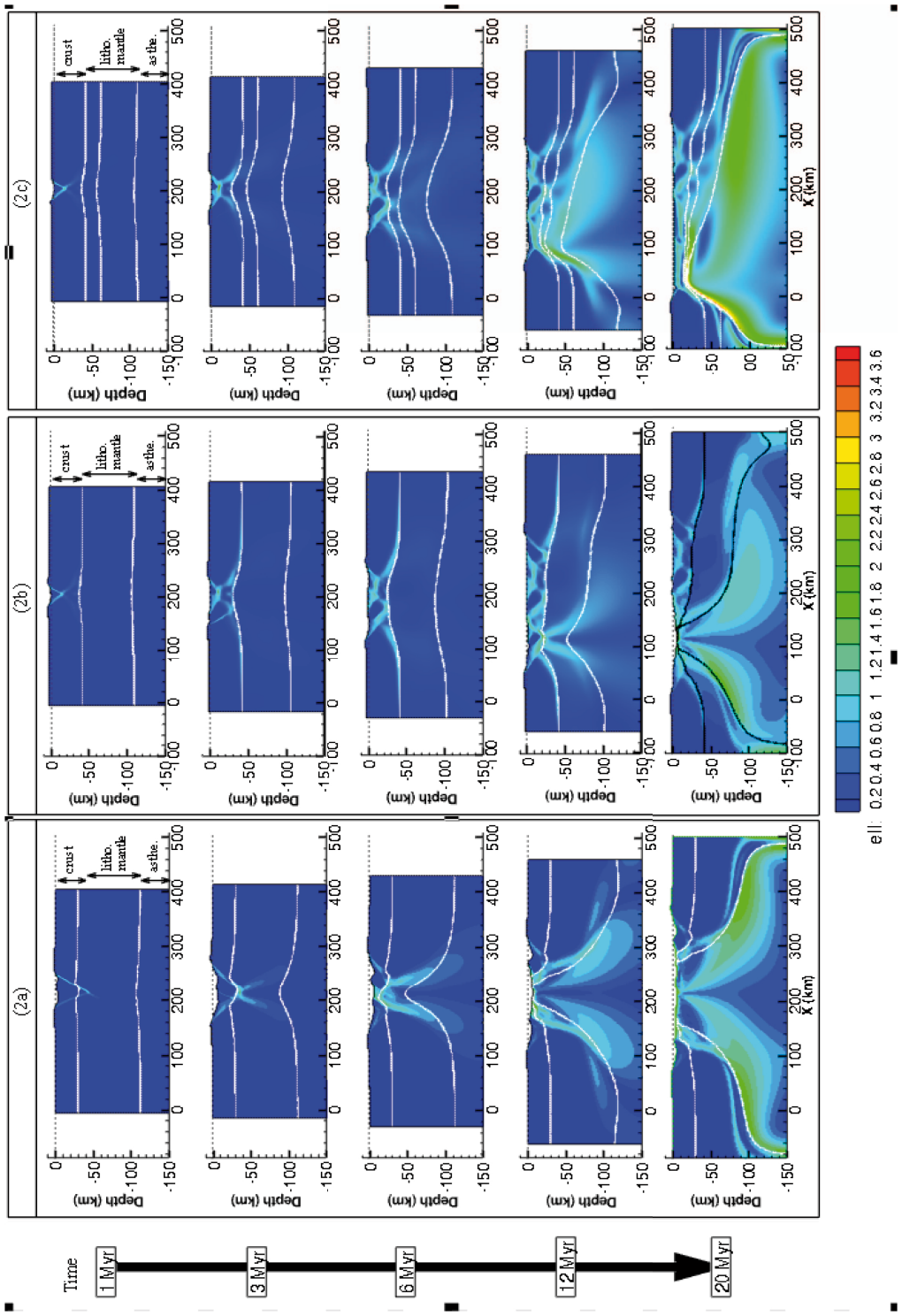

Fig. 2.: Effective accumulated strain field overlay (eII) for models with crust dominated by plagioclase rheology and an initial geotherm corresponding to a $500\,\mathrm{Myr}$ old lithosphere. From top to bottom, the models experience $200\,\mathrm{km}$ of extension over $20\,\mathrm{Myr}$ (extension velocity of $1\,\mathrm{cm/yr}$). At the left, the time after the onset of rifting for each of the five stages of the evolution depicted for the three experiments. (2 a) $30\,\mathrm{km}$ initial crust, and dry olivine mantle; (2 b) $45\,\mathrm{km}$ initial crust, and dry olivine mantle; and, (2 c) $45\,\mathrm{km}$ initial crust, and wet olivine mantle. White solid lines depict the boundaries between crust and mantle (Moho), and between litospheric mantle and asthenosphere (LAB, $1300\,^{\circ}\mathrm{C}$).

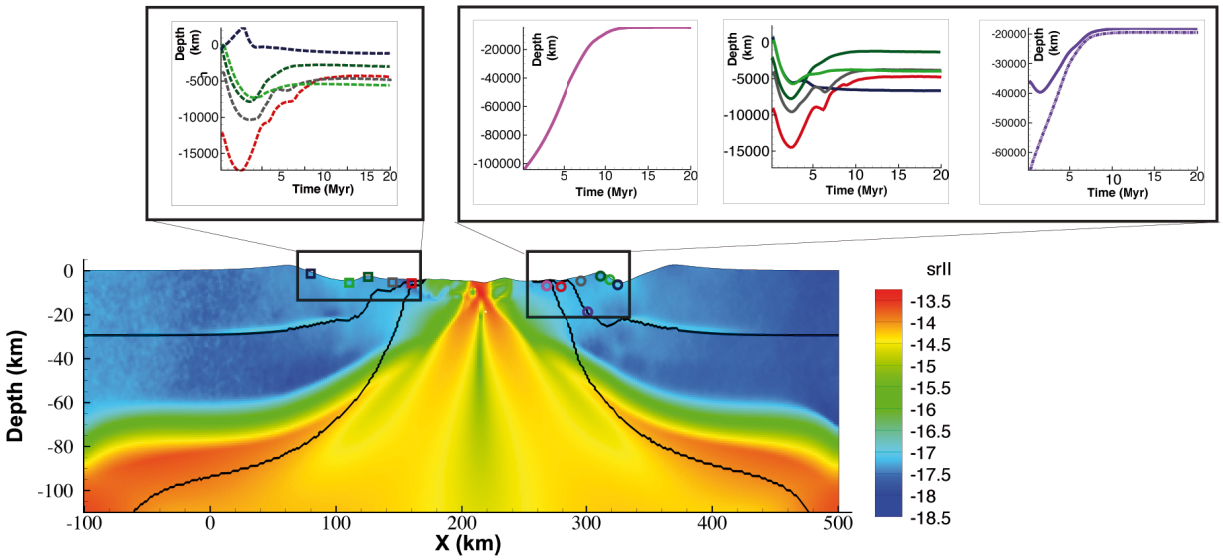

Fig. 3.: On the top, subsidence or exhumation curves (Depth vs. Time) of the particles extracted from the experiment depicted in Figure 2a. Solid lines correspond to subsidence/exhumation histories of particles at the right margins; dashed lines, to the left margin. The color of each line corresponds to the circles (right margin) and squares (left margins) plotted on the section at the bottom, which displays the strain rate of the experiment after 20 Myr of extension.

not enough to result in shallow water conditions.

The processes controlling rif evolution vary depending on initial conditions. We interpret that whether deformation localizes in block H or delocalizes into a wide margin is due to: strengthening of the upper crust, weakening or strengthening of the strong upper mantle below the initial zone of deformation, and the presence or absence of a significant thickness of ductile lower crust. The later is not defined here as a separate layer of the crust with different composition. Ductile lower crust thickness increases with crustal thickness and geothermal gradient (when Moho is above 600 °C significant thickness of the lower crust can flow). Moreover, if the crust is thick, bending stresses are high enough to result in upper crust hardening, forcing the deformation to migrate outside of the initial zone of crustal deformation (Lavier et al., 2000). This lateral migration is later reinforced by three other processes: strengthening of the middle to lower crust due to viscous flow at high strain rates, lateral lower crustal flow from the undeformed to the deformed area, and strengthening of the lithosphere as the mantle uplifts (Buck, 1991) As a result wide margins can form (figure 2). When the strong mantle is weakened sufficiently, deformation localizes there and thinning and exhumation may follow (figure 2, a and b). Brittle faulting or heat transfer in the strong mantle can cause sufficient weakening to initiate thinning and exhumation. But it also possible that diking could provide the necessary weakening.

References

Aslanian, D., & Moulin, M. (2013). Palaeogeographic consequences of conservational models in the South Atlantic Ocean. Geological Society, London, Special Publications, 369(1), 75-90.

Blaich, O. A., Faleide, J. I., Tsikalas, F., Lilletveit, R., Chiossi, D., Brockbank, P., & Cobbold, P. (2010, January). Structural architecture and nature of the continent-ocean transitional domain at the Camamu and Almada Basins (NE Brazil) within a conjugate margin setting. In

Geological Society, London, Petroleum Geology Conference series (Vol. 7, pp. 867-883). Geological Society of London.

Buck, W. R. (1991). Modes of continental lithospheric extension. Journal of Geophysical Research: Solid Earth (1978–2012), 96(B12), 20161-20178.

Buck, W. R., Lavier, L. L., & Poliakov, A. N. (1999). How to make a rift wide.PHILOSOPHICAL TRANSACTIONS-ROYAL SOCIETY OF LONDON SERIES A MATHEMATICAL PHYSICAL AND ENGINEERING SCIENCES, 671-689.

Heine, C., Zoethout, J., & Müller, R. D. (2013). Kinematics of the South Atlantic rift. Solid Earth, 4(2).

Huismans, R., & Beaumont, C. (2011). Depth-dependent extension, two-stage breakup and cratonic underplating at rifted margins. Nature, 473(7345), 74-78.

Kusznir, N. J., & Park, R. G. (1987). The extensional strength of the continental lithosphere: its dependence on geothermal gradient, and crustal composition and thickness. Geological Society, London, Special Publications,28(1), 35-52.

Lavier, L. L., Buck, W. R., & Poliakov, A. N. (2000). Factors controlling normal fault offset in an ideal brittle layer. Journal of Geophysical Research: Solid Earth (1978–2012), 105(B10), 23431-23442.

Lavier, L. L., & Manatschal, G. (2006). A mechanism to thin the continental lithosphere at magma-poor margins. Nature, 440(7082), 324-328.

Mohriak, W. U., & Leroy, S. (2013). Architecture of rifted continental margins and break-up evolution: insights from the South Atlantic, North Atlantic and Red Sea–Gulf of Aden conjugate margins. Geological Society, London, Special Publications, 369(1), 497-535.

Péron-Pinvidic, G., & Manatschal, G. (2009). The final rifting evolution at deep magma-poor passive margins from Iberia-Newfoundland: a new point of view.International Journal of Earth Sciences, 98(7), 1581-1597.

Peron-Pinvidic, G., Manatschal, G., & Osmundsen, P. T. (2013). Structural comparison of archetypal Atlantic rifted margins: A review of observations and concepts. Marine and Petroleum Geology, 43, 21-47.

Quirk, D. G., Hertle, M., Jeppesen, J. W., Raven, M., Mohriak, W. U., Kann, D. J., ... & Mendes, M. P. (2013). Rifting, subsidence and continental break-up above a mantle plume in the central South Atlantic. Geological Society, London, Special Publications, 369(1), 185-214.

Sakariassen, R. (2007). North Namibia margin: regional tectonic evolution based on integrated analysis of seismic reflection and potential field data and modelling.

Van Avendonk, H. J., Holbrook, W. S., Nunes, G. T., Shillington, D. J., Tucholke, B. E., Louden, K. E., ... & Hopper, J. R. (2006). Seismic velocity structure of the rifted margin of the eastern Grand Banks of Newfoundland, Canada. Journal of Geophysical Research: Solid Earth (1978–2012), 111(B11).

Van Avendonk, H. J., Lavier, L. L., Shillington, D. J., & Manatschal, G. (2009). Extension of continental crust at the margin of the eastern Grand Banks, Newfoundland. Tectonophysics, 468(1), 131-148.

Zalán, P. V., Severino, M. D. C. G., Rigoti, C. A., Magnavita, L. P., de Oliveira, J. A. B., & Vianna, A. R. (2011, April). An entirely new 3D-view of the crustal and mantle structure of a South Atlantic passive margin–Santos, Campos and Espírito Santo basins, Brazil. In Americal Association of Petroleum Geology, Annual Convention and Exhibition.

Influence of Melting on the Long-Term Thermo-Chemical Evolution of Earth's Deep Mantle

Paul J. Tackley[1], Diogo Lourenço[2], Ilya Fomin[1], Takashi Nagawaga[2]

[1]*Institute of Geophysics, Department of Earth Sciences, ETH Zurich, Switzerland*
[2]*IFREE, JAMSTEC, Japan*
e-mail: *ptackley@ethz.ch*
session: *Geodynamics*

Melting has always played a key role in Earth evolution. Early solidification of a magma ocean may have left the mantle compositionally stratified and may have continued in the form of a long-lived basal magma ocean (BMO). Ongoing upper mantle/transition zone melting, perhaps associated with water and carbonate, may have caused "internal differentiation", resulting in dense enriched products that sink. Throughout Earth's history melting in the shallow mantle has produced crust, most of which was recycled into the interior and some of which may have segregated above the core-mantle boundary, joining possible enriched products from early differentiation, internal differentiation and BMO solidification to produce a Basal Melange (BAM). Here we investigate the thermal and chemical evolution of Earth's interior from the ~molten state to billions of years later using global-scale numerical simulation. Our previously-published models that included only oceanic crustal production and recycling (e.g. Nakagawa & Tackley, 2014 GCubed) indicated that (i) a layer of subducted crust can rapidly build up above the CMB, (ii) early-formed layering above the CMB may have been necessary to avoid rapid early core cooling and a too-large present-day inner core, (iii) magmatism is the dominant heat transport mechanism early on, (iv) melting acts as a thermostat, buffering mantle temperature. Here we improve the models to handle deep melting including melt fractions of up to 100 %, fractional melting using a eutectic model, segregation of melt and solid, and a parameterized magma ocean treatment at high melt fractions (using an eddy diffusivity based on mixing length theory, similar to previous 1-D treatments). We investigate and characterize the evolution of deep mantle structure in the limits of negatively buoyant melt and positively buoyant melt. We focus on the interplay of deep melting and melt migration, primordial layering, recycled crust and harzburgite, and products of upper mantle internal differentiation, in producing a heterogeneous deep mantle BAM.

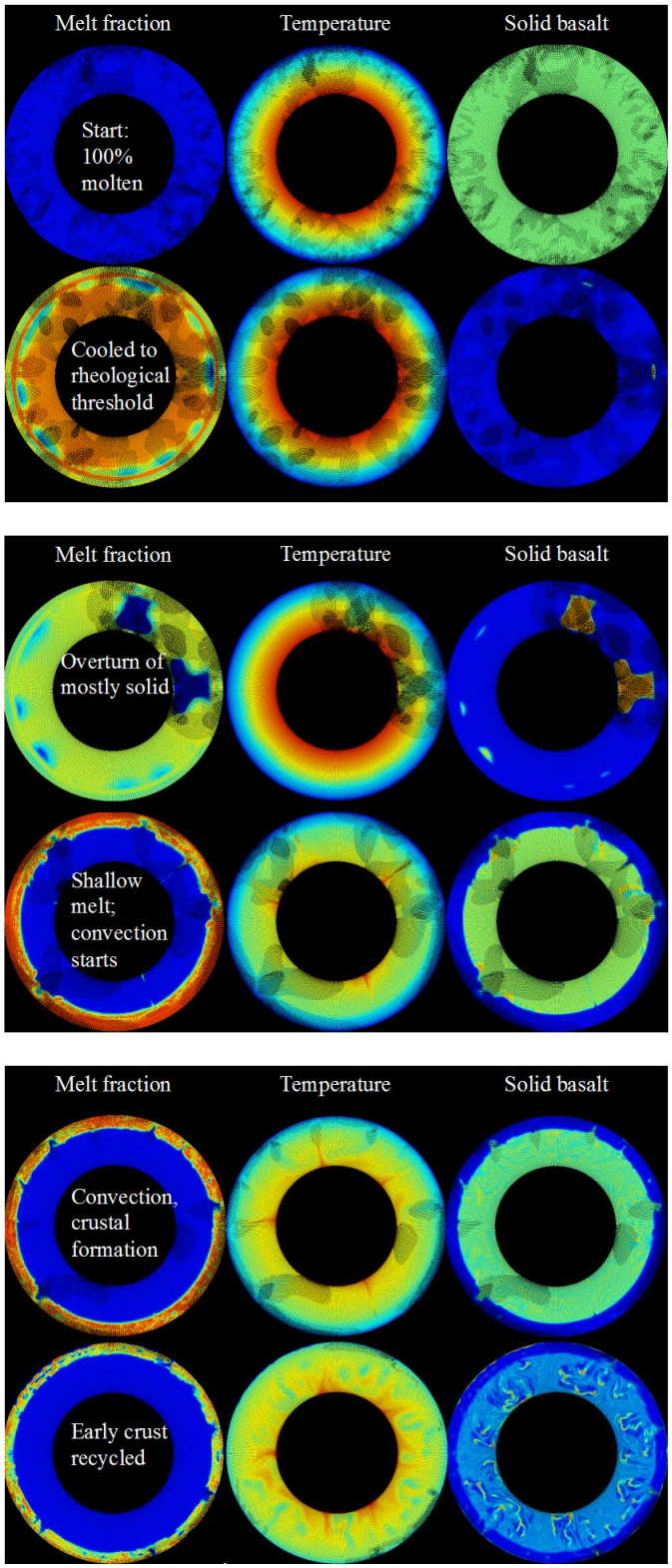

Fig. 1.: Sequence of events in the early ($< 1\,\mathrm{Byr}$) evolution of an Earth-like planet starting from a 100 % molten state. Quantities are scaled to minimum and maximum values.

A two- and three-dimensional numerical modelling benchmark of slab detachment

Cedric Thieulot[1,2], Anne Glerum[1,4], Bram Hillebrand[1], Stefan Schmalholz[3], Wim Spakman[1,2,4], Trond Torsvik[2]

[1] *Utrecht University, Dept. of Earth Sciences, Utrecht, Netherlands*
[2] *Centre for Earth Evolution and Dynamics, Oslo, Norway*
[3] *Institute of Earth Sciences , University of Lausanne, Switzerland*
[4] *The Netherlands Research Centre for Integrated Solid Earth Science*
e-mail: *c.thieulot@uu.nl*
session: *Geodynamics*

Subduction is likely to be the most studied phenomenon in Numerical Geodynamics. Over the past 20 years, hundreds of publications have focused on its various aspects (influence of the rheology and thermal state of the plates, slab-mantle coupling, roll-back, mantle wedge evolution, buoyancy changes due to phase change, ...) and results were obtained with a variety of codes.

Slab detachment has recently received some attention (e. g. Duretz, 2012) but remains a field worth exploring due to its profound influence on dynamic topography, mantle flow and subsequent stress state of the plates, and is believed to have occured in the Zagros, Carpathians and beneath eastern Anatolia, to name only a few regions.

Following the work of Schmalholz (2011), we propose a two- and three-dimensional numerical benchmark of slab detachment. The geometry is simple: a power-law T-shaped plate including an already subducted slab overlies the mantle whose viscosity is either linear or power-law. Boundary conditions are free-slip on the top and the bottom of the domain, and no-slip on the sides.

When the system evolves in time, the slab stretches out vertically and shows buoyancy-driven necking, until it finally detaches. The benchmark is subdivided into several sub-experiments with a gradual increase in complexity. An array of objective measurements is recorded throughout the simulation such as the width of the necked slab over time and the exact time of detachment. The experiments will be run in two-dimensions and repeated in three-dimensional, the latter case being designed so as to allow both poloidal and toroidal flow.

We show results obtained with a multitude of Finite Element and Finite Difference codes, using either compositional fields, level sets or tracers to track the compositions. A good agreement is found for most of the measurements in the two-dimensional case, and preliminary three-dimensional measurements will be shown.

References

Duretz et al (2012), Thermomechanical modeling of slab eduction, JGR, vol. 117.

Schmalholz (2011), A simple analytical solution for slab detachment, EPSL, vol. 304, p 45-54.

The effect of strong heterogeneities in the upper mantle rheology on the dynamic topography and geoid

Anthony Osei Tutu

GFZ German Research Centre for Geoscience (Section 2.5), Potsdam, Germany
e-mail: *oseitutu@gfz-potsdam.de*
session: *Geodynamics*

The undulating nature of the earth surface (topography) on both continents and sea floor and the observed geoid anomaly are influenced by the convective processes within the Earth's mantle driven by density anomalies. Hot, less dense material tends to rise and push the overlying lithosphere upward, whereas cold, denser material tends to sink and pull the lithosphere downward (Steinberger, 2014). This mechanism is simplistically illustrated in figure 1.

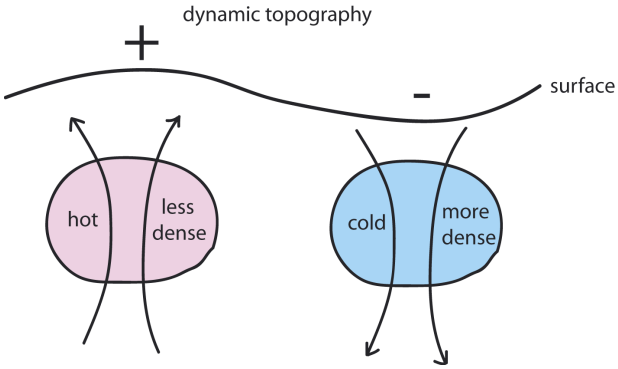

Fig. 1.: The concept of dynamic topography (Steinberger, 2014)

Evidence from ancient coastal areas currently submerged (Hartley et al. 2011) suggests significant changes in topography of several hundred meters relative to the present day Europe. The effect of such changes on the present-day relief and land area would drastically change the face of Europe as shown in figure 2.

The geoid is about 90 % (Hager & Richards, 1989) determined by both the density anomalies driving the mantle flow and the dynamic topography caused at the Earth surface and the core-mantle boundary. The remainder is largely due to strong heterogeneities in the lithospheric mantle and the crust, which also need to be taken into account. Surface topography caused by density anomalies both in the sub-lithospheric mantle and within the lithosphere depend on lithosphere rheology. Here we investigate these effects by assessing the differences between modelled dynamic topography and geoid from the spectral mantle flow code (Hager & O'Connell, 1981) and a fully coupled code of the lithosphere and mantle accounting for strong heterogeneities in the upper mantle rheology (Popov & Sobolev, 2008).

The coupled code approach simulates the visco-elasto-plastic rheology of the lithosphere and the radial and lateral viscosity variations in the material in the uppermost 300 km of the Earth interior including the lithosphere-asthenosphere boundary. In contrast, the mantle flow code simulates a 3-D density structure inferred from shear wave seismic tomography and assumes a radial viscosity variation from the CMB to the surface to compute a deviatoric normal stress, which is then converted to the dynamic topography using a scaling coefficient.

This study is the first step towards, linking global mantle dynamics with lithosphere dynamics using the observed geoid as a major constraint and results from both codes will be presented and compared with the observed geoid and dynamic topography. This effort will also serve as a benchmark of the two existing numerical codes developed for geodynamic modelling.

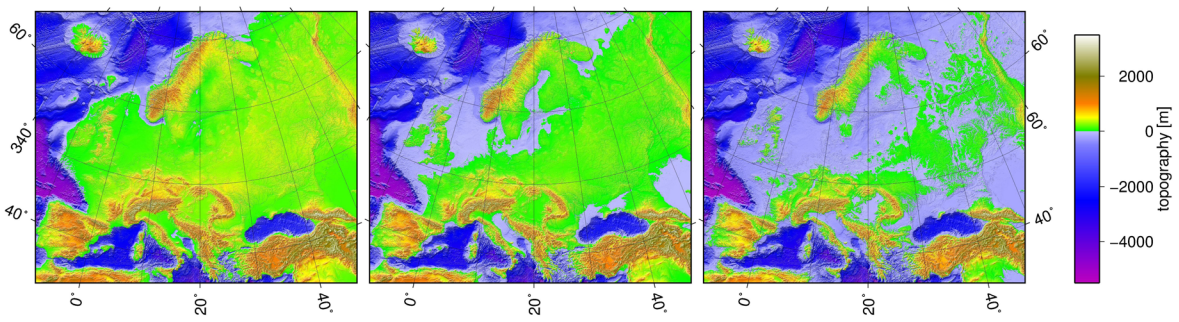

Fig. 2.: Topography of Europe: A) Present-day $+150\,\mathrm{m}$; B) Present-day C) Present-day $-150\,\mathrm{m}$ (Steinberger, 2014)

References

Hager B.H & O'Connell R.J., 1981. A simple global model of plate dynamics and mantle convection, J.geophys. Res. 86, 4843-4867.

Hager B.H. & Richards M.A., 1989. Long-wavelength variations in Earth's geoid: physical models and dynamical implications, Phil. Trans. R. Soc. Lond., A348, 309-327.

Hartley, R.A., Roberts, G.G., White, N. & Richardson, C., 2011. Transient convective uplift of an ancient buried landscape, it Nat. Geosci., 4, 562-565.

Popov A.A., Sobolev S.V., 2008. SLIM3D: A tool for three-dimensional thermomechanical modelling of lithospheric deformation with elasto-visco-plastic rheology.

Steinberger B., 2014. Dynamic topography: Acomparison between observations and models based on seismic tomography.

The role of weak seeds in numerical modelling of continental extensional systems

Iris van Zelst[1], Cedric Thieulot[1,2], Susanne J. H. Buiter[2,3], John Naliboff[3], Wim Spakman[1,2]

[1] *Department of Earth Sciences, Utrecht University, Utrecht, The Netherlands*
[2] *Centre for Earth Evolution and Dynamics, University of Oslo, Oslo, Norway*
[3] *Geodynamics Team, Geological Survey of Norway, Trondheim, Norway*
e-mail: *i.vanzelst@students.uu.nl*
session: *Geodynamics*

Numerical models that investigate the dynamics of the lithosphere and upper mantle need to start from an initial geometry with a set of prescribed mechanical and thermal conditions. Initial conditions are required in order to localize and initiate deformation. Without such initial conditions, deformation may take a long model time to localize, up to millions of years. The reason for this is that these models need to accumulate numerical disturbance to create starting points for the deformation. A method that is often used in models of extension of continental lithosphere to localize deformation faster is to use "seeds" to initiate extension. These seeds are usually small regions that are weaker than the surrounding crust and lithosphere. Multiple ways of prescribing weak seeds are found in the literature.

One way of implementing a weak seed is through thermal effects. A weak region can be achieved by a temperature anomaly in the crust or lithosphere, which can be created by directly imposing a temperature difference, by assigning high radiogenic heat production, by perturbing the basal heat flow, or by modelling a thermal upwelling in the mantle below. For models with a temperature-dependent viscosity, the elevated temperature reduces the viscosity. An advantage of using an imposed temperature anomaly is that it will dissipate with time, thus reducing the impact on later model stages.

Another way of implementing a weak region is to compose the seed of a material with a lower rheological strength than its surroundings. This can be achieved by imposing a lower viscosity, a lower value for the angle of internal friction, or assigning different material properties, such as a von Mises seed in a frictional plastic material. Prescribing the weak seed as a region which already has accumulated strain, leading to strain-weakening, is also a frequently used approach. In the literature a variety of shapes and sizes for this kind of weak seeds can be found. Examples include square seeds, fault-shaped weak inclusions and rectangular seeds with different aspect ratios. Randomly distributed seeds have also been used.

A weak zone can also be created by an abrupt variation in the thickness of the crust and/or lithosphere. A locally thinned crust can be thought to be caused by a previous rifting phase, whereas a thicker crust could represent preceding mountain building. These variations in thickness affect the mechanical strength and impose a thermal anomaly.

The literature is scarce concerning the effects of the different methods of implementing a weak zone on the results of the model. However, the variety in shape, size, orientation, mechanical and thermal properties and depth of the seed(s) begs the question whether these different approaches could have an effect on model evolution. We therefore present a series of numerical models conducted with the codes ELEFANT and SULEC that aims at investigating the role of weak seeds

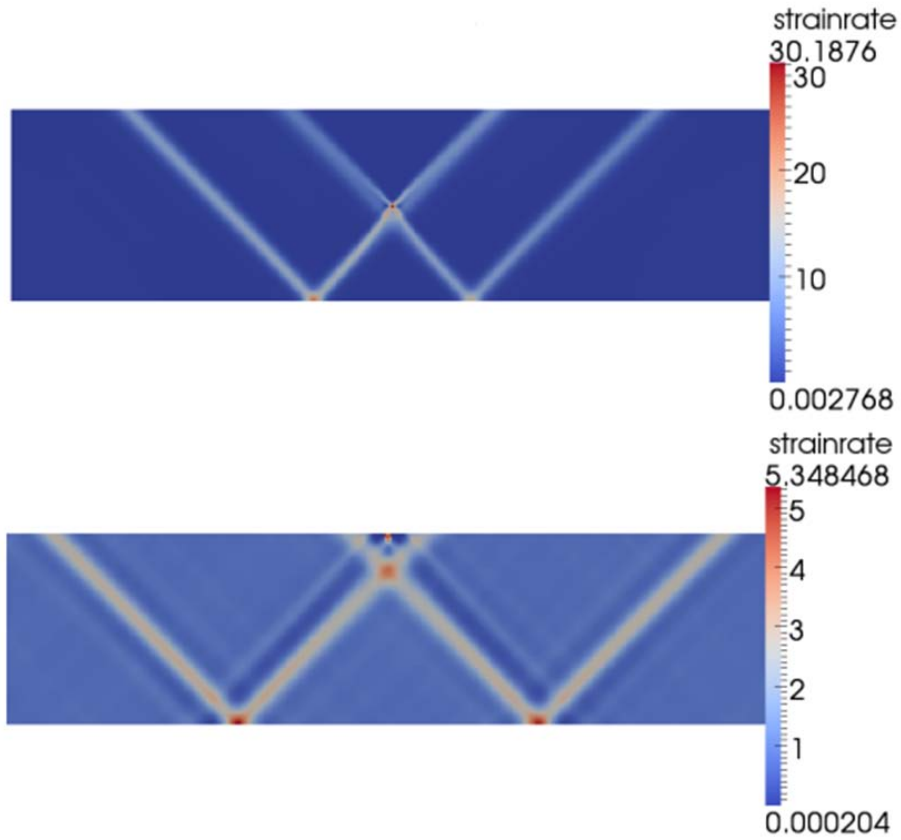

Fig. 1.: Results for different vertical positions of the weak seed in a dimensionless single layer extensional system. The internal angle of friction ϕ is 15. In the top figure, the weak seed is placed in the middle of the model domain, while in the bottom figure the weak seed is placed at the top. Results are calculated with ELEFANT.

in the initial and later stages of continental extension. The basis model is always the same (a multi-layered thermo-mechanically coupled extension model of the upper mantle), the only difference between the models is formed by the size and nature of the weak seed. In figure 1 preliminary results concerning the placement of the weak seed are shown for a simple, dimensionless, one layer model. The viscosity of the layer is 10^5. On the poster for GeoMod2014, results will be presented for the more complex, multi-layered extension model of the upper mantle.

The up side down logic of orogenic collision: on the formation of low-topography mountain ranges

Katharina Vogt[1], Liviu Matenco[1], Taras Gerya[2], Sierd Cloetingh[1]

[1]*Department of Earth Sciences, Utrecht University, Budapestlaan 4, 3584CD Utrecht, Netherlands*
[2]*Institute of Geophysics, ETH Zürich, Sonneggstrasse 5, 8092 Zürich, Switzerland*
e-mail: *k.j.vogt@uu.nl*
session: *Geodynamics*

Abstract

Present models of orogeny generally assume that mountains grow upwards by gradual accretion of crustal material during continental collision. This mechanism is characterized by high topographic build-up and material transport within the pro- and retro-wedge. However, at least half of the mountain ranges worldwide are characterized by low and distributed topographies with little or no exhumation in retro-wedges. In this study we analyse if mountain chains may grow downwards, by active accretion of crustal material to the lower plate. In this model the upper crust is decoupled and deformed, while the lower crust is subducted to mantle depth and subjected to slab retreat. This mechanism allows a foreland shift in the timing of exhumation and the location of the main subduction zone, explaining the often geometrical misfit between the crustal position of the lower plate and the geometry of slabs inferred by teleseismic tomography.

Introduction

When the continental crust reaches a subduction zone continental collision forms generally high topography, because of the excess of low-density material accumulated at the plate margin. Analogue and numerical models demonstrated the gradual accretion of crustal material to the upper plate along retro-shears (Beaumont et al., 1996). In these models continental subduction results in upper plate deformation and formation of double-vergent orogens. Typical examples include the Swiss Alps and the Pyrenees (Schmid et al., 1996; Beaumont et al., 2000). These are dominantly high-convergence orogens with low angles of subduction and where the contact between the collisional plates is positioned in line with the location of slabs detected by teleseismic mantle tomography.

The other half of worldwide orogens forms low-topography mountain ranges at retreating subduction boundaries, where the rapid roll-back of subducted slabs is accommodated by upper plate extension and formation of back-arc basins (e. g., Faccenna et al., 2004). A common feature of these orogens is the geometrical misfit between the crustal position of the lower plate and the geometry of slabs inferred by teleseismic tomography. The aim of this study is to analyse numerically the physical concepts and implications of such low topography mountain ranges.

Methods

The study of collisional systems and the evolution in time of associated deformation was analysed by the means of high-resolution thermo-mechanical numerical modelling designed to investigate the physical processes related to orogenic building. All numerical experiments were performed with the I2VIS code (Gerya and Yuen, 2003). This code is based on conservative finite differences and a marker-in-cell technique. The momentum,

continuity and energy equations are solved on Eulerian frame, and Lagrangian markers that move according to the velocity field interpolated from the fix grid transport physical properties. The model uses non-Newtonian visco-plastic rheologies to simulate multiphase flow.

Model Setup: The computational domain spans 1000 km × 200 km and contains a (600 km wide) high-resolution area of 0.5 km × 0.5 km. Constant velocities are applied to the to simulate a total convergence of 1 cm/a. A rheologically weak zone at the bottom of the continental crust represents a suture zone, separating two continental domains after the closure of an ocean. The continental crust is homogeneous and has a total thickness of 35 km. It is subdivided into 20 km of felsic and 15 km of mafic rocks. The underlying mantle is composed of dry olivine. The initial temperature field of the continental lithosphere was varied. It increases linearly from 0 °C at the surface to 400 °C to 800 °C at the crust-mantle boundary (Moho) and 1300 °C at the lithosphere-asthenosphere boundary at 120 km to 160 km depth. For the asthenospheric mantle a thermal gradient of 0.5 °C km^{-1} is used. To allow for topographic build up of the lithosphere a layer of 20 km and low viscosity (1018 Pa s) and low density (1 kg m^{-3}) is implemented above the lithosphere. The large viscosity contrast between this layer and the lithosphere minimizes shear stresses (< 104 Pa) making it an efficient free surface (e. g. Schmeling et al., 2008). The topography of the model (air/crust interface) evolves according to a transport equation that is solved at each time-step on the Eulerian grid and accounts for erosion and sedimentation (Gorczyk et al., 2007).

Results

Our numerical results indicate that (i) deformation might be localized in lower orogenic plates and (ii) collisional systems are able to develop solely by foreland-vergent deformation and migration of the main subduction zone.

Similar to the orogenic retro-wedge scenarios, the onset of contraction leads to an initially symmetric situation in which pro- and retro- shears display limited offsets at the scale of the orogen. The subsequent localized deformation within the weak (subduction) zone leads to a concentration of deformation almost exclusively in pro-shears. This causes a large-scale asymmetry, where deformation and associated exhumation gradually migrate towards the foreland. The large displacement in the pro-wedge accommodates almost the entire shortening and allows for the subduction of lower crust. The upper crust decouples and records significant internal shortening during the foreland propagation of the deformation front, while the upper orogenic plate is passively exhumed and deformed, although with significant lower values than normally observed in typical retro-wedges. The resulting orogenic geometry is highly asymmetric and almost exclusively oriented towards the foreland, deformation and exhumation migrating in the same direction.

Discussion

Our numerical results indicate that (i) deformation might be localized in lower orogenic plates and (ii) collisional systems are able to develop solely by foreland-vergent deformation and migration of the main subduction zone.

Similar to the orogenic retro-wedge scenarios, the onset of contraction leads to an initially symmetric situation in which pro- and retro- shears display limited offsets at the scale of the orogen. The subsequent localized deformation within the weak (subduction) zone leads to a concentration of deformation almost exclusively in pro-shears. This causes a large-scale asymmetry, where deformation and associated exhumation gradually migrate towards the foreland. The large displacement in the pro-wedge accommodates almost the entire shortening and allows for the subduction of lower crust. The upper crust decouples and records significant internal shortening during the foreland propagation of the deformation front, while the upper orogenic plate is passively ex-

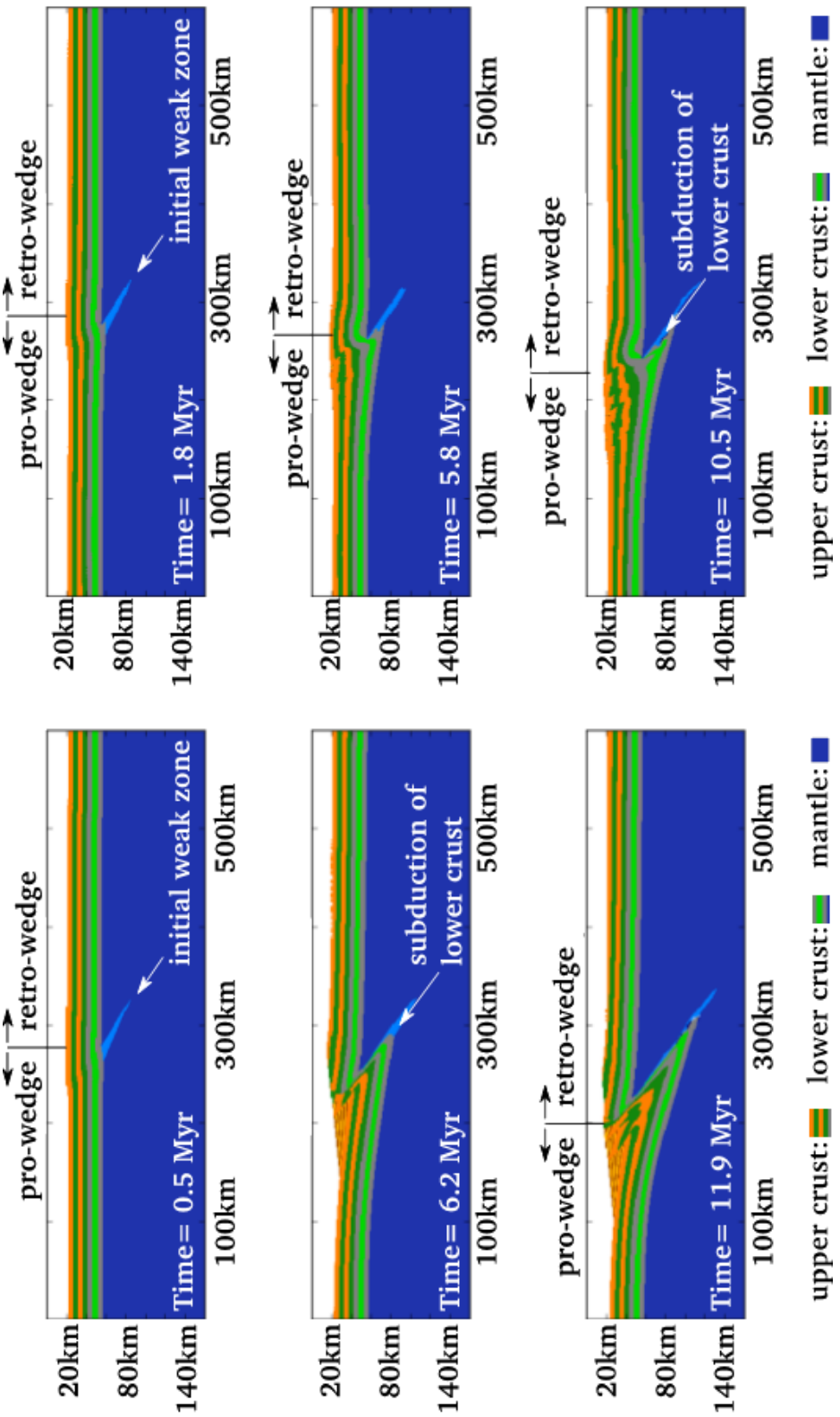

Fig. 1.: Tectonic model of a continent-continent collision zone. Compositional map.

humed and deformed, although with significant lower values than normally observed in typical retro-wedges. The resulting orogenic geometry is highly asymmetric and almost exclusively oriented towards the foreland, deformation and exhumation migrating in the same direction.

References

Beaumont, C., Ellis, S., Hamilton, J., Fullsack, P., 1996. Mechanical model for subduction collision tectonics of Alpine-type compressional orogens. Geology 24, 675-678.

Beaumont, C., Munoz, J.A., Hamilton, J., Fullsack, P., 2000. Factors controlling the Alpine evolution of the central Pyrenees inferred from a comparison of observations and geodynamical models. Journal of Geophysical Research 105, 8121-8145.

Faccenna, C., Piromallo, C., Crespo-Blanc, A., Jolivet, L., Rosetti, F., 2004. Lateral slab deformation and the origin of the western Mediterranean arcs. Tectonics 23, TC1012, doi:1010.1029/2002TC001488.

Gorczyk, W., Willner, A.P., Gerya, T.V. and Connolly, J.A.D. and Burg, J.-P., 2007. Physical controls of magmatic productivity at Pacific-type convergent margins: Numerical modelling. Physics of the Earth and Planetary Interiors. 163, 209–232.

Gerya, T.V., and Yuen, D.A., 2003, Characteristics-based marker-in-cell method with conservative finite differences schemes for modeling geological flows with strongly variable transport properties: Physics of the Earth and Planetary Interiors, v. 140, p. 293–318, doi:10.1016/j.pepi.2003.09.006.

Jolivet, L., Faccenna, C., 2000. Mediterranean extension and the Africa-Eurasia collision. Tectonics 19, 1095-1106.

Schmeling H., Babeyko, A., Enns, A., Faccenna, C., Funiciello, F., Gerya, T., Globalek, G., Grigull, S., Kaus, B., Morra, G., van Hunen, 2008. A benchmark comparison of spontaneous subduction models - toward a free surface. Physics of the Earth and Planetary Interiors 171, 198-223.

Schmid, S.M., Berger, A., Davidson, C., Giere, R., Hermann, J., Nievergelt, P., Puschnig, A.R., Rosenberg, C., 1996. The Bergell pluton (Southern Switzerland, Northern Italy): overview acompanying a geological-tectonic map of the intrusion and surrounding country rocks. Schweizerische Mineralogische und Petrographische Mitteilungen 76, 329-355.

Willingshofer, E., Sokoutis, D., Luth, S.W., Beekman, F., and Cloething, S., 2013. Subduction and deformation of the continental lithosphere in response to plate and crust-mantle coupling. Geology, 41, 1239-1242.

Implementing fluid flow in SLIM-3D

Marius Walter, Javier Quinteros, Stephan V. Sobolev

GeoForschungsZentrum, Telegrafenberg, 14473 Potsdam, Germany
e-mail: *mwalter@gfz-potsdam.de*
session: *Geodynamics*

SLIM-3D is a three-dimensional thermomechanical code capable of simulating lithospheric deformation with elasto-visco-plastic rheology (Popov and Sobolev, 2008). It incorporates an arbitrary Lagrangian Eulerian formulation, free surface, and changes in density and viscosity, due to endothermic and exothermic phase transitions. It has been successfully applied to model different geodynamic processes at divergent (Brune and Autin, 2013; Melnick et al., 2012), convergent (Quinteros and Sobolev, 2013; Quinteros and Sobolev, 2010) and transform (Popov et al., 2012) plate boundaries. However, although SLIM-3D already includes many features, fluid flow has not been incorporated into the model yet.

The aim of the here presented study is to overcome this shortcoming of SLIM-3D. We are especially interested in modeling subduction evolution with respect to fluid flow. Fluids play a crucial role in subduction evolution. For example, excess mechanical weakening along tectonic interfaces, due to excess fluid pressure, may enable oceanic subduction (Dymkova & Gerya, 2013). Hence, the water content may be a critical parameter for subduction initiation. Studies have also shown a correlation between the location of slab dehydration and intermediate seismic activity (Hacker et al., 2003). Furthermore, expelled fluids from the subduction slab affect the melting temperature, consequently, contributing to partial melting in the wedge above the downgoing plate and resulting in chemical changes in earth interior and extensive volcanism (Cagnioncle et al., 2007). In summary, fluids have a great impact on tectonic processes and therefore should be incorporated into geodynamic numerical models.

Here we use existing approaches to implement fluid flow into SLIM-3D (McKenzie, 1984; Morency et al., 2007). The coupling between solid and fluid flow rests upon the assumption that fluids flow through a porous and deformable solid. Thus, we couple the solid momentum equation, continuity equation for solid and fluid, as well as the Darcy equation. This system of equations becomes, however, nonlinear, because permeability is assumed to be a power-law function of porosity. Ultimately, the evolution of porosity is governed by the compaction pressure and the advection of the porous solid.

We plan to show the implementation of the fluid flow into the existing thermo-mechanical finite element code and present first results. Eventually, we will carry out experiments to better understand controls on magma emplacement and variations in the temperature field. We are especially interested in the coupling of subduction processes and the evolution of the magmatic arc. Thereby, we will study the migration of the volcanic front in respect to subduction processes and geometry in order to identify models that best fit the geodynamic evolution of the Central Andes.

References

Brune, S. and Autin, J.: The rift to break-up evolution of the Gulf of Aden: Insights from 3D numerical lithospheric-scale modelling, Tectonophysics, 607, 65–79.

Cagnioncle, A.-M., Parmentier E. M., Elkins-Tanton L. T. (2007). Effect of solid flow above a subducting slab on water distribution and

melting at convergent plate boundaries, J. Geophys. Res., 112 (B09402), 1–19.

Dymkova, D., Gerya, T., 2013. Porous fluid flow enables oceanic subduction initiation on Earth. Geophysical Research Letters 40 (21), 5671–5676.

Hacker, B. R., Peacock S. M., Abers G. A., Holloway S. D. (2003). Subduction factory: Are intermediate-depth earthquakes in subducting slabs linked to metamorphic dehydration reactions?, J. Geophys. Res., 108 (B1), 1–8.

McKenzie, D., (1984). The generation and compaction of partially molten rock. Journal of Petrology 25 (3), 713–765.

Morency, C., Huismans, R., Beaumont, C., Fullsack, P, (2007), A numerical model for coupled fluid flow and matrix deformation with applications to disequilibrium compaction and delta stability, Jour. Geophys. Res., 112 (B10404), 1–24.

Popov, A. A., Sobolev, S. V., 2008. Slim3d: A tool for three-dimensional thermo-mechanical modeling of the lithospheric deformation with elasto-visco-plastic rheology. Physics of the Earth Interiors 171, 55–75.

Quinteros, J., Sobolev, S. V., 2012. Constraining kinetics of metastable olivine in Marianas slab from seismic observations and dynamic models. Tectonophysics 526–529 (0), 48–55.

Quinteros, J. and Sobolev, S. V.: Why has the Nazca plate slowed since the Neogene?, Geology, 41, 31–34, doi:10.1130/G33497.1, 2013.

Quinteros, J., Sobolev, S. V., and Popov, A. A.: Viscosity in transition zone and lower mantle: Implications for slab penetration, Geophysical Research Letters, 37, L09 307, doi:10.1029/2010GL043140, 2010.

The mechanical erosion of refertilized continental lithosphere by plume driven mantle flow

Hongliang Wang[1], Jeroen van Hunen[1], D. Graham Pearson[2]

[1] *Department of Earth Science, University of Durham, Durham, England, United Kingdom*
[2] *Department of Earth & Atmospheric Sciences, University of Alberta, Edmonton, AB, Canada*
e-mail: *godormag@gmail.com*
session: *Geodynamics*

Abstract

Mantle plumes are amongst the most influential thermal events for continental lithosphere as they provide extra heat and strong mantle flow that could change and erode the originally depleted continental root. Xenolith research shows that many Precambian lithospheres show a multistage modification/enrichment through mantle metasomatism process that might change the buoyancy and rheology of continental root. We performed new numerical experiments to explore the lithosphere dynamics of a plume impacting continental lithosphere. A combined rheology with parameters close to dislocation and diffusion creep experiments is applied. Our models demonstrate that the mechanical erosion of lithosphere mainly focuses on the edge of the continental root, and it is strongly affected by the internal buoyancy and rheology of the portion of the root that is exposed to the plume flow. Models with increased plume flux or closer plume proximity, however, are not found to induce more erosion. By either losing their high viscosity or chemical buoyancy, a significant part of continental root might be eroded away during tens of Myrs by the plume impact. Thus, our results indicate that metasomatic refertilization that could change the buoyancy and rheology of lithosphere, is an essentia for the destruction of continental roots. Furthermore, our results demonstrate how a plume event could have caused the significant thinning of Proterozoic lithosphere beneath SW Namibia in southern Africa, at 70 Ma.

Introduction

The heterogeneity of lithosphere with cratonic, platform and oceanic lithosphere, is one of the most salient features of modern plate tectonic. The long lasting thick cratonic lithosphere is considered to be generally stable and not subject to change since it is formed in Archean, at least in terms of geodynamics. However, the finding that North China Craton [Gao et al., 2008; Zhu and Zheng, 2009] has lost significant part of its root shows that craton might also be affected by mantle dynamic activities. With the development of modern geosciences techniques, more and more new evidences show that the physically stable cratons might also experience some mantle dynamics and be modified in different aspects such as seismic properties, chemical composition [Chesley et al., 2004; Carlson et al., 1995, 2005; Simon et al., 2003; James et al., 2001; Griffin et al., 2003a]. Consider the significant lithosphere heterogeneity observed, either from the different thickness of different types of lithosphere or from the geochemical modifications (e. g. mantle metasomatism), the geodynamical modelling of its effects is required. Mantle plumes are suggested to be responsible to some observations related to mantle dynamics. Therefore, it is interesting to know how lithospheric refertilization and mantle plume influence the stability of the continental lithosphere. Numerical experiments are performed to explore the erosion process when a plume impact thick continental root with different buoyancy and strength.

Model setup

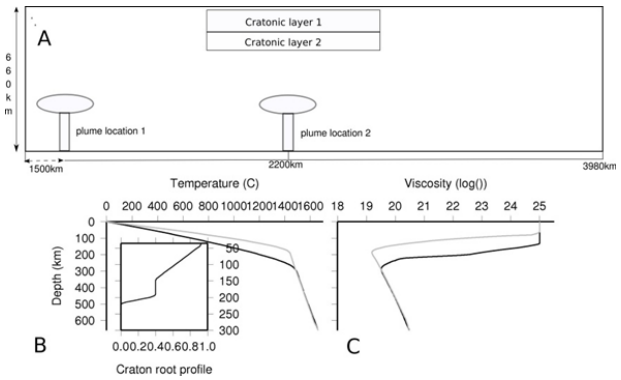

Fig. 1: A) Two-layer Cratonic root setup: 1) a highly depleted layer from Moho to 150 km with the chemically tracking value gradually decrease from 1 to $C\eta$; 2) a less depleted layer from 150 km to 200 km with constant chemically tracking value $C\eta$. B) Typical geotherms of cratonic (black) and normal lithosphere (gray) as the initial thermal condition and chemical profile of cratonic layer (zoomed box). C) Typical viscosity profile corresponding to the geotherms in B.

Results and discussion

Figure 2 show the plume craton interaction for about 125 Myrs through temperature, buoyancy and viscosity evolution. When the plume arrives at around 30 Myrs, the lower cratonic root become relatively more gravitational unstable as the deep blue area indicates and is strongly sheared at the edge by the plume induce flow (30.7 Myr in Fig. 2 B). However, the high viscosity of cratonic root prevent the significant development of gravity instability in this model and only the root material at edge of cratonic root is eroded away. After the major plume flow impact, small scale convection develops underneath the normal lithosphere and it propagates to the edge of cratonic root and cause further erosion (41.7 Myr in Fig. 2 B). Once the plume material cools down, the lower part of cratonic root returns back to neutrally buoyant (125 Myrs in Fig. 2 B). Comparing the cratonic root before and after the plume, we can see the main impact and erosion is focused on the edge of thick continental root.

As the first layer of the root has little effects on the dynamics, we parameterize the chemical buoyancy and strengthening factor ($\Delta\rho$ and $\Delta\eta$ in Fig. 3) of the second layer to explore their effects on the erosion of cratonic root by plumes. We calculate average thermal thickness and chemical root remain at the left cratonic edge at every time step in order to monitor the extent of erosion. Figure 3 A and 3 B show these two quantities at 50 Myr (20 Myrs after the plume rising up) for a range of models. Four models are selected to demonstrate the evolution histories of these two quantities in Figure 3 C and 3 D, in which the impact of plume arrival is clearly indicated by the kink points near 30 Myrs for all of these lines. After the plume, the average thermal thicknesses grows slowly as the mantle cools down (Fig. 3 C), while the erosion of chemical root might still continue (red and blue lines in Fig. 3 D) or slows down (green line in Fig. 3 D). As it shows, the craton edge in the model with $\Delta\rho = 31.5\,\mathrm{kg\,m^{-3}}$ and $\Delta\eta = 4$ maintains an average thermal thickness around 190 km and 90 % of its original cratonic root at 50 Myrs. By either reducing the buoyancy (e. g. $10\,\mathrm{kg\,m^{-3}}$) or the strengthening factor (e. g. < 2), the erosion of cratonic root edge would increase considerably; if both the buoyancy and strengthening factor are reduced, even more significant erosion could be observed (Fig 3 A, 3 B). Therefore, the erosion of cratonic root is strongly depended on the buoyancy and strength of the cratonic root.

Our geodynamical models demonstrate how the continental root would be eroded by the hot mantle flow induced by plume and find the buoyancy and strength of the lowermost root play a dominant role on this process. The effects of plume induced flow on a typical chemical cratonic root with $\Delta\rho \approx 30\,\mathrm{kg\,m^{-3}}$ and mild compositional strengthening factor (3–4) is quite limited. By either losing the chemical buoyancy or reducing the compositional strengthening factor, significant erosion of continental root by plumes could happen. The most likely mechanism for continental root to lose the chemical distinguished characteristics is lithosphere refertilization through mantle metasomatism. By decreasing the Mg#

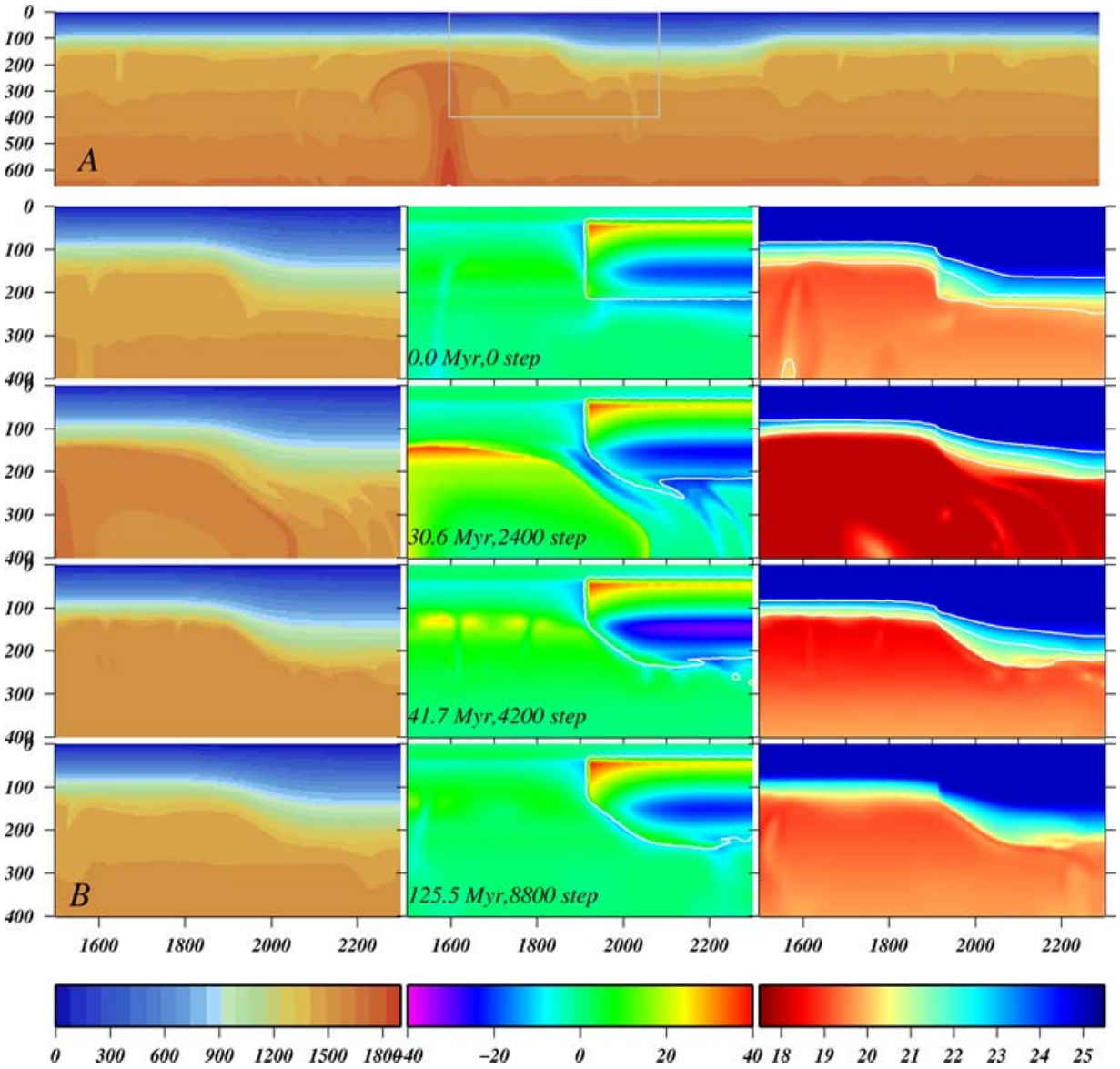

Fig. 2.: A): The full image of temperature field when plume rise up near cratonic root. The area within the gray box is zoomed out in Fig. 2 B. B): The evolution of temperature (left), horizontal buoyancy (middle) and viscosity (right) when plume impact thick cratonic root. The four time snapshots are: 0 Myrs, 30.67 Myr, 41.7 Myr and 125.5 Myrs. The plume rises up at 30 Myr. This model has $\Delta\rho = 21\,\mathrm{kg\,m^{-3}}; \Delta\eta = 3$ as showed in Figure 3.

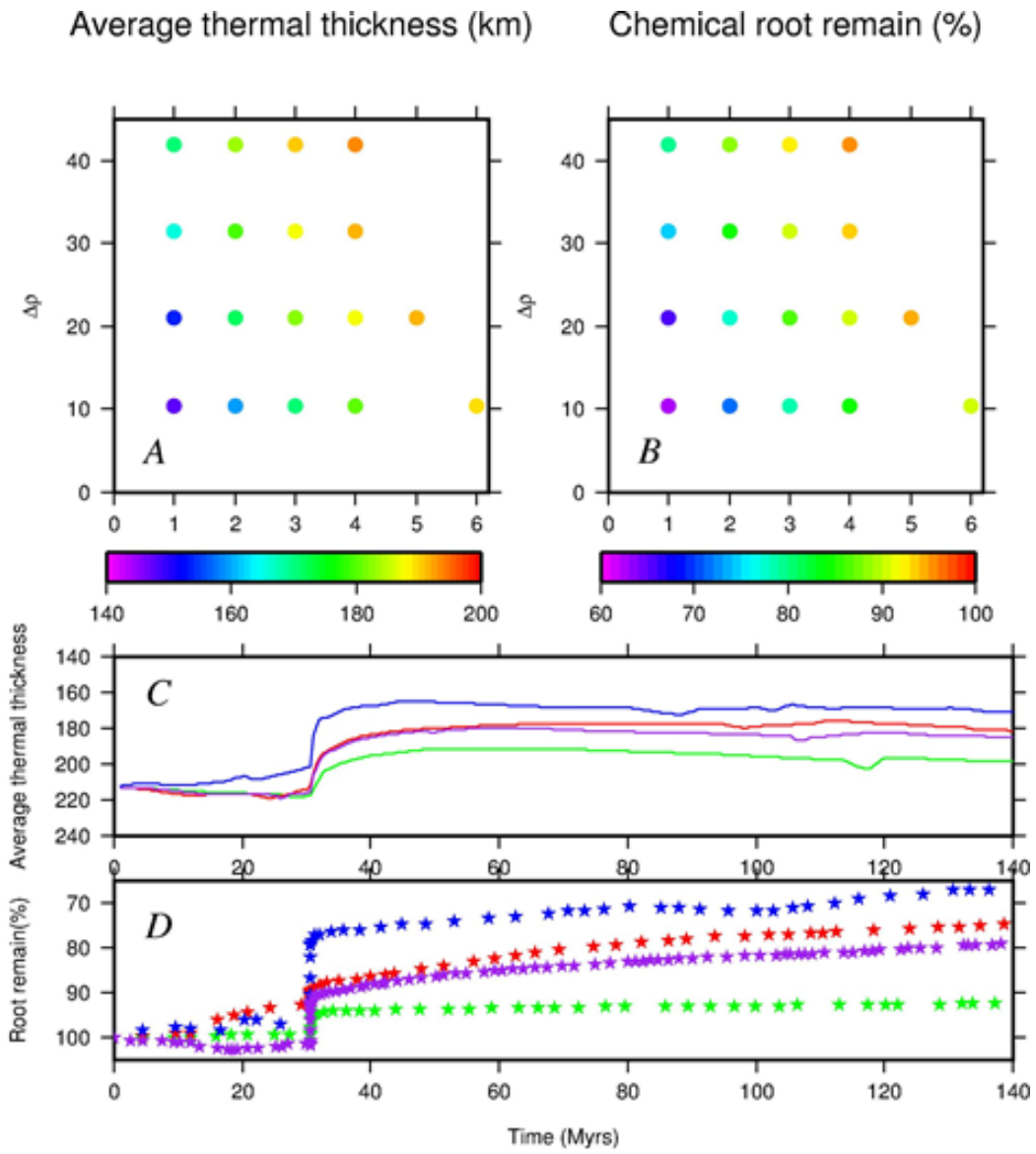

Fig. 3.: Effects of buoyancy and viscosity of the second cratonic layer on the erosion of cratonic root edge. (A) and (B) shows the average thermal thickness and chemical root remain of craton edge ($1914\,\mathrm{km}$ to $2046\,\mathrm{km}$) at 50 Myrs, respectively. C) and D) shows the 140 Myrs evolutions of four selected models in A and B: green lines for ($\Delta\rho = 31.5\,\mathrm{kg\,m^{-3}}; \Delta\eta = 4$); red lines for ($\Delta\rho = 10.5\,\mathrm{kg\,m^{-3}}; \Delta\eta = 4$); blue lines for ($\Delta\rho = 31.5\,\mathrm{kg\,m^{-3}}; \Delta\eta = 1$) purple lines for ($\Delta\rho = 21\,\mathrm{kg\,m^{-3}}; \Delta\eta = 3$).

of the originally depleted continental lithosphere and raising its pyroxene and garnet content, the chemical buoyancy/density of the SCLM would decrease/increase substantially[Griffin et al., 2003(b); Carlson et al., 2005]. Another important aspect of refertilization through mantle metasomatism is thermal effects. Through the heat advection from the metasomatism agents (hot fluid or melts) and enriched radiogenic element, the temperature of refertilized lithosphere would increase accordingly, but its effects would be smaller than the change of Mg# [Griffin et al., 2003(b)]. The influence of metasomatic refertilization on the viscosity of mantle rock is unclear due to the lack of related research, but the research about elastic thickness of Slave province in Canada shows that the metasomatic refertilization might also affects the rheology [Poudjom Djomani et al. 2005]. However, the heating of continental root itself has a rheological effect as the temperature is the main factor of mantle rheology, especially for the root material at the rheological boundary. Therefore, it's reasonable to link the change of buoyancy and strengthening factor in our models to metasomatic refertilization that happen to the continental root, even though we didn't include this process in our numerical models due to the lack of mathematic description.

Conclusion

1. For any significant thinning of cratonic root, it is most likely that one of the factor of buoyancy and viscosity or both were changed significantly, otherwise the chemically buoyant and strengthened root would strongly resist the erosion and deformation.

2. Metasomatic refertilization, as the main mechanism to change the composition of continental root, has an important geodynamic meaning for the continental lithosphere.

References

Carlson, R. R. W., D. G. Pearson, and D. D. E. James (2005), Physical, chemical, and chronological characteristics of continental mantle, Rev. Geophys., (2004), 1–24, doi:10.1029/2004RG000156.1.INTRODUCTION.

Djomani, Y. P., and S. O'Reilly (2001), The density structure of subcontinental lithosphere through time, Earth Planet. Sci. Lett., 184, 605–621.

Gao, S. et al. (2008), Recycling deep cratonic lithosphere and generation of intraplate magmatism in the North China Craton, Earth Planet. Sci. Lett., 270(1-2), 41–53, doi:10.1016/j.epsl.2008.03.008.

Griffin, W., S. O'Reilly, L. Natapov, and C. Ryan (2003a), The evolution of lithospheric mantle beneath the Kalahari Craton and its margins, Lithos, 71, 215–241, doi:10.1016/j.lithos.2003.07.006.

Griffin, W. ., S. . O'Reilly, N. Abe, S. Aulbach, R. . Davies, N. . Pearson, B. . Doyle, and K. Kivi (2003b), The origin and evolution of Archean lithospheric mantle, Precambrian Res., 127(1-3), 19–41, doi:10.1016/S0301-9268(03)00180-3.

Simon, N., G. R. Irvine, and G. Davies (2003), The origin of garnet and clinopyroxene in "depleted" Kaapvaal peridotites, Lithos, 71(2-4), 289–322, doi:10.1016/S0024-4937(03)00118-X

James, D. E., M. J. Fouch, J. C. Vandecar, and S. Van Der Lee (2001), Tectospheric structure beneath southern Africa, Geophys. Researc Lett., 28(13), 2485–2488.

Chesley, J., K. Righter, and J. Ruiz (2004), Large-scale mantle metasomatism: a Re–Os perspective, Earth Planet. Sci. Lett., 219(1-2), 49–60, doi:10.1016/S0012-821X(03)00698-8.

Deformation of forearcs during ridge subduction

Stefanie Zeumann, Andrea Hampel

Institut für Geologie, Leibniz Universität Hannover, Callinstraße 30, 30167 Hannover
e-mail: *zeumann@geowi.uni-hannover.de*
session: *Geodynamics*

Subduction of oceanic ridges causes considerable deformation of the forearc. Depending on the orientation of the ridge relative to the plate convergence direction, the ridge may either be stationary (e. g. Cocos Ridge at the Central American margin) or migrate along the margin (e. g. Nazca Ridge at the Peruvian margin). Here we use the finite Element program Abaqus to investigate the tectonic evolution of forearcs affected by ridge subduction.

The 3D models consist of a wedge-shaped forearc, under which an oceanic plate carrying the ridge is subducted (fig. 1). Following the approach of Cailleau and Oncken (2008) we use a cylindrical shape with a radius of 225 km for the subducting plate. Since the focus is on the deformation of the forearc we consider the oceanic plate as rigid. The plate interface is divided into the coupling zone with a variable friction coefficient and a frictionless section. The coupling zone along the plate interface is up to 30 km deep (fig. 1).

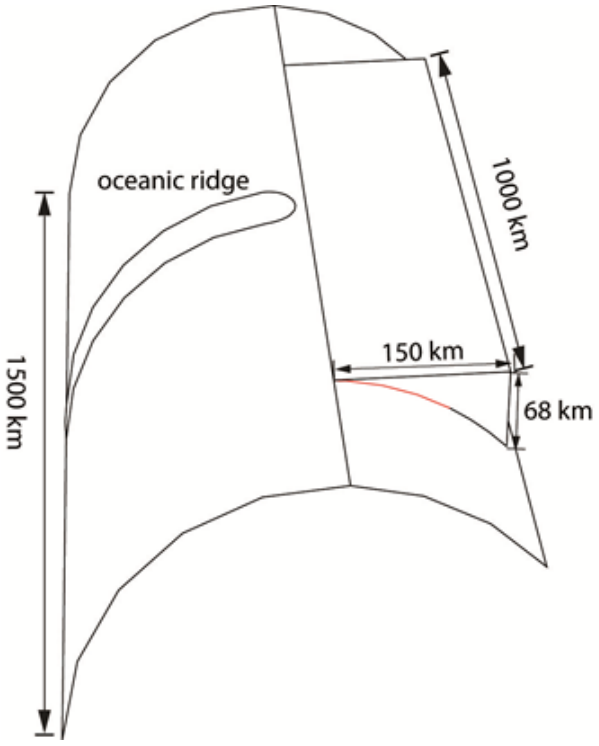

Fig. 1.: Model geometry includes a deformable wedge and a rigid slab carrying the oceanic ridge. The red line indicates the coupling zone along the plate interface.

In a systematic series of experiments, we consider migrating and non-migrating ridges by changing the angle between ridge and plate convergence direction. We further varied the ridge shape, the mechanical strength of the forearc and the frictional behaviour of the plate interface to identify the most crucial parameter for forearc deformation.

First results with a purely elastic forearc show that in all models the forearc is uplifted (fig. 2 a) and moved sideward during ridge subduction. For a stationary ridge, where the plate convergence direction is parallel to the ridge and perpendicular to the trench, the deformation pattern is symmetrical with respect to the ridge axis (fig. 2 a-d). The strain components show co-existing domains of both shortening and extension. Along the ridge axis, contraction occurs at the ridge tip and extension behind it (Fig 2 b). The strain component parallel to the margin (i. e. perpendicular to the ridge axis) reveals extension at the ridge tip and contraction above the flanks of the ridge (fig. 2 d-e). In models with a migrating ridge, the strain field becomes asymmetric with respect

to the ridge axis (fig. 2 e-f). The maximum contraction is found above the leading flank of the ridge.

A preliminary parameter study shows that the displacement and strain fields depend on the ridge shape (height, width), on the friction coefficient along the plate interface and, to a lesser extent, on the Young's moduli of the forearc. A higher ridge increases the amount of uplift whereas a broader ridge enlarges the region of uplift. A higher friction coefficient results in lower uplift for constant ridge height. Shortening and extension perpendicular to the margin increase with increasing ridge height or decreasing Young's moduli of the forearc layers. In contrast, a higher friction coefficient leads to lower extension but higher contraction. The strain component parallel to the margin is primarily affected by the ridge shape whereas material properties of the forearc and friction coefficient along the plate interface have nearly no influence. Increasing the ridge height increases the magnitude of both the extension at the ridge tip and the contraction above the ridge flanks. In contrast, a wider ridge decreases the overall amount of strain. In all models the ridge indents the forearc wedge (fig. 2 c). The indentation increases if a) the Young's moduli of the forearc layers decrease, b) the ridge is higher and c) the friction coefficient of the plate interface is increased. For example, increasing the ridge height from 1000 m to 2000 m enlarges the indentation by nearly 300 m after one million years of modelling time. Furthermore, the indentation depends on the frictional coupling between the two plates, with higher friction coefficients leading to larger re-entrants.

Future models will include the implementation of plastic behaviour to investigate the permanent deformation of forearcs during ridge subduction.

References

Cailleau, B. and O. Oncken (2008), Past forearc deformation in Nicaragua and coupling at the megathrust interface: Evidence for subduction retreat?, Geochem. Geophys. Geosyst., 9, Q03016, doi:10.1029/2007GC001754

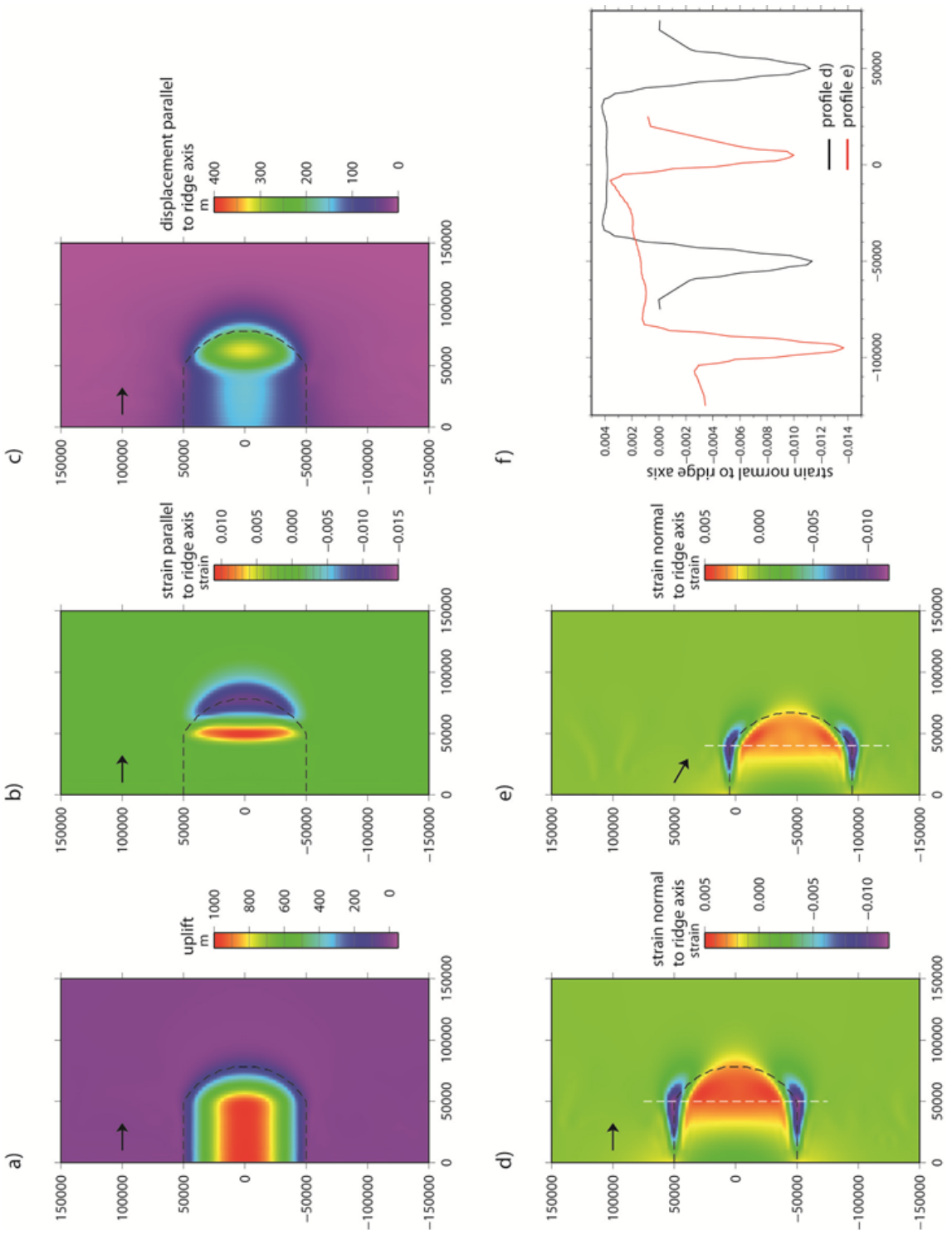

Fig. 2.: Central part of the model surface at 1 Ma of model time for a $100\,\mathrm{km}$ broad and $1\,\mathrm{km}$ high ridge. Black arrows indicate the plate convergence direction and black dashed line mark the ridge position. a) Uplift, b) strain component along the ridge axis, c) displacement along the ridge axis, and d) strain component normal to the ridge axis for a model with a plate convergence direction normal to the margin. e) Strain component normal to the ridge axis for a model with a plate convergence direction $60°$ oblique to the margin. f) Comparison of the strain component normal to the ridge axis for the white profiles in pictures d (black) and e (red).

Scientific Programme

GeoMod2014 - Conference Outline

Time	31. August	1. September	2. September	3. September
08:45 - 09:00	-	Welcome	-	-
09:00 - 11:00	-	(Seismo-)tectonics (orals)	Volcanism and Volcanotectonics (orals)	Rheology (orals)
11:00 - 13:00	-	(Seismo-)tectonics (posters)	Volcanism and Volcanotectonics (poster)	Rheology (poster)
13:00 - 14:00	-	Lunch break	Lunch break	Lunch break
14:00 - 16:00	-	Tectonics and Surface processes (orals)	Geodynamics (orals)	Fluids and Deformations (orals)
16:00 - 18:00	-	Tectonics and Surface processes (poster)	Geodynamics (posters)	Fluids and Deformations (poster)
18:00 - 21:00	Ice Breaker Party	-	-	-
19:00 - 22:00	-		Joint Conference Dinner	-

GeoMod2014 - Short course on "Constitutive Laws: from Observation to Implementation in Models" by Onno Oncken, Mathias Rosenau, Fabio Corbi, Georg Dresen Erik Rybacki, Stephan Sobolev, and Sascha Brune
Thursday 4 September: 09:00 - 18:00
Friday 5 September: 09:00 - 14:00

GeoMod2014 - Hands-on tutorial on "ASPECT: a next-generation geodynamic modelling software" by Anne Glerum and Juliane Dannberg
Thursday 4 September: 09:00 - 18:00: Tutorial
Friday 5 September: 09:00 - 18:00: ASPECT Strategy Workshop (for Advanced Users) - voluntary

GeoMod2014 Conference Programme (31 August - 3 September)

Sunday 31 August 2014

18:00 - 21:00: Ice Breaker Party at the 'Theaterschiff Potsdam' (Schiffbauergasse 9b, 14467 Potsdam)

Monday 1 September 2014

08:45 - 09:00: Welcome by Prof. Dr. Dr. h.c. Reinhard Hüttl and Prof. Dr. Onno Oncken

09:00 - 11:00: (Seismo-)tectonics Orals (chairs: B. Kaus, O. Oncken)

- 09:00 - 09:30: **Kelin Wang:** *Thermal Expressions of Stick-slip and Creeping Subduction Megathrusts* (keynote)
- 09:30 - 10:00: **Bertrand Maillot:** *The long-term Evolution of Fold-and-Thrust Belts: Consistency of Numerical Approaches and Physical Experiments* (keynote)
- 10:00 - 10:20: **Tasca Santimano** et al.: *Smart or Beautiful? Accretionary wedge evolution seen as a competition between minimum work and critical taper*
- 10:20 - 10:40: **Lorenzo Bonini** et al.: *The role of pre-existing frictional weaknesses on the propagation of extensional faults*
- 10:40 - 11:00: **Ylona van Dinther** et al.: *Seismo-thermo-mechanical modeling of subduction zone seismicity*

11:00 - 13:00: (Seismo-)tectonics Posters (chairs: B. Kaus, O. Oncken)

13:00 - 14:00: Lunch break

14:00 - 16:00: Tectonics and Surface processes Orals (chairs: F. Graveleau, N. Hovius)

- 14:00 - 14:30: **Ritske Huismans:** *Interaction and feedback between surface processes and mountain building* (keynote)
- 14:30 - 15:00: **Stéphane Dominguez:** *Joint analogue modelling of marine and terrestrial geological processes: state of the art and new developments* (keynote)
- 15:00 - 15:15: **Utsav Mannu** et al.: *Dynamic Modelling of Accretionary Prisms and Stratigraphy of Forearc basins*
- 15:15 - 15:30: **Karen Leever:** *3D Analogue Modelling of the Effect of Fan Sedimentation on Accretionary Wedge Dynamics – the Magdalena Fan case, South Caribbean Margin, Colombia*
- 15:30 - 15:45: **Frank Zwaan**, Guido Schreurs: *4D Transfer Zone Modeling in Continental Rift Systems*
- 15:45 - 16:00: **Sergei Medvedev**, Ebbe H. Hartz: *Evolution of topography of post-Devonian Scandinavia: Effects and rates of erosion*

16:00 - 18:00: Tectonics and Surface processes Posters (chairs: F. Graveleau, N. Hovius)

Tuesday 2 September 2014

09:00 - 11:00: Volcanism and Volcanotectonics Orals (chairs: O. Galland, E. Holohan)

- 09:00 - 09:30: **Rikke Pedersen:** *Surface deformation simulations of volcanic and tectonic processes in Iceland* (keynote)
- 09:30 - 10:00: **Olivier Roche**, Yarko Niño: *Mechanisms of entrainment of a granular substrate by pyroclastic density currents: insights from laboratory experiments and models, and implications for flow dynamics* (keynote)
- 10:00 - 10:15: **Rosanne Heistek** et al.: *Temporal changes in mantle wedge geometry and magma generation processes in the Central Andes: towards linking petrological data to thermomechanical models*
- 10:15 - 10:30: **Francesco Maccaferri** et al.: *The gravitational unloading due to rift depression: A mechanism for the formation of off-rift volcanoes in (continental) rift zones*
- 10:30 - 10:45: **Lola Chanceaux**, Thierry Menand: *Solidification effects on sill formation: an experimental approach*
- 10:45 - 11:00: Max Gallagher, **Ben Kennedy** et al.: *Megatsunami generation from caldera subsidence*

11:00 - 13:00: Volcanism and Volcanotectonics Posters (chairs: O. Galland, E. Holohan)

13:00 - 14:00: Lunch break

14:00 - 16:00: Geodynamics Orals (chairs: F. Funiciello, S. Sobolev)

- 14:00 - 14:30: **Anne Davaille:** *Plumes to Plate Tectonics: Insights from Laboratory Experiments* (keynote)
- 14:30 - 15:00: **Bernhard Steinberger** et al.: *On the relation between plate tectonics, large-scale mantle flow and mantle plumes: Some recent results and many open questions* (keynote)
- 15:00 - 15:15: **Paul J. Tackley** et al.: *Influence of Melting on the Long-Term Thermo-Chemical Evolution of Earth's Deep Mantle*
- 15:15 - 15:30: **Maria V. Chertova** et al.: *3-D numerical modeling of subduction evolution of the western Mediterranean region*
- 15:30 - 15:45: Tobias Baumann, **Boris Kaus**, A. Popov: *Constraining the rheology of the lithosphere through geodynamic inverse modelling*
- 15:45 - 16:00: **Elisa Calignano** et al.: *Strain localization during compression of a laterally heterogeneous lithosphere*

16:00 - 18:00: Geodynamics Posters (chairs: F. Funiciello, S. Sobolev), Methods and Materials Posters (chairs: M. Frehner, M. Rosenau)

19:00 - 22:00 Joint conference dinner in Potsdam on the ship 'Belvedere' (Lange Brücke 6, 14467 Potsdam)

Wednesday 3 September 2014

09:00 - 11:00: Rheology Orals (chairs: G. Dresen, H. Sone)

- 09:00 - 09:30: **Yuri Fialko:** *Numerical models of ductile roots of mature strike-slip faults* (keynote)
- 09:30 - 10:00: **Laurent Montési:** *Localization processes on Earth, Mars, and Venus* (keynote)
- 10:00 - 10:20: **Suzon Jammes** et al.: *Localization of deformation in a polymineralic material*
- 10:20 - 10:40: **Sebastian P. Müller** et al.: *Rheology of bubble- and crystal-bearing magma: new analogue experimental data and an effective-medium model*
- 10:40 - 11:00: **Maria A. Nikolinakou** et al.: *Modeling stress evolution around a rising salt diapir*

11:00 - 13:00: Rheology Posters (chairs: G. Dresen, H. Sone)

13:00 - 14:00: Lunch break

14:00 - 16:00: Fluids and Deformations Orals (chairs: S. Miller, M. Moreno)

- 14:00 - 14:30: **Boris Galvan** et al.: *Towards a general simulation tool for complex fluid-rock lithospheric processes: merging pre-processing, processing and post-processing in state-of-the-art computational devices* (keynote)
- 14:30 - 15:00: **Takeshi Tsuji:** *Digital rock physics: Insight into fluid flow and elastic deformation of porous media* (keynote)
- 15:00 - 15:15: **Thomas Heinze** et al.: *Numerical Modelling of earthquake swarms in the Vogtland / West- Bohemia*
- 15:15 - 15:30: **Samuel Angiboust** et al.: *Effect of Fluid Circulation on Intermediate-Depths Subduction Dynamics: From Field Observations to Numerical Modelling*
- 15:30 - 15:45: Magdalena Scheck-Wenderoth, **Judith Sippel** et al.: *Heat transport mechanisms at different scales – a 3D modelling workflow*
- 15:45 - 16:00: **Antoine Jacquey** et al.: *Modelling of fractured reservoirs: Fluid-rock interactions within fault domains*

16:00 - 18:00: Fluids and deformations Posters (chairs: S. Miller, M. Moreno)

The posters will be presented during the entire conference. Each poster session starts with a 1-2 min. short presentation of all participating posters.

GeoMod2014 - Short course on "Constitutive Laws: from Observation to Implementation in Models"

Thursday 4 September 2014

Morning Session: Onno Oncken, Mathias Rosenau, and Fabio Corbi

- 09:00 - 10:00: **Onno Oncken:** Observing deformation kinematics and localization: Observations from the field, geophysical imaging, and geodetic monitoring
- 10:00 - 10:15: Coffee Break
- 10:15 - 11:00: **Mathias Rosenau:** Rheology of rock analogues 1: Elastoplasticity and its application in seismotectonic simulation
- 11:00 - 11:15: Coffee Break
- 11:15 - 12:00: **Fabio Corbi:** Rheology of rock analogues 2: Viscoelasticity and its application in seismotectonic simulation
- 12:00 - 13:00: **Visit to the GFZ Analogue Lab**

13:00 - 14:00: Lunch break

Afternoon Session: Georg Dresen and Erik Rybackii

- 14:00 - 15:15: Rheology of the lower crust : Reconciling laboratory data and field observations
- 15:15 - 15:30: Coffee Break
- 15:30 - 16:45: **Visit to the GFZ rock mechanics lab**
- 16:45 - 17:00: Coffee Break
- 17:00 - 18:00: Rock fracture processes and stick slip sliding –What do we learn from analyzing nanofemto seismicity?

Friday 5 September 2014

Morning Session: Stephan Sobolev and Sascha Brune

- 09:00 - 10:00: **Stephan Sobolev:** Rheology and geodynamic modeling: key controls in plate tectonics and beyond
- 10:00 - 10:15: Coffee Break
- 10:15 - 11:30: **Sascha Brune:** Rock rheology in numerical models: PC exercises and application to rift dynamics
- 11:30 - 11:45 Coffee Break
- 11:45 - 12:30: **Stephan Sobolev:** Rheology and cross-scale modeling: towards understanding of great earthquakes
- 12:30 - 13:00: Discussion

13:00 - 14:00: Lunch and end of the short course

GeoMod2014 – Hands-on tutorial on"ASPECT: a next-generation geodynamic modelling software" by Anne Glerum and Juliane Dannberg

Thursday 4 September 2014

08:30 - 9:00: Registration

- 09:00 - 10:00: **Tutorial 1:** First Steps – Compiling and Running ASPECT, **Lecture:** How to run and visualize simple models
- 10:00 - 11:15: **Lecture** ASPECT – A next-generation geodynamic modelling software, **Tutorial 2:** Convection in a 2D box
- 11:15 - 11:30: Coffee Break
- 11:30 - 13:00: **Tutorial 3:** Using the adaptive mesh refinement and spherical shell geometry **Lecture:** How to run and visualize simple models

13:00 - 14:00: Lunch break

- 14:00 - 15:15: **Tutorial 4:** Using the adaptive mesh refinement and spherical shell geometry and using the function parser
- 15:15 - 15:30: Coffee Break
- 15:30 - 17:00: **Tutorial 5:** Averaging at the example of subduction and using a “sticky air” layer
- 17:00 - 18:00: **Voluntary:** Installing ASPECT on personal computers

18:30: Joint Dinner (to be payed by the participants)

Friday 5 September 2014

09:00 - 18:00: ASPECT Strategy Workshop for Advanced Users: Perspectives for Modelling with ASPECT

Index